Thermodynamic investigations of microbial metabolism and abiotic organic synthesis in seafloor hydrothermal systems

Michael Hentscher

Dissertation
zur Erlangung des Doktorgrades Dr. rer. nat.
Bremen, 2012

Fachbereich Geowissenschaften

Universität Bremen

Thermodynamics
- fit for fun ...

Referent:
Prof. Dr. Wolfgang Bach

Korreferent:
Prof. Dr. Kai Uwe Hinrichs

Tag des öffentlichen Promotionskolloquiums:
27.06.2012 18:00 Uhr

Table of Contents

Abstract

Hydrothermal circulation of seawater within the oceanic crust creates conditions suitable for chemosynthesis-based microbial life. Synthesis of abiotic organic compounds takes place during seawater-basement rock interaction at elevated temperatures. Low temperature circulation in the recharge zone allows chemolithoautotrophs to gain energy by oxidizing or reduction of minerals, while deeper and hotter regions (reaction zone) are dominated by rock alteration and produce the reduced conditions which are required in abiotic organic synthesis. The discharge zone, where cold seawater mixes with upwelling hydrothermal fluid is another habitat for diverse microbial life and locus of abiotic organic synthesis.

Thermodynamic calculations are helpful in assessing these processes in hydrothermal systems. In this thesis thermodynamic reaction path models have been used to simulate water-rock interactions in the oceanic lithosphere to evaluate the potential of abiotic organosynthesis in sub-seafloor environments. Batch mixing models were used to determine the Gibbs energy available for metabolic reaction along given mixing paths for hydrothermal fluid and seawater. The results highlight the important role variable water-to-rock ratios (W/R), fluid mixing ratios and temperature play in influencing abiotic organosynthesis processes. By merging model results with geochemical field data and microbiological observations it is possible to elucidate the bioenergetics of microbial metabolism in a range of hydrothermal environments from diffuse vent fields to ridge flank seawater aquifers.

Furthermore, thermodynamic computations were used to test the hypothesis that changing vent fluid compositions directly impact vent biology. In an example from the East Pacific Rise (EPR) 9°50'N the energy yield of a wide range of catabolic reactions in diffuse vents was calculated. From these calculations it is apparent that the energy for sulfide oxidizing dropped notably before the demise of the colonies of *Riftia* (a giant tubeworm living in symbiosis with sulfur oxidizing bacteria). In a second vent field of the EPR 9°50'N area the catabolic activity of microbial communities in the subsurface was assessed by geochemical modeling. Elements behaving conservatively during the fluid mixing process were used to infer the mixing ratio of seawater and hydrothermal vent fluid. Concentrations of non-conservative elements were then compared with the actually measured composition of diffuse fluids. The difference between measured and calculated fluid composition is indicative of the consumption or the release of a chemical species. The growth of hydrogenotrophic communities effective lowers the hydrogen concentration in a hydrothermal fluid. Indeed, the calculations show that the fluid composition measured at the vent site allows subseafloor methanogenesis. The results are in line with these findings and indicate that a period of active growth of hydrogenotrophic communities was followed by a period of steady state.

In a second study, the potential for abiotic organosynthesis in serpentinization systems was examined by reaction path modeling of harzburgite – seawater interactions at a range of temperatures. Serpentinization reactions release hydrogen, which drives the reduction of dissolved inorganic carbon to organic compounds (e.g., formic acid, methanol, and methane). While methane is the thermodynamically stable species, there is evidence from hydrothermal experiments indicative of sluggish reduction from methanol to methane. In calculations

of metastable stability of intermediate organic species, I could show that in fluid-dominated systems (W/R ≥ 4–5) organic synthesis is more likely than under more rock-dominated conditions. This relation exists because calcite precipitation is predicted to take place at small W/R, which considerably lowers the concentration of DIC and diminishes the driving force for abiotic organic synthesis. When applied to the Lost City hydrothermal vent field, these results indicate that methane formation may have taken place at W/R greater than those proposed for the reaction zone (W/R=2–4). The calculation results also suggest that organosynthesis reactions likely occur in the deepest part of the recharge zone. In contrast, the fate of DIC in the more rock-buffered reaction zone of the Lost City system is predicted to be the formation of carbonate.

The third chapter of this Thesis examines bioenergetic constraints in hydrothermal systems. By using batch mixing models, Gibbs energies were calculated for a range of metabolic reactions supported microbial growth in hydrothermal systems. Firstly, published vent fluid compositional data from hydrothermal areas hosted in different rock types and situated in varied geotectonic settings are used to assess which catabolic and anabolic reactions are favored in these different environments. From this theoretical study it is concluded that peridotite-hosted systems can be distinguished from basalt hosted systems by a higher number of possible catabolic reactions as well as anabolic reactions that are more favored (dissipate less Gibbs energy). These differences are largely related to the higher hydrogen concentrations in peridotite-hosted systems. Secondly, ridge flank microbial metabolism was examined by using pore fluid chemistry and microbiological observation in a colonizing experiment from the eastern flank of the Juan de Fuca Ridge. It could be shown that the observed shift in microbial community was caused by the shift in the energy yields of catabolic reactions when the borehole returned to its natural state. Thirdly, combined microbiological and thermodynamic studies were used to infer about the conditions of habitats formed by the subseafloor mixing at the Mid-Atlantic Ridge 5°S and 9°S hydrothermal fields. These studies indicate that the metabolic diversity appears to be a function of overall energy availability. Furthermore, the extent of seawater entrainment in these systems apparently imparts a strong control on the microbial community structure of diffuse vents.

In summary, thermodynamic computations can be used in different ways to enhance our understanding of hydrothermal processes. This has been demonstrated for microbial metabolism as well as for abiotic organic synthesis within the ocean crust. A particular strength of thermodynamics is that it fosters bridging between several scientific disciplines (biology, chemistry, geology, etc.) to further our understanding of varied aspects of hydrothermal systems in the sense of a ‘follow-the-energy approach’.

Zusammenfassung

Hydrothermale Zirkulation von Meerwasser innerhalb der ozeanischen Kruste schafft geeignete Bedingungen für mikrobielles chemotrophisches Leben. Durch die Wechselwirkung von Meerwasser mit dem Untergrund wird zudem abiotische Synthese von organischen Verbindungen ermöglicht. Die Zirkulation von kühlem Meerwasser in der oberen Kruste ermöglicht chemolithoautotrophen Organismen, Energie durch das Oxidieren oder Reduzieren von Mineralen zu gewinnen, während die tieferen und heißeren Bereiche (Reaktionszone) überwiegend durch die abiotische Gesteinsalteration beeinflusst werden. Alteration von ozeanischer Kruste erzeugt reduzierende Bedingungen, die für die abiotische organische Synthese benötigt werden. Dort, wo sich kaltes Meerwasser mit der aufsteigenden hydrothermalen Lösung mischt (die Aufstiegs- and Austragszone), werden verschiedene Bereiche geschaffen, welche für Mikroorganismen einen potentiellen Lebensraum bilden, aber auch abiotische organische Synthese ermöglichen.

Thermodynamische Berechnungen stellen ein geeignetes Mittel dar, um die Prozesse in hydrothermalen Systemen vorherzusagen. So wurden in dieser Dissertation thermodynamische Reaktionspfadmodelle benutzt, um die Gesteinsalteration durch Meerwasser zu simulieren und im nächsten Schritt daraus abzuschätzen, wie wahrscheinlich der Ablauf der abiotischen organische Synthese in der Reaktionszone ist. Ebenso wurden mit Hilfe eines Mischungsmodelles die Gibbsenergien für metabolische Reaktionen bestimmt, die ermöglicht werden, wenn Meerwasser sich mit hydrothermalen Lösungen mischt. Der Schwerpunkt dieser Berechungen liegt auf die Beurteilung des Einflusses von Wasser-Gesteinsverhältnissen sowie der Mischungsverhältnisse bei hydrothermalen Prozessen. Die Ergebnisse der Modellberechnungen wurden in Kombination mit geochemischen Daten und mikrobiologischen Beobachtungen angewandt, um Rückschlüsse auf die mikrobiologischen Stoffwechsel in verschieden hydrothermalen Systemen zu ziehen. Die untersuchten hydrothermalen Systeme reichen von diffusen Quellen bis zu Meerwasseraquiferen an ozeanischen Rückenflanken

In einem Anwendungsbeispiel wurden thermodynamische Berechnungen verwendet, um die Hypothese zu testen, dass eine Änderung der hydrothermalen Flüssigkeitszusammensetzung die massive Veränderung der hydrothermalen Biozönose am Ostpazifischen Rücken (East Pacific Rise, EPR) 9°50’N verursacht hat. Die Berechnung der katabolischen Energiegehalte für die diffusen Quellen dieses Gebietes zeigen, dass der Energiegehalt, insbesondere für Sulfidoxidation, sank bevor die *Riftia*- (Riesenröhrenwürmer aus der Familie der Bartwürmer, die in Symbiose mit schwefeloxidierenden Bakterien leben) Kolonien starben. Außerdem konnte für eine zweite Lokalität mit Hydrothermalquellen am EPR 9°50’N gezeigt werden, dass die katabolische Aktivität der im Untergrund lebenden mikrobiellen Lebensgemeinschaft durch geochemische Modellierung quantifiziert werden kann. Dazu wurde zunächst das Mischungsverhältnis von Meerwasser und hydrothermaler Lösung anhand sich beim Mischungsprozess konservativ verhaltender Elemente bestimmt und eine entsprechende diffuse Lösung modelliert. Im folgenden Schritt wurden dann die Konzentrationen sich nicht konservativ verhaltenden Komponenten mit denen aus der gemessenen

Mischung verglichen. Der Unterschied zwischen den gemessenen und modellierten Konzentrationen weist auf den Verbrauch beziehungsweise die Abgabe dieser chemischen Spezies hin. So verringert das Wachstum einer hydrogenothrophen Lebensgemeinschaft die Konzentration von Wasserstoff in der Lösung; hierbei konnte zudem gezeigt werden, dass eben diese Fluide den Ablauf von Methanogenese im Meeresboden fördern. Die Ergebnisse der thermodynamischen Berechnungen stehen im Einklang mit diesen Resultaten und zeigen, dass nach einer Periode von aktivem Wachstum von hydrogenotrophen Organismen sich ein stationärer Zustand einstellte

In einer zweiten Studie wurde das Potential für abiotische organische Synthese innerhalb von Serpentinisierungssystemen mittels eines Reaktionspfadmodelles untersucht. Das Modell simuliert die Alteration von Harzburgit durch Meerwasser in bestimmten Temperaturbereichen. Bei der Serpentinisierung werden große Mengen an Wasserstoff (H_2) erzeugt, welcher die Reduktion von gelöstem anorganischem Kohlenstoff zu organischen Verbindungen (z.B. Ameisensäure, Methanol und Methan) antreibt. Während Methan in Serpentinisierungsfluiden die thermodynamisch stabile organische Spezies ist, gibt es jedoch Hinweise aus hydrothermalen Experimenten, dass die Reduktion von Methanol zu Methan sehr langsam ist, was die Bildung von intermediären organischen Spezies ermöglicht. Mit Hilfe der Berechnung von thermodynamisch metastabilen Gleichgewichten für diese intermediären organischen Spezies konnte gezeigt werden, dass organische Synthese unter fluiddominierten Bedingungen (Wasser-Gesteins-Verhältnis W/R$\geq$4–5) wahrscheinlicher ist als unter gesteinsdominierten Bedingungen. Dieser Zusammenhang lässt sich damit erklären, dass die prognostizierte Bildung von Kalzit bei niedrigenWasser-Gesteins-Verhältnissen dazu führt, dass die Konzentration von gelöstem anorganischem Kohlenstoff sinkt und damit auch die Triebkraft für abiotische organische Synthese. Wendet man diese Ergebnisse auf das Lost City-Hydrothermalfeld an, zeigt sich, dass die Wasser-Gestein-Verhältnisse bei der Methanbildung vermutlich höher waren als bei der allgemein angenommen Reaktionzone (W/R=2-4). Die Modellergebnisse deuten auch darauf hin, dass die abiotische organische Synthese im untersten Teil der sogenannten “recharge zone” abläuft, während es in der gesteinsgepufferten Reaktionszone des Lost City-Systems zur Karbonatausfällung kommt.

Das dritte Kapitel der vorliegenden Dissertation untersucht die bioenergetischen Grenzen in hydrothermalen Systemen. Mit Hilfe von Mischungsmodellen wurden Gibbsenergien für eine Reihe von Stoffwechselreaktionen berechnet, die mikrobielles Wachstum in hydrothermalen Systemen unterstützen. Zunächst wurden veröffentlichte chemische Daten von Hydrothermalfluiden aus verschiedenen geotektonischen Milieus und von verschiedenen Gesteinstypen verwendet, um zu beurteilen, welche anabolischen und katabolischen Reaktionen in den jeweiligen Umgebungen die Ansiedlung von Lebensformen potentiell begünstigen . Aus dieser theoretischen Studie ließ sich schlussfolgern, dass sich Hydrothermalsysteme auf Peridotit von Systemen auf Basalt durch die Anzahl möglicher katabolischer als auch anabolischer Reaktionen unterscheiden. Diese Unterschiede lassen sich durch höhere Wasserstoffkonzentration in Peridotitsystemen erklären. Zudem wurde der mikrobielle Stoffwechsel in Rückenflankensystemen untersucht. Grundlage der Studie bildeten chemischen Daten von Porenwässern und mikrobiologische Beobachtungen, die während eines Kolonisierungsexperiments an der östlichen Flanke des Juan de Fuca-Rückens gesam-

melt wurden. Es konnte gezeigt werden, dass der beobachtete Wechsel der mikrobiellen Lebensgemeinschaft durch die Änderung im Energiegehalt der katabolischen Reaktionen verursacht wurde, als sich das natürliche Gleichgewicht im Bohrloch wieder einstellte. Schließlich wurden mikrobiologische und thermodynamische Studien kombiniert, um auf die Lebensbedingungen im Ozeanboden zu schließen, die durch das Mischen von Meerwasser mit hydrothermalen Lösungen (Hydrothermalfelder 5°S und 9°S des Mittelatlantischen Rücken) entstehen. Es kann gezeigt werden, dass die metabolische Diversität scheinbar eine Funktion der allgemeinen Verfügbarkeit von Energie ist. Darüber hinaus scheint das Ausmaß der Meerwasserzirkulation einen starken Einfluss auf die mikrobielle Zusammensetzung der Lebensgemeinschaft an diffusen Quellen zu haben.

Im Rahmen dieser Arbeit konnte gezeigt werden, dass thermodynamische Berechnungen auf unterschiedlichste Weise verwendet werden können, um das Verständnis von hydrothermalen Prozessen zu verbessern. Dies gilt sowohl für mikrobiellen Stoffwechsel als auch für abiotische organische Synthese in der Ozeankruste. Eine besondere Stärke der Thermodynamik ist, dass sie eine Brücke zwischen verschiedenen wissenschaftlichen Disziplinen (Biologie, Chemie, Geologie, etc.) schlägt, welche unser Verständnis für die verschiedenen Aspekte in hydrothermalen Systemen im Sinne des Ansatzes „Folge der Energie“ fördert.

1. Introduction

1.1 Hydrothermal systems in the deep sea

Energy transfer from the earth's interior to the ocean is the cause for hydrothermal circulation beneath the seafloor. Mantle upwelling leads to partial melting and the formation of new oceanic crust along mid-ocean spreading ridges, such as the Mid-Atlantic-Ridge. The high heat flux associated with this process induces the circulation of seawater through the crust. Stein and Stein (1994) estimated that cooling of the lithosphere by seawater circulation accounts for nearly a quarter of the global heat loss and corresponds to round about $7 \cdot 10^{12}$ to $11 \cdot 10^{12}$ W. Between $1 \cdot 10^{12}$ and $4 \cdot 10^{12}$ W of that heat loss takes place by seawater circulation through crust within a few kilometers at the spreading ridges (Sleep, 1991; Stein and Stein, 1994), while the rest is transferred by off-axis seawater circulation in older permeable crust at lower temperatures (Elderfield and Schultz, 1996). Sediments are restrictive to the hydrothermal circulation and thickening of the sediment cover with time leads to a loss in permeability and limits the exchange between ocean and basement to areas where the crust is exposed (Fisher and Wheat, 2010).

Seawater is not only responsible for the heat transfer from the lithosphere to the ocean, but also for the alteration of the oceanic crust. Increasing temperatures of the fluid enhance the kinetic rate for water-rock reaction and modifies the crust as well as the fluid. The uptake of water is the dominant alteration process of the rock. Seawater in hydrothermal systems undergoes a decrease of Mg content and an increase in Ca content as temperatures go up. Mg is incorporated in various alteration phases, such as chlorite, of the crust but can also precipitate as magnesium-hydroxide-sulfate-hydrate directly from the seawater (Bischoff and Seyfried, 1978; Janecky and Seyfried, 1983). Ca in contrast is leached from the rock and is removed along with sulfate from the fluid by precipitation of anhydrite. The loss of Mg in hydrothermal fluids is virtually complete, so that the amount seawater entrained during sampling of hydrothermal vent fluids can be calculated by mass balance (Von Damm et al., 1985).

Seawater-rock interactions cause a significant change of the redox state of the fluid from oxic to reduced conditions. Fe^{2+}, Mn^{2+} and other metals are leached from the host rock. Reduced compounds like H_2S, H_2 or CH_4 are produced by abiotic reactions at high temperature. The same compounds may be produced or consumed by microbial activity at lower temperatures. The highest temperatures for circulation fluids are reached in vicinity of a heat source like a magma chamber. Crystallizing magma can also release gases to the fluid, like SO_2, H_2 and CO_2 (Mottl et al., 2011; Reeves et al., 2011). These gases can be very reactive; for instance, SO_2 disproportionates to H_2S and SO_4^{2-} following the reaction $4\,SO_2 + 4\,H_2O = H_2S + 3\,SO_4^{2-} + 6\,H^+$ and acidify the solution (Kusakabe et al., 2000). At low pH the leaching of the metal from the rocks is more efficient because the solubility of metals in the fluids is increased.

Hydrothermal systems hosted in ultramafic rock (mantle peridotite) appear to be less influenced by magma degassing than basalt hosted hydrothermal systems. In the former

water-rock reactions produce substantial amounts of H_2, which may reduce dissolved CO_2 to methane and other organic compounds (e.g., Berndt et al., 1996; Charlou et al., 2002; Konn et al., 2006; Proskurowski et al., 2008; Konn et al., 2009). H_2 is produced in these systems, when heated seawater reacts with olivine and orthopyroxene to form serpentine, brucite, and magnetite (Klein et al., 2009; McCollom and Bach, 2009).

In the hottest part of the reaction zone the fluid can undergo phase separation at temperatures and pressures above the critical point of seawater (405°C, 297 bar; Bischoff and Rosenbauer, 1988). During supercritical phase separation two separate fluid phases form, one that is enriched in gases and depleted in salt, and a second one that has high salt freight and low amounts of dissolved gas. It has been observed that the gas-rich fluids vent earlier than the corresponding brine, likely because they are less dense and more buoyant (Von Damm et al., 2003; Schubert et al., 2010). The buoyant hydrothermal fluids rise up to the seafloor in narrow upflow zones and undergo adiabatic and conductive cooling in addition to mixing with seawater. When these hot vent fluids mix with seawater the properties of the fluid (e.g., temperature and pH) change, which can induce the precipitation of minerals, in particular anhydrite and metal sulfides. This process causes the formation of black smoker chimneys at the seafloor and plume particles in the water column. Besides this focused venting of hydrothermal fluid large areas diffuse venting in the vicinity of the vents are commonly observed. Diffuse venting results from mixing of hydrothermal vent fluid with entrained seawater in the subseafloor. Although diffuse fluids are lower in temperature, they have been proposed to transport more heat from the system than the focused vents (Rona and Trivett, 1992; Schultz et al., 1992).

1.2 Habitats created by hydrothermal circulation of seawater

Mixing of hot, reduced vent fluids with cold, oxic seawater supports some of the most impressive ecosystems in the deep sea. Habitats must satisfy two criteria: (1) the physical and chemical conditions must be suitable for life, and (2) energy for metabolic activity has to be available. The highest temperature of a cultured growing microorganism (an dissimilatory Fe-reducer using formate as energy source) is 121°C (Kashefi and Lovley, 2003). At higher temperatures this microorganism was able to survive but did not grow. It is conceivable that microorganisms in the subsurface inhabit zones in the subseafloor that do not exceed this temperature limit.

Primary production in the deep sea depends on chemotrophy because other energy sources as like light for photosynthesis are unavailable. A prerequisite for chemotrophy is that a chemical disequilibrium is present which can be exploitable by microorganisms. Disequilibria prevail, when the properties of the system change at rates faster than the rates at which the thermodynamically favored reactions proceed. Mixing of high temperature vent fluid with cold oxygenated seawater is a process that fulfills these criteria. The mixing lowers the temperature to temperatures suited for microorganism and the supply flux of reduced components like H_2, H_2S, CH_4 and Fe^{2+} (in vent fluid) and electron acceptors like O_2, SO_4^{2-} and HCO_3^- (in seawater) generates thermodynamic drive for various redox reactions and allow microorganisms to gain energy for their catabolism (McCollom and Shock, 1997;

Shock and Canovas, 2010; Amend et al., 2011). Actively venting chimneys (Takai et al., 2001; Tivey, 2004; Kormas et al., 2006; Takai et al., 2009) and hydrothermal plumes (Cowen et al., 1986; de Angelis et al., 1993) are places that are colonized by microorganisms, which form the basis of the food web in these ecosystems. The high energy flux from the subsurface enables also higher organisms like tube worms and mussels, which are living in symbiosis with microorganisms, to colonize vent areas (Childress et al., 1991; Le Bris et al., 2005; Tunnicliffe et al., 2009; Petersen et al., 2011). Evidently, the mixing zone in the subsurface provides exploitable energy for microbial metabolism at favorable conditions. The longer residence times of the mixed fluids in the subsurface and the abundance of diffuse vents on the seafloor indicate that this type of habitat may support the production of high biomass.

1.3 Bioenergetics of hydrothermal vents

Thermodynamic calculations have been applied to assess the bioenergetics of hydrothermal vent systems in terms of the bioenergetics of catabolic and anabolic metabolism (Amend and Shock, 1998; Shock and Schulte, 1998; Amend et al., 2003; Shock and Holland, 2004; McCollom and Amend, 2005; Amend et al., 2011). The potential energy yield of vent fluid-seawater mixtures supporting vent habitats can be estimated by the thermodynamic relation

$$\Delta_r G = \Delta_r G^\circ + RT \ln(\mathrm{Q}_r) \qquad \text{(eq. 1)}$$

where R is the universal gas constant and T the temperature in Kelvin. $\Delta_r G^\circ$ is the Gibbs energy for the reaction at standard temperature and pressure, and Q_r expresses the activities of species participating a specific reaction in the actual fluid mixture. Q_r is evaluated through equation (2):

$$\mathrm{Q}_r = \prod_i a_i^{\,v_{ir}} \qquad \text{(eq. 2)}$$

where a_i represents the activity of the chemical species in the reaction, v_{ir} denotes the stoichiometric coefficient for the ith chemical species in the reaction, which is positive for products and negative for reactants. If $\Delta_r G$ for a reaction is negative, then the reaction is favored and the microorganism can gain energy; if it is greater than zero, than the reaction will proceed in the opposite direction and the microorganism can only gain energy if it uses the reverse reaction.

The activity of all chemical species involved in a reaction can be calculated from compositional data of vent fluids. For a given reference state (p, T), the potential Gibbs energy for the various redox reactions can then be determined to infer which kind of microbial metabolism is possible in a specific mixing zone. By using a batch mixing computations for seawater and endmember hydrothermal vent fluids, one can calculate the Gibbs energy for

different mixing ratios to examine the change in catabolic energies as a function of increasing seawater entrainment.

The composition of the host rock and volcanic activity greatly affect vent fluid chemistry, with profound consequences for the bioenergetics of vent microorganisms (Amend et al., 2011). While oxidation of H_2S is the most commonly available energy source in basalt-hosted vent systems (McCollom and Shock, 1997), other systems are rich in hydrogen that can be used by microorganism for catabolic reactions such as the reduction Fe(III) or sulfate reduction, methanogenesis and manganese reduction (Huber et al., 2003; Shock and Holland, 2004; Takai and Nakamura, 2010).

Besides the habitats supported by mixing of hydrothermal fluids with seawater, ridge flank water-rock interactions may also support primary production of biomass. When seawater recharges into the crust, oxygen and other oxidized compounds like sulfate or nitrate are introduced into the system. These compounds can be used by chemolithoautotrophic microorganism to oxidize the reduced Fe(II) and sulfide of the crustal rocks. This process may support quantities of biomass similar to that in hydrothermal vent settings (Bach and Edwards, 2003). Mn(II) and dissolved and particulate organic substrate may also fuel metabolism in the ridge flank habitats. Low temperatures in these systems slow down the rates of abiotic reactions that allow slow-growing microorganisms to harness the Gibbs energy of rock weathering reactions. With increasing temperatures, these microorganisms may not the able to outcompete the abiotic reactions. Ridge flanks are therefore likely to be inhabited by groups of microorganisms that differ substantially from those found in vent settings (e.g., Edwards et al., 2005).

1.4 Abiotic organosynthesis

The reduced conditions in hydrothermal systems may generate potential to drive abiotic reduction of CO_2 to organic compounds (Shock, 1990). Indeed, high concentrations of organic compounds, especially methane, were measured in vent fluids rich in H_2 (Charlou et al., 2002). The highest concentrations of methane are measured from sediment-hosted environments, but carbon isotopic ratios indicate that these high concentrations are produced by thermal decomposition (pyrolysis) of organic matter within these sediments (Welhan and Lupton, 1987; Lilley et al., 1993; Proskurowski et al., 2008). High concentrations of methane (1-2 mM) were also measured in ultramafic-hosted systems, such as the Lost City, Rainbow and Logatchev vent fields. The $\delta^{13}C_{PDB}$ values of CH_4 from theses systems are heavy (Lost City -14 to -9‰, Rainbow -16‰, Logatchev -14‰) in contrast to isotopic light values of thermogenic CH_4 (-50 to -30‰) (Sherwood Lollar et al., 2006). This isotopic difference and the lack of large sediment covers indicate abiotic organosynthesis of methane (Proskurowski et al., 2008). Abiotic synthesis of methane is kinetically sluggish (McCollom and Seewald, 2001), but the production of precursor compounds, such as formic acid and methanol, is much faster (Seewald et al., 2006). Driving the formation of abiotic organic compounds in these ultramafic-hosted systems is the high concentration of H_2 in the vent fluids. The H_2 is

produced by the alteration of olivine with seawater (serpentinization) by following general reaction after Klein et al. (2009):

olivine + H_2O → serpentine + brucite + magnetite + H_2 (≤ 330°C)

and

olivine + H_2O + SiO_2 → serpentine + magnetite + H_2 (≤ 400°C)

The activity of hydrogen in the fluid is strongly influenced by the water to rock ratio and temperature in the system. McCollom and Bach (2008) and Klein et al. (2009) used a thermodynamic modeling method to estimate H_2 concentrations during serpentinization. These computations indicate that H_2 concentrations may be as high as several hundred millimolal, suggesting a very large potential for the formation of organic compounds in serpentinization systems.

Mixing of H_2-rich hydrothermal fluids with seawater may also drive abiotic organosynthesis reaction (Amend and Shock, 1998; Shock and Schulte, 1998; Amend and McCollom, 2009; Shock and Canovas, 2010; Amend et al., 2011). However, the time scales of mixing are short relative to the rates at which organic synthesis reactions proceed. This may be different in subseafloor hydrothermal mixing zones, where residence times of the mixed fluids are increased.

1.5 Motivation and outline of this thesis

The aim of this thesis is to enhance the understanding of microbial metabolism and abiotic organic synthesis related to hydrothermal circulation of seawater within the oceanic crust from a thermodynamic perspective. Hydrothermal systems offer an interesting field for interdisciplinary research, and many aspects, in particular the interface between geochemical and microbial processes, can be elucidated using thermodynamic relations. The alteration of oceanic crust and the associated change of fluid composition can be predicted and compared with actual findings. In the case of large and consistent differences between predictions and observations, these models can be adjusted to account for metastable equilibria. This iterative process improves the predictive power of the models in order to guide in the interpretation and understanding of the system. Thermodynamics can be particularly valuable in examining chemotrophy-based vent ecosystems. The exploitable energy for microbial metabolism depends on the disequilibria formed by either mixing of seawater with reduced hydrothermal fluid or fluid-rock interaction. The maximum amount of Gibbs energy available for chemotrophic microorganism can be by quantified by thermodynamic computations. By quantifying the amount of exploitable energy, metabolic strategies of microbes inhabiting a given systems can be assessed. These are only two examples which show how thermodynamics can enhance our understanding of hydrothermally related processes in the deep sea. The versatility of thermodynamics in bridging between several scientific disciplines (biology, chemistry, geology, etc.) to further our understanding of various aspects of hydrothermal systems in the sense of a ‘follow-the-energy approach’ will be presented in the following chapters:

Chapter 2: "Geochemically induced shifts in catabolic energy yields explain past ecological changes of diffuse vents in the East Pacific Rise 9°50'N area"

This chapter highlights the relation between vent fluid chemistry and vent fauna in the East Pacific Rise 9°50'N area. This area is known for a profound change in the vent fauna caused by a change in fluid chemistry (Shank et al., 1998; Von Damm and Lilley, 2004). To test this hypothesis I conducted free energy calculations for a range of catabolic reactions. The calculations are based on a comprehensive dataset for diffuse and high temperature fluids from the vent site. In a second case study from this vent area, the results from similar calculations in combination with fluid chemistry data are used to infer the inhabiting microbial community in the subsurface. This chapter is complemented by a detailed method section detailing the relevant calculations.

Chapter two is published:

Hentscher, M., Bach, W., 2012. Geochemically induced shifts in catabolic energy yields explain past ecological changes of diffuse vents in the East Pacific Rise 9°50'N area. Geochemical Transactions 13, 2.

Chapter 3: "Geochemical modeling of CO_2 behavior in water-peridotite interactions: organic synthesis versus carbonate precipitation"

Chapter 3 deals with the possible fate of CO_2 during the alteration of peridotite with seawater (serpentinization). Serpentinization produces substantial amounts of hydrogen which creates the driving force for the reduction of dissolved inorganic carbon to organic molecules. Serpentinization releases dissolved Ca and increases the alkalinity of the interaction fluid, which facilitates the precipitation of calcite. Using reaction path modeling I examine the fate of organic C1 and C2 compounds as a function of water-to-rock ratio and temperature during serpentinization. Kinetic constraints are included in the discussion of the computational results. Finally, a scenario for the natural serpentinization system Lost City is presented, which provides a plausible explanation for nature of the fluids venting from that system.

Chapter three will be submitted to Chemical Geology

Michael Hentscher, Wolfgang Bach, Frieder Klein
"Geochemical modeling of CO_2 behavior in water-peridotite interactions: organic synthesis versus carbonate precipitation"

Chapter 4 "Thermodynamic assessment of catabolic and anabolic energetics in submarine hydrothermal systems"

Chapter 4 is a synthesis of four published articles I co-authored. In these articles I performed thermodynamic calculations and was strongly involved in their interpretation as well as in the writing of the methods sections. The chapter begins with a comprehensive and systematic assessment of energetics of chemolithoautotrophs in deep-sea hydrothermal systems. It provides a thermodynamic perspective on catabolic metabolism fuelling chemolithoautotrophs in high temperature hydrothermal systems in relation to the rock type and fluid chemistry. This approach is also used to estimate the energy which these microbes have to spend to form biomass and to examine which temperature and mixing ratio of hydrothermal fluid with seawater will minimize these costs (Amend et al., 2011). Further, the potential for ridge flank microbial processes by the example of a incubation study in ridge flank hydrothermal systems is discussed (Orcutt et al., 2011).

In addition it will be shown from the difference between predicted and observed concentrations of non-conservative species in diffuse fluids that energetically feasible catabolic pathways can be identified and that they provide insights into subseafloor microbial metabolism. This will be demonstrated by two examples from combined microbiological and thermodynamic studies of diffuse fluids from Mid-Atlantic Ridge 5°S and 9°S hydrothermal vent sites (Perner et al., 2009; Perner et al., 2011).

The published articles are:

Amend, J.P., McCollom, T.M., **Hentscher, M.**, Bach, W., 2011. Catabolic and anabolic energy for chemolithoautotrophs in deep-sea hydrothermal systems hosted in different rock types. Geochimica et Cosmochimica Acta 75, 5736-5748.

Orcutt, B.N., Bach, W., Becker, K., Fisher, A.T., **Hentscher, M.**, Toner, B.M., Wheat, C.G., Edwards, K.J., 2011. Colonization of subsurface microbial observatories deployed in young ocean crust. ISME Journal 5, 692-703.

Perner, M., Bach, W., **Hentscher, M.**, Koschinsky, A., Garbe-Schönberg, D., Streit, W.R., Strauss, H., 2009. Short-term microbial and physico-chemical variability in low-temperature hydrothermal fluids near 5°S on the Mid-Atlantic Ridge. Environmental Microbiology 11, 2526-2541.

Perner, M., **Hentscher, M.**, Rychlik, N., Seifert, R., Strauss, H., Bach, W., 2011. Driving forces behind the biotope structures in two low-temperature hydrothermal venting sites on the southern Mid-Atlantic Ridge. Environmental Microbiology Reports 3, 727-737.

In the course of my thesis work, I coauthored another publication, in which I conducted the geochemical modeling and helped with the data interpretation.

Klevenz, V., Bach, W., Schmidt, K., **Hentscher, M.**, Koschinsky, A., Petersen, S., 2011. Geochemistry of vent fluid particles formed during initial hydrothermal fluid-seawater mixing along the Mid-Atlantic Ridge. Geochemistry, Geophysics, Geosystems 12, Q0AE05.

Chapter 5 "Synthesis and outlook"

This chapter summarizes my thesis work and examines how thermodynamic calculation can improve the understanding of processes in hydrothermal systems. It is also discussed how this computational method can be refined and extended to cross between geology and biology in hydrothermal vent research.

1.6 References

Amend, J.P., Shock, E., 1998. Energetics of Amino Acid Synthesis in Hydrothermal Ecosystems. Science 281, 1659-1662.

Amend, J.P., McCollom, T.M., 2009. Energetics of Biomolecule Synthesis on Early Earth, Chemical Evolution II: From the Origins of Life to Modern Society. American Chemical Society, pp. 63-94.

Amend, J.P., McCollom, T.M., Hentscher, M., Bach, W., 2011. Catabolic and anabolic energy for chemolithoautotrophs in deep-sea hydrothermal systems hosted in different rock types. Geochimica et Cosmochimica Acta 75, 5736-5748.

Amend, J.P., Rogers, K.L., Shock, E.L., Gurrieri, S., Inguaggiato, S., 2003. Energetics of chemolithoautotrophy in the hydrothermal system of Vulcano Island, southern Italy. Geobiology 1, 37-58.

Bach, W., Edwards, K.J., 2003. Iron and sulfide oxidation within the basaltic ocean crust: implications for chemolithoautotrophic microbial biomass production. Geochimica et Cosmochimica Acta 67, 3871-3887.

Berndt, M.E., Allen, D.E., Seyfried, W.E., 1996. Reduction of CO_2 during serpentinization of olivine at 300°C and 500 bar. Geology 24, 351-354.

Bischoff, J.L., Rosenbauer, R.J., 1988. Liquid-vapor relations in the critical region of the system NaCl-H2O from 380 to 415°C: A refined determination of the critical point and two-phase boundary of seawater. Geochimica et Cosmochimica Acta 52, 2121-2126.

Bischoff, J.L., Seyfried, W.E., 1978. Hydrothermal chemistry of seawater from 25 degrees to 350 degrees C. American Journal of Science 278, 838-860.

Charlou, J.L., Donval, J.P., Fouquet, Y., Jean-Baptiste, P., Holm, N., 2002. Geochemistry of high H_2 and CH_4 vent fluids issuing from ultramafic rocks at the Rainbow hydrothermal field (36°14'N, MAR). Chemical Geology 191, 345-359.

Childress, J.J., Fisher, C.R., Favuzzi, J.A., Kochevar, R.E., Sanders, N.K., Alayse, A.M., 1991. Sulfide-Driven Autotrophic Balance in the Bacterial Symbiont-Containing Hydrothermal Vent Tubeworm, *Riftia pachyptila* Jones. Biological Bulletin 180, 135-153.

Cowen, J.P., Massoth, G.J., Baker, E.T., 1986. Bacterial scavenging of Mn and Fe in a mid- to far-field hydrothermal particle plume. Nature 322, 169-171.

de Angelis, M.A., Lilley, M.D., Baross, J.A., 1993. Methane oxidation in deep-sea hydrothermal plumes of the endeavour segment of the Juan de Fuca Ridge. Deep Sea Research Part I: Oceanographic Research Papers 40, 1169-1186.

Edwards, K.J., Bach, W., McCollom, T.M., 2005. Geomicrobiology in oceanography: microbe–mineral interactions at and below the seafloor. Trends in Microbiology 13, 449-456.

Elderfield, H., Schultz, A., 1996. Mid-ocean ridge hydrothermal fluxes and the chemical composition of the ocean. Annual Review of Earth and Planetary Sciences 24, 191-224.

Fisher, A.T., Wheat, C.G., 2010. Seamounts as conduits for massive fluid, heat, and solute fluxes on ridge flanks. Oceanography 23, 74-87.

Huber, J.A., Butterfield, D.A., Baross, J.A., 2003. Bacterial diversity in a subseafloor habitat following a deep-sea volcanic eruption. FEMS Microbiology Ecology 43, 393-409.

Janecky, D.R., Seyfried, W.E., 1983. The solubility of magnesium-hydroxide-sulfate-hydrate in seawater at elevated temperatures and pressures. American Journal of Science 283, 831-860.

Kashefi, K., Lovley, D.R., 2003. Extending the Upper Temperature Limit for Life. Science 301, 934.

Klein, F., Bach, W., Jöns, N., McCollom, T., Moskowitz, B., Berquó, T., 2009. Iron partitioning and hydrogen generation during serpentinization of abyssal peridotites from 15°N on the Mid-Atlantic Ridge. Geochimica et Cosmochimica Acta 73, 6868-6893.

Konn, C., Charlou, J.L., Donval, J.P., Holm, N.G., Dehairs, F., Bouillon, S., 2009. Hydrocarbons and oxidized organic compounds in hydrothermal fluids from Rainbow and Lost City ultramafic-hosted vents. Chemical Geology 258, 299-314.

Konn, C., Holm, N.G., Charlou, J.L., Donval, J.P., Dehairs, F., Bouillon, S., 2006. Biogenic or abiogenic organics in hydrothermal fluids from ultramafic-hosted vents of the Mid Atlantic Ridge: The first step to the origin of life? Geochimica et Cosmochimica Acta 70, 28-28.

Kormas, K.A., Tivey, M.K., Von Damm, K., Teske, A., 2006. Bacterial and archaeal phylotypes associated with distinct mineralogical layers of a white smoker spire from a deep-sea hydrothermal vent site (9°N, East Pacific Rise). Environmental Microbiology 8, 909-920.

Kusakabe, M., Komoda, Y., Takano, B., Abiko, T., 2000. Sulfur isotopic effects in the disproportionation reaction of sulfur dioxide in hydrothermal fluids: implications for the $\delta^{34}S$ variations of dissolved bisulfate and elemental sulfur from active crater lakes. Journal of Volcanology and Geothermal Research 97, 287-307.

Le Bris, N., Zbinden, M., Gaill, F., 2005. Processes controlling the physico-chemical micro-environments associated with Pompeii worms. Deep Sea Research Part I: Oceanographic Research Papers 52, 1071-1083.

Lilley, M.D., Butterfield, D.A., Olson, E.J., Lupton, J.E., Macko, S.A., McDuff, R.E., 1993. Anomalous CH_4 and NH_4^+ concentrations at an unsedimented mid-ocean-ridge hydrothermal system. Nature 364, 45-47.

McCollom, T.M., Amend, J.P., 2005. A thermodynamic assessment of energy requirements for biomass synthesis by chemolithoautotrophic micro-organisms in oxic and anoxic environments. Geobiology 3, 135-144.

McCollom, T.M., Bach, W., 2009. Thermodynamic constraints on hydrogen generation during serpentinization of ultramafic rocks. Geochimica et Cosmochimica Acta 73, 856-875.

McCollom, T.M., Shock, E.L., 1997. Geochemical constraints on chemolithoautotrophic metabolism by microorganisms in seafloor hydrothermal systems. Geochimica et Cosmochimica Acta 61, 4375-4391.

Mottl, M.J., Seewald, J.S., Wheat, C.G., Tivey, M.K., Michael, P.J., Proskurowski, G., McCollom, T.M., Reeves, E., Sharkey, J., You, C.F., Chan, L.H., Pichler, T., 2011. Chemistry of hot springs along the Eastern Lau Spreading Center. Geochimica et Cosmochimica Acta 75, 1013-1038.

Orcutt, B.N., Bach, W., Becker, K., Fisher, A.T., Hentscher, M., Toner, B.M., Wheat, C.G., Edwards, K.J., 2011. Colonization of subsurface microbial observatories deployed in young ocean crust. ISME Journal 5, 692-703.

Perner, M., Bach, W., Hentscher, M., Koschinsky, A., Garbe-Schönberg, D., Streit, W.R., Strauss, H., 2009. Short-term microbial and physico-chemical variability in low-temperature hydrothermal fluids near 5°S on the Mid-Atlantic Ridge. Environmental Microbiology 11, 2526-2541.

Perner, M., Hentscher, M., Rychlik, N., Seifert, R., Strauss, H., Bach, W., 2011. Driving forces behind the biotope structures in two low-temperature hydrothermal venting sites on the southern Mid-Atlantic Ridge. Environmental Microbiology Reports 3, 727-737.

Petersen, J.M., Zielinski, F.U., Pape, T., Seifert, R., Moraru, C., Amann, R., Hourdez, S., Girguis, P.R., Wankel, S.D., Barbe, V., Pelletier, E., Fink, D., Borowski, C., Bach, W., Dubilier, N., 2011. Hydrogen is an energy source for hydrothermal vent symbioses. Nature 476, 176-180.

Proskurowski, G., Lilley, M.D., Seewald, J.S., Früh-Green, G.L., Olson, E.J., Lupton, J.E., Sylva, S.P., Kelley, D.S., 2008. Abiogenic Hydrocarbon Production at Lost City Hydrothermal Field. Science 319, 604-607.

Reeves, E.P., Seewald, J.S., Saccocia, P., Bach, W., Craddock, P.R., Shanks, W.C., Sylva, S.P., Walsh, E., Pichler, T., Rosner, M., 2011. Geochemistry of hydrothermal fluids from the PACMANUS, Northeast Pual and Vienna Woods hydrothermal fields, Manus Basin, Papua New Guinea. Geochimica et Cosmochimica Acta 75, 1088-1123.

Rona, P.A., Trivett, D.A., 1992. Discrete and diffuse heat transfer Atashes vent field, Axial Volcano, Juan de Fuca Ridge. Earth and Planetary Science Letters 109, 57-71.

Schubert, M., Regler, J.W., Vogel, F., 2010. Continuous salt precipitation and separation from supercritical water. Part 1: Type 1 salts. The Journal of Supercritical Fluids 52, 99-112.

Schultz, A., Delaney, J.R., McDuff, R.E., 1992. On the Partitioning of Heat Flux Between Diffuse and Point Source Seafloor Venting. Journal of Geophysical Research 97, 12299-12314.

Seewald, J.S., Zolotov, M.Y., McCollom, T., 2006. Experimental investigation of single carbon compounds under hydrothermal conditions. Geochimica et Cosmochimica Acta 70, 446-460.

Shank, T.M., Fornari, D.J., Von Damm, K.L., Lilley, M.D., Haymon, R.M., Lutz, R.A., 1998. Temporal and spatial patterns of biological community development at nascent deep-sea hydrothermal vents (9°50'N, East Pacific Rise). Deep Sea Research Part II: Topical Studies in Oceanography 45, 465-515.

Sherwood Lollar, B., Lacrampe-Couloume, G., Slater, G.F., Ward, J., Moser, D.P., Gihring, T.M., Lin, L.H., Onstott, T.C., 2006. Unravelling abiogenic and biogenic sources of methane in the Earth's deep subsurface. Chemical Geology 226, 328-339.

Shock, E., Canovas, P., 2010. The potential for abiotic organic synthesis and biosynthesis at seafloor hydrothermal systems. Geofluids 10, 161-192.

Shock, E., Holland, M.E., 2004. Geochemical energy sources that support the subsurface biosphere, in: Wilcock, W.S.D., DeLong, E.F., Kelley, D.S., Baross, J.A., Cary, S.C. (Eds.), The Subseafloor Biosphere at Mid-Ocean Ridges. American Geophysical Union, Washington, DC, pp. 153-165.

Shock, E.L., 1990. Geochemical constraints on the origin of organic compounds in hydrothermal systems. Origins of Life and Evolution of Biospheres 20, 331-367.

Shock, E.L., Schulte, M.D., 1998. Organic synthesis during fluid mixing in hydrothermal systems. Journal of Geophysical Research 103, 28513-28528.

Sleep, N.H., 1991. Hydrothermal Circulation, Anhydrite Precipitation, and Thermal Structure at Ridge Axes. Journal of Geophysical Research 96, 2375-2387.

Stein, C.A., Stein, S., 1994. Constraints on hydrothermal heat flux through the oceanic lithosphere from global heat flow. Journal of Geophysical Research 99, 3081-3095.

Takai, K., Komatsu, T., Inagaki, F., Horikoshi, K., 2001. Distribution of Archaea in a Black Smoker Chimney Structure. Applied and Environmental Microbiology 67, 3618-3629.

Takai, K., Nakamura, K., 2010. Compositional, Physiological and Metabolic Variability in Microbial Communities Associated with Geochemically Diverse, Deep-Sea Hydrothermal Vent Fluids, in: Barton, L.L., Mandl, M., Loy, A. (Eds.). Springer Netherlands, pp. SP - 251-283.

Takai, K., Nunoura, T., Horikoshi, K., Shibuya, T., Nakamura, K., Suzuki, Y., Stott, M., Massoth, G.J., Christenson, B.W., deRonde, C.E.J., Butterfield, D.A., Ishibashi, J.-i., Lupton, J.E., Evans, L.J., 2009. Variability in Microbial Communities in Black Smoker Chimneys at the NW Caldera Vent Field, Brothers Volcano, Kermadec Arc. Geomicrobiology Journal 26, 552-569.

Tivey, M.K., 2004. Environmental conditions within active seafloor vent structures: sensitivity to vent fluid composition and fluid flow, in: Wilcock, W.S.D., DeLong, E.F., Kelley, D.S., Baross, J.A., Cary, S.C. (Eds.), The Subseafloor Biosphere at Mid-Ocean Ridges. American Geophysical Union, Washington, DC, pp. 137-152.

Tunnicliffe, V., Davies, K.T.A., Butterfield, D.A., Embley, R.W., Rose, J.M., Chadwick Jr, W.W., 2009. Survival of mussels in extremely acidic waters on a submarine volcano. Nature Geoscience 2, 344-348.

Von Damm, K.L., Edmond, J.M., Grant, B., Measures, C.I., Walden, B., Weiss, R.F., 1985. Chemistry of submarine hydrothermal solutions at 21 °N, East Pacific Rise. Geochimica et Cosmochimica Acta 49, 2197-2220.

Von Damm, K.L., Lilley, M.D., 2004. Diffuse Flow Hydrothermal Fluids from 9 50'N East Pacific Rise: Origin, Evolution and Biogeochemical Controls, in: Wilcock, W.S.D., DeLong, E.F., Kelley, D.S., Baross, J.A., Cary, S.C. (Eds.), The Subseafloor Biosphere at Mid-Ocean Ridges. American Geophysical Union Washington, DC, pp. 245-268

Von Damm, K.L., Lilley, M.D., Shanks III, W.C., Brockington, M., Bray, A.M., O'Grady, K.M., Olson, E., Graham, A., Proskurowski, G., 2003. Extraordinary phase separation and segregation in vent fluids from the southern East Pacific Rise. Earth and Planetary Science Letters 206, 365-378.

Welhan, J., Lupton, J., 1987. Light hydrocarbon gases in Guaymas Basin hydrothermal fluids: thermogenic versus abiogenic origin. AAPG Bulletin 71, 215-223.

2. Geochemically induced shifts in catabolic energy yields explain past ecological changes of diffuse vents in the East Pacific Rise 9°50'N area

Michael Hentscher[1§], Wolfgang Bach [1]

[1] *Department of Geoscience, University of Bremen, Klagenfurter Straße, 28359 Bremen, Germany*

[§]*Corresponding author: hentscher@uni-bremen.de*

wbach@uni-bremen.de

2.1 Abstract

The East Pacific Rise (EPR) at 9°50'N hosts a hydrothermal vent field (Bio9) where the change in fluid chemistry is believed to have caused the demise of a tubeworm colony. We test this hypothesis and expand on it by providing a thermodynamic perspective in calculating free energies for a range of catabolic reactions from published compositional data. The energy calculations show that there was excess hydrogen sulfide (H_2S) in the fluids and that oxygen (O_2) was the limiting reactant from 1991 to 1997. Energy levels are generally high, although they declined in that time span. In 1997, sulfide availability decreased substantially and H_2S was the limiting reactant. Energy availability dropped by a factor of 10 to 20 from what it had been between 1991 and 1995. The perishing of the tubeworm colonies began in 1995 and coincided with the timing of energy decrease for sulfide oxidizers. In the same time interval, energy availability for iron oxidizers increased by a factor of 6 to 8, and, in 1997, there was 25 times more energy per transferred electron in iron oxidation than in sulfide oxidation. This change coincides with a massive spread of red staining (putative colonization by Fe-oxidizing bacteria) between 1995 and 1997.

For a different cluster of vents from the EPR 9°50'N area (Tube Worm Pillar), thermodynamic modeling is used to examine changes in subseafloor catabolic metabolism between 1992 and 2000. These reactions are deduced from deviations in diffuse fluid compositions from conservative behavior of redox-sensitive species. We show that hydrogen is significantly reduced relative to values expected from conservative mixing. While H_2 concentrations of the hydrothermal endmember fluids were constant between 1992 and 1995, the affinities for hydrogenotrophic reactions in the diffuse fluids decreased by a factor of 15 and then remained constant between 1995 and 2000. Previously, these fluids have been shown to support subseafloor methanogenesis. Our calculation results corroborate these findings and indicate that the 1992-1995 period was one of active growth of hydrogenotrophic communities, while the system was more or less at steady state between 1995 and 2000.

2.2 Introduction

Microorganisms have the ability to gain energy for their metabolism by promoting a large range of redox reactions. Well-known energy sources are for example aerobic oxidation of methane (CH_4) or hydrogen sulfide (H_2S), methanogenesis, fermentation, and sulfate reduction under anaerobic conditions (Jannasch, 1995). In habitats like hydrothermal systems or mines, lacking sunlight and organic carbon sources, the primary production depends on electron donors that are released by water-rock reactions. High-temperature (>400°C) processes of water-rock interaction determine the composition of seawater-derived hydrothermal fluids that are equilibrated with rocks at depths as much as several kilometers (Figure 2-1). Upon upwelling, these fluids cool (conductively and/or adiabatically) and mix with cold seawater to varying extents. High temperature fluids, venting focused via black smoker chimneys, often show little evidence for subseafloor mixing and are typically used as "hydrothermal endmember" compositions. Commonly, sites of diffuse venting are developed around the black smokers, and the temperature-composition relations of the fluids issuing through the seafloor there indicate that the diffuse fluids formed by subseafloor cooling and mixing of hot hydrothermal fluids with cold seawater. The seafloor underneath these diffuse vent sites is a particularly favorable environment for a variety of chemosynthetic microorganisms in terms of suitable temperature and large energy availability (Figure 2-1). The composition of the upwelling hydrothermal fluids in these diffuse vent sites imposes a major control on the metabolic diversity in the colonizing ecosystem. Because of this tight relation between vent ecosystem and fluid compositions, chemical changes in the fluid may directly influence the ecosystem.

Thermodynamic calculations based on geochemical compositions of waters in these habitats provide insights into the energy availability and can determine possible reactions that can support primary production in these systems (McCollom and Shock, 1997; Shock and Holland, 2004; Houghton and Seyfried Jr, 2010; Amend et al., 2011). Tight relations between the availability of geochemical energy and microbial processes have been demonstrated for a variety of submarine hydrothermal environments, including chimney walls, diffuse fluids, and vent mussels (Huber et al., 2003; Kormas et al., 2006; Reysenbach et al., 2006; Perner et al., 2009; Petersen et al., 2011).

In this study we use geochemical data from two hydrothermally active vents in the East Pacific Rise 9°50'N area to show that thermodynamic modeling can help interpret the microbial metabolism in such systems. For the first area, our calculations provide clues to the biological evolution of a vent site influenced by dynamic changes in fluid chemistry and, consequently, catabolic energy. The other case shows that microbial processes in the subseafloor may be deciphered by determining and comparing free energies of reactions for catabolic reactions of hypothetical fluids derived from conservative mixing of seawater and hydrothermal fluid with the diffuse fluid actually sampled.

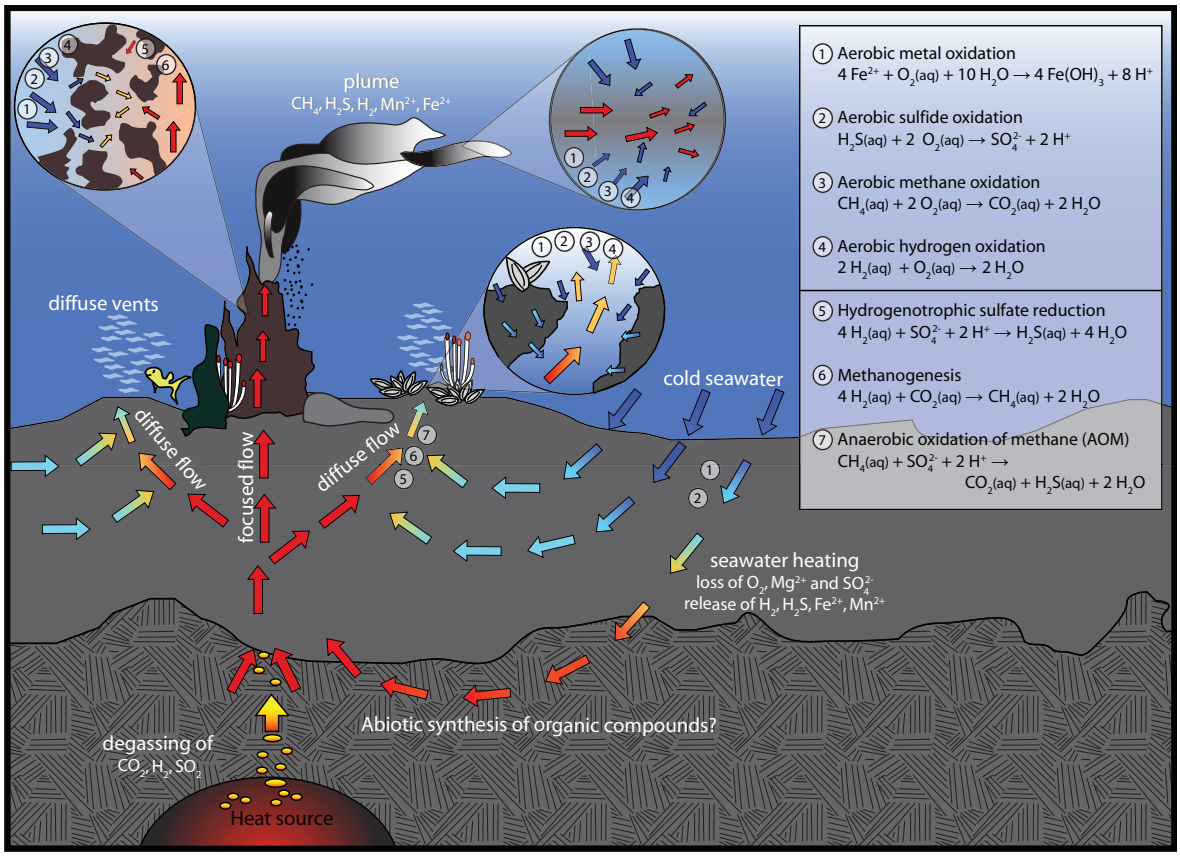

Figure 2-1: Sketch of idealized fluid flow within a hydrothermal system and potential catabolic reactions in different environments (chimney wall, plume, recharge zone, and subseafloor mixing zone).
Upwelling hot, reducing hydrothermal fluids mix with entrained cold, oxygenated seawater in subseafloor mixing zones. For these zones, the affinities of the catabolic reactions provided in the inset are examined in this chapter

2.3 Methods

2.3.1 Calculation of affinity

Free energy for catabolic reactions is available only if the system is out of geochemical equilibrium. Disequilibrium prevails when the properties of the system change at rates faster than the rates at which the thermodynamically favored reactions proceed. The abiotic rates of many redox reactions are sluggish, in particular at temperatures conducive of life (<120°C) (Houghton and Seyfried Jr, 2010). Microbes use enzymes to catalyze these redox reactions and harness the free energy by controlling electron transfers and converting a sizable fraction of the catabolic energy in ATP production for their anabolic metabolism (Amend and Shock, 2001). The maximum quantity of free energy that microorganisms can catabolize (Δ_rG) is given by the Gibbs energy at a reference state [$\Delta_rG^o = -RT\ln(K_r)$] representing the intensive parameters (P, T) and an extensive term [$RT\ln(Q_r)$] that captures the compositions of the vent solutions

$$\Delta_r G = -RT\ln\left(K_r\right) + RT\ln\left(Q_r\right) \qquad \text{(eq. 1)}$$

where R is the universal gas constant and T the temperature in Kelvin. K_r is the calculated equilibrium for the temperature and pressure of interest, and Q_r expresses the activities of species participating a specific reaction. Q_r is evaluated through equation (2):

$$Q_r = \prod_i a_i^{v_{ir}} \qquad \text{(eq. 2)}$$

where a_i represents the activity of the chemical species in the reaction, v_{ir} denotes the stoichiometric coefficient for the ith chemical species in the reaction, which is positive for products and negative for reactants. If $\Delta_r G$ for a reaction is negative, then the reaction should proceed from left to right; if it is greater than zero, the reaction will proceed in the opposite direction. By convention a negative sign indicates that the reaction should take place spontaneously and energy can be gained by microbes catalyzing this reaction.

Commonly, affinity is used instead of $\Delta_r G$ for a reaction (Helgeson, 1979). Affinities express the change of the Gibbs energy with reaction progress (ξ).

$$A_r = -\left(\frac{\partial \Delta_r G}{\partial \xi}\right) \qquad \text{(eq. 3)}$$

It follows that the reaction is favorable if the affinity is positive. Combining equations 1 and 3, the affinity can be evaluated through

$$A_r = RT \ln\left(\frac{K_r}{Q_r}\right) \qquad \text{(eq. 4)}$$

This relation demonstrates that, if $K_r > Q_r$, then $A_r > 0$ and the reaction may proceed while free energy is released (Helgeson, 1979).

Two types of computations were employed in this study: (1) calculation of concentrations and activities of dissolved species in diffuse fluids, and (2) calculation of affinities of potential catabolic reactions in these fluids. These calculations were conducted for actual diffuse fluids sampled and analyzed by Von Damm and Lilley (2004) and for hypothetical mixtures of endmember vent fluids (Von Damm, 2004) and ambient seawater. It is assumed here that the diffuse fluids form by subseafloor mixing of ascending hydrothermal fluids with seawater. The endmember hydrothermal fluid composition is taken from black smoker vent fluids issuing within a few meters of the diffuse vent site (Von Damm, 2004; Von Damm and Lilley, 2004). The percentage of hydrothermal fluid is estimated using a simple mass balance for silica:

$$\text{Hydrothermal Fluid\%} = 100 \cdot \frac{C_{SiO_2(aq)}\text{diffuse fluid} - C_{SiO_2(aq)},\text{sw}}{C_{SiO_2(aq)}\text{hydrothermal fluid} - C_{SiO_2(aq)},\text{sw}} \quad \text{(eq. 5)}$$

Silica is known to precipitate slowly at low temperatures from mildly acidic fluids (Carroll et al., 1998) and can be assumed to behave conservatively at the time scales of fluid mixing (Edmond et al., 1979).

Geochemist Workbench® (GWB) was used to conduct the thermodynamic calculations (Bethke, 1996). A Log K_r database was created, covering temperatures from 0 to 350°C at a pressure of 25 MPa, using SUPCRT92 (Johnson et al., 1992) and the thermodynamic database OBIGT (Dick, 2008), and including all speciation reactions in an aqueous system with Na, Ca, Mg, Fe, Sr, K, SiO_2, Cl, sulfate, sulfide, oxygen, hydrogen and carbon dioxide. Likewise, equilibrium constants for the following catabolic reactions were calculated.

Aerobic sulfide oxidation
$$H_2S(aq) + 2\ O_2(aq) \rightarrow SO_4^{2-} + 2\ H^+ \quad (1)$$

Aerobic methane oxidation
$$CH_4(aq) + 2\ O_2(aq) \rightarrow CO_2(aq) + 2\ H_2O \quad (2)$$

Aerobic iron oxidation
$$Fe^{2+} + ¼\ O_2(aq) + 2.5\ H_2O \rightarrow Fe(OH)_3 + 2\ H^+ \quad (3)$$

Aerobic hydrogen oxidation
$$2\ H_2(aq) + O_2(aq) \rightarrow 2\ H_2O \quad (4)$$

Hydrogenotrophic sulfate reduction
$$4\ H_2(aq) + SO_4^{2-} + 2\ H^+ \rightarrow H_2S(aq) + 4\ H_2O \quad (5)$$

Hydrogenotrophic methanogenesis
$$4\ H_2(aq) + CO_2(aq) \rightarrow CH_4(aq) + 2\ H_2O \quad (6)$$

Anaerobic oxidation of methane
$$CH_4(aq) + SO_4^{2-} + 2\ H^+ \rightarrow H_2S(aq) + CO_2(aq) + 2\ H_2O \quad (5)$$

Published compositions of endmember vent fluids (Von Damm, 2004; Von Damm and Lilley, 2004) issuing from black smoker chimneys in proximity (few meters) to the diffuse vent site were used in the calculations of affinities for these reactions (Table 2-1). In determining Q_r (eq. 2), the extended Debye–Hückel equation was used to calculate activity coefficients with extended parameters and hard core diameters for each species from Wolery and Jove-Colon (2004). Dissolved neutral species were assigned an activity coefficient of one,

except non–polar species for which CO_2 activity coefficients were used (Drummond, 1981). Reported pH values of hydrothermal vents (measured at 25°C) were used in determining the in situ pH (Table 2-1) by re-speciating the fluids at the temperatures of venting (Tivey et al., 1995). The percentage of hydrothermal endmember fluid in the diffuse fluids derived from the silica mass balance was used to calculate idealized mixed fluids, assuming conservative behavior of all elements. These hypothetical fluids were also speciated and compared with actual compositions of diffuse fluids in terms of concentrations and affinities (Table 2-1 and Table 2-2). Deviations from conservative behavior in the diffuse fluids indicate that removal or release processes take place in the subseafloor mixing zones in which the diffuse fluids are formed. In the calculations, the activities of species in the hypothetical diffuse fluids (ideal conservative mixing) were determined in a batch mixing model simulating titration of hot hydrothermal endmember fluid into cold seawater and tracking the chemical speciation changes in the mixed fluid. In these calculations, redox reactions were suppressed, while kinetically fast reactions like protonation of bases, dissociation of acids, and complex formation are allowed to take place spontaneously. Redox reactions were suppressed, because these reactions are not expected to proceed at the low temperatures of the diffuse fluids and on the short time scales of the mixing process (Foustoukos et al., 2011). This procedure has the advantage that disequilibria formed during mixing can be determined and the affinities of selected redox reactions may be calculated. GWB also allows suppressing the Knallgas reaction, so elevated concentrations of both O_2 and H_2 in the mixed fluids could be accounted for (Perner et al., 2009).

The precipitation of minerals was also suppressed. The thermodynamically stable Fe-minerals in the diffuse fluids are hematite and pyrite. If these phases were allowed to precipitate, Fe concentrations would drop to extremely low values in the hypothetical mixed fluids. The measured diffuse fluids have Fe concentrations that are many orders of magnitude higher than values corresponding to pyrite and hematite solubility. They are hence strongly oversaturated with respect to pyrite and hematite and indicate that precipitation of these minerals was largely inhibited. The concentrations of Fe and H_2S calculated for the hypothetical mixed fluids represent maximum values.

The affinities calculated (Table 2-2) represent the maximum energy content for the different catabolic reactions, disregarding the fact that limiting electron donors and acceptors, which appear in several reactions, can still only be used once within the ecosystem (McCollom, 2007). Moreover, comparisons of the raw affinities do not reflect differences in the numbers of electrons transferred in these reactions. This is problematic, because a given quantity of proton motive force driving chemiosmosis is generated by a set number of electrons transferred. The fact that the reactions considered have between one and eight electron transferred therefore skews a comparison of the affinities of different reactions. We hence report the affinities in values per electron transferred (Table 2-2). Furthermore, the energy flux into the system is controlled by the concentration of the limiting reactant in the upwelling fluid. To examine these combined effects on energy availability, we normalized affinity to kg vent fluid by multiplying the energy with the concentration of the limited reactant, and divided by the fraction of endmember vent fluid in the mix (McCollom, 2007). These normalized affinities provide us with a meaningful parameter for assessing the fluxes

Table 2-1: Compositions of discrete and diffuse vent fluids

		Temperature (°C)	pH (25°C) (1)	in situ pH	Mg^{2+} mM	Na^{+} mM (1)	Cl^{+} mM	SiO_2 (aq) mM	H_2 (aq) µM	H_2S (aq) mM	Fe^{2+} µM	CH_4 (aq) µM	CO_2 (aq) mM	O_2 (aq) µM (5)	SO_4^{2-} mM (1, 6)	% hydrothermal fluid (4)
	Seawater	1.8	7.8	8.1	52.2	464	540	0.16	0	0	0	0	2.3	100	28.2	0
Northern Area																
Apr 91	hot endmember	368	2.6	3.2	0	139	154	9.9	3030	23.2	2190	172	44.8	-	0	100
	diffuse, measured	22	-	-	49.7	-	530	0.88	0.36	0.9	151	0.07	5.9	-	-	7.39
	diffuse, calculated	22	5.7	5.7	48.3	440	511	0.88	225	1.72	162	12.8	5.46	92.6	26.1	7.39
December 1993	hot endmember	365	3.6	5.7	0	188	212	11.3	700	7.3	1060	1000	204	-	0.18	100
	diffuse, measured	30.9	-	-	49.6	-	522	0.57	0.33	0.28	24.2	5.8	9.57	-	-	3.68
	diffuse, calculated	30.9	5.5	5.5	50.3	454	528	0.57	25.9	0.27	39.3	37.1	9.77	96.3	27.2	3.68
March 1994	hot endmember	363	3.5	5.1	0	222	249	12.6	680	8.5	1430	112	187	-	0.04	100
	diffuse, measured	29.9	-	-	50.4	-	525	0.79	1.9	0.27	25	6.58	9.57	-	-	5.06
	diffuse, calculated	29.9	5.4	5.4	49.6	452	525	0.79	34.5	431	72.5	5.68	11.7	94.9	26.8	5.06
October 1994	hot endmember	364	3.2	4.8	0	279	325	14.1	530	6.2	2730	86	146	-	1.55	100
	diffuse, measured	32.3	-	-	48.1	-	524	0.92	6.79	0.11	69.9	4.83	8.54	-	-	5.45
	diffuse, calculated	32.3	5.5	5.4	49.3	454	528	0.92	29.2	0.34	150	4.74	10.2	94.5	26.7	5.45
November 95	hot endmember	366	3	3.9	0	391	466	14.8	360	6.7	6030	84	139	-	0	100
	diffuse, measured	33.3	-	-	46.3	-	550	1.14	2.5	0.19	277	5.37	9.01	-	-	6.69
	diffuse, calculated	33.3	5.4	5.3	48.7	459	535	1.14	24.2	0.45	406	5.65	11.5	93.3	26.3	6.69
November 97	hot endmember	373	3.1	4.1	0	342	400	13.4	330	8.6	6640	95	117	-	0	100
	diffuse, measured	27.2	-	-	50.5	-	534	0.72	0.75	0	170	2.52	4.7	-	-	4.23
	diffuse, calculated	27.2	5.7	5.7	50	459	534	0.72	14.1	0.37	284	4.07	7.21	95.7	27	4.23

Table 2-1 continued: Compositions of discrete and diffuse vent fluids

		Temperature (°C)	pH (25°C) (1)	in situ pH	Mg^{2+} mM	Na^{+} mM (1)	Cl^{+} mM	SiO_2 (aq) mM	H_2(aq) µM	H_2S (aq) mM	Fe^{2+} µM	CH_4 (aq) µM	CO_2 (aq) mM	O_2 (aq) µM (5)	SO_4^{2-} mM (1, 6)	% hydrothermal fluid (4)
Southern Area																
April 91	diffuse, measured	55	-	-	46.7	-	504	1.95	2.17	8.46	2.4	505	10.1	-	-	-
February-March	hot endmember	160	3 (2)	3.7	0	126 (3)	136	12.7	6460	20.7	4080	213	31	-	-	100
1992	diffuse, measured	23.3	-	-	48.2	-	529	0.69	14.9	0.66	2	94	4.57	-	-	4.28
	diffuse, calculated	23.3	6.2	6.2	50	479	523	0.69	277	0.89	175	9.12	3.53	95.7	27	4.28
December 1993	diffuse, measured	15.4	-	-	50.5	-	532	0.23	0.13	0	9.2	2.87	2.7	-	-	-
March 1994	hot endmember	20.5	-	-	0	-	269	5.57	8910	11.2	200	748	118	-	-	100
October 1994	hot endmember	351	3 (2)	3.8	0	229 (3)	235	12.5	8390	14.3	1590	116	104	-	-	100
	diffuse, measured	20.4	-	-	49.7	-	526	0.66	6.75	0.21	11.5	15.6	4.96	-	-	4.05
	diffuse, calculated	204	-	5.8	50.1	484	528	0.66	343	0.58	65	4.74	6.46	95.9	27	4.05
November 95	hot endmember	341	3 (2)	3.7	0	297 (3)	301	13.8	4930	14	1550	106	95.7	-	-	100
	diffuse, measured	24.7	-	-	50.3	-	531	0.85	0.75	0.53	9.9	15.9	5.8	-	-	5.06
	diffuse, calculated	24.7	5.7	5.7	49.5	484	528	0.85	250	0.71	78.7	5.38	7.04	94.9	26.8	5.06
November 97	hot endmember	307	3 (2)	3.4	0	326 (3)	330	16.1	3550	11.3	742	121	81.9	-	-	100
	diffuse, measured	18.2	-	-	51.5	-	530	0.57	0.67	0.24	27	4.09	3.84	-	-	2.57
	diffuse, calculated	18.2	6	6.1	50.9	490	535	0.57	91.3	0.29	19.1	3.11	4.35	97.4	27.5	2.57
April 00	hot endmember	279	3 (2)	3.3	0	355 (3)	359	16.8	2700	11.2	517	108	77	-	-	100
	diffuse, measured	11.9	-	-	50.4	-	529	0.23	0.15	0.06	23	0.47	2.57	-	-	0.42
	diffuse, calculated	11.9	7	6.9	52	494	539	0.23	12.5	0.05	2.39	0.5	2.65	99.5	28.1	0.42

Fluid data for high temperature fluids and measured diffuse fluids are from Von Damm and Lilley (2004)
Northern Area: Hot vent fluids are from Bio9 and Bio9' and the associated diffuse fluids from BM9Rifia, BM91o and BM12
Southern Area: High temperature fluids are from Tube Worm Pillar (TWP) and the diffuse fluids from Y vent at the base of TWP
(1) pH, sodium and sulfate concentrations of vent fluids are from Von Damm (2004), unless otherwise indicated
(2) pH was not measured but is approximated by comparison with similar vent fluids from Von Damm (2004)
(3) Na^{+} calculated by charge balance
(4) Calculated assuming conservative behavior of SiO_2(aq)

of energy for different catabolic reactions into a system. While affinities expressed in both notations are reported in Table 2-2, the following discussion will primarily use normalized affinity, i.e., energy flux.

Table 2-2: Affinities for different catabolic reactions in kJ and normalized affinities in J per e^- and Kg Vent-fluid at the Southern Area (TWP)

Southern Area	5 Hydrogenotrophic sulfate reduction		6 Hydrogenotrophic methanogenesis		7 Anaerobe oxidation of methane	
	Measured	Predicted	Measured	Predicted	Measured	Predicted
	kJ		kJ		kJ	
February-March 1992	128.6	156.7	94.1	128.0	34.5	28.7
October 1994	129.3	165.1	93.4	135.3	35.9	29.8
November 1995	104.3	161.2	70.1	130.8	34.2	30.4
November 1997	103.9	151.1	73.8	122.5	30.1	28.7
April 2000	88.4	130.4	63.9	105.7	24.7	24.5
	J per e^- and kg vent fluid		J per e^- and kg vent fluid		J per e^- and kg vent fluid	
February-March 1992	1.34	30.28	0.98	24.73	9.07	0.73
October 1994	0.64	41.50	0.46	34.01	1.64	0.41
November 1995	0.05	23.57	0.03	19.13	1.27	0.38
November 1997	0.08	16.34	0.06	13.24	0.58	0.42
April 2000	0.09	10.95	0.06	8.88	0.31	0.33

2.4 Results and Discussion

2.4.1 Case studies

The sample locations are situated in the axial summit caldera of the fast spreading (11 cm/yr full rate) ridge EPR at 9°50'N at a water depth of 2500 meters. In both case studies we use data from time series studies conducted in the 1990s. Venting temperatures are ≤55°C, and fluids issue from cracks in the seafloor or from lava pillars that are fissured near the base. Compositions of vent fluids from the two sites are reported in Von Damm and Lilley (2004) and Von Damm (2004). These publications also present a detailed description of the geological setting and vent field characteristics, so we here highlight only the key features of these localities.

The northern area is characterized by the high temperature vents Bio9 and Bio9' and the associated diffuse flow sites BM9Riftia (BM9R), BM91o and BM12. The data set for this system (hereinafter referred to as Bio9 area) is the most detailed, because the site was the target of long-term measurements of fluid composition and temperature (Fornari et al., 1998) and seismic activity (Sohn et al., 1998). Sohn et al. (1998) documented a seismic swarm in 1995 in this area, followed by a temperature increase in the Bio9 vent with a delay of a few days (Fornari et al., 1998). Temperatures of the diffuse fluid samples range between 22.0 and 33.3°C (Table 2-1).

The southern area (Tube Worm Pillar, TWP) features high temperature venting through an 11-m high sulfide structure on top of a lava pillar. Discrete venting of 351°C fluid is restricted to the top of the chimney, while leakage of diffuse fluids is observed from around the base of the chimney. Eponymous for the site name, a large tubeworm colony inhabits the area of diffuse venting. The associated diffuse fluid samples were retrieved from Y vent, an adjacent broken-off lava pillar that issued fluids of temperatures between 20 and 25°C in 1992-1995, dropping to 18°C in 1997 and finally to 12°C in 2000.

Case study 1 – Bio9 area

Shank et al. (1998) studied the change in the vent community during the time period from 1991 to 1995 at the vents in the Bio9 area. These authors report of a magmatic event in 1991, followed by venting of fluids high in H_2S. These conditions boosted the establishment of a strong population of the tubeworm *Riftia*. During the following cruises in 1994, Shank et al. (1998) observed the development of rusty spots that appeared within the *Riftia* colonies. In 1995, the rusty spots had spread and covered large areas of the *Riftia* population. In 1997, the *Riftia* population had broken down largely, while the rust had extended to cover much of the *Riftia* patch (Von Damm and Lilley, 2004).

The temporal evolution of the fluid compositions in that time span reveals a decrease in hydrogen sulfide concentrations over the entire period after 1992 with a slight increase in November of 1995 (Figure 2-2). Before March of 1994, soluble iron follows the H_2S concentration; afterwards the iron content increased and reached maximum concentrations during November of 1995. In November of 1997, the Fe concentration had dropped slightly, but was still much higher than during the beginning of the time series.

It has been suggested that the biological development of this area depends on the bioavailability of iron and H_2S (Von Damm and Lilley, 2004). This interpretation is plausible, because Riftia live in symbiosis with sulfide oxidizing bacteria (Cavanaugh, 1983) and depend on the energy associated with sulfide oxidation. Also, Fe-oxidizing bacteria oxidize Fe^{2+} in the fluids to ferric hydroxide (Toner et al., 2009). So the "rust" in the study area is an indicator that these microorganisms are thriving.

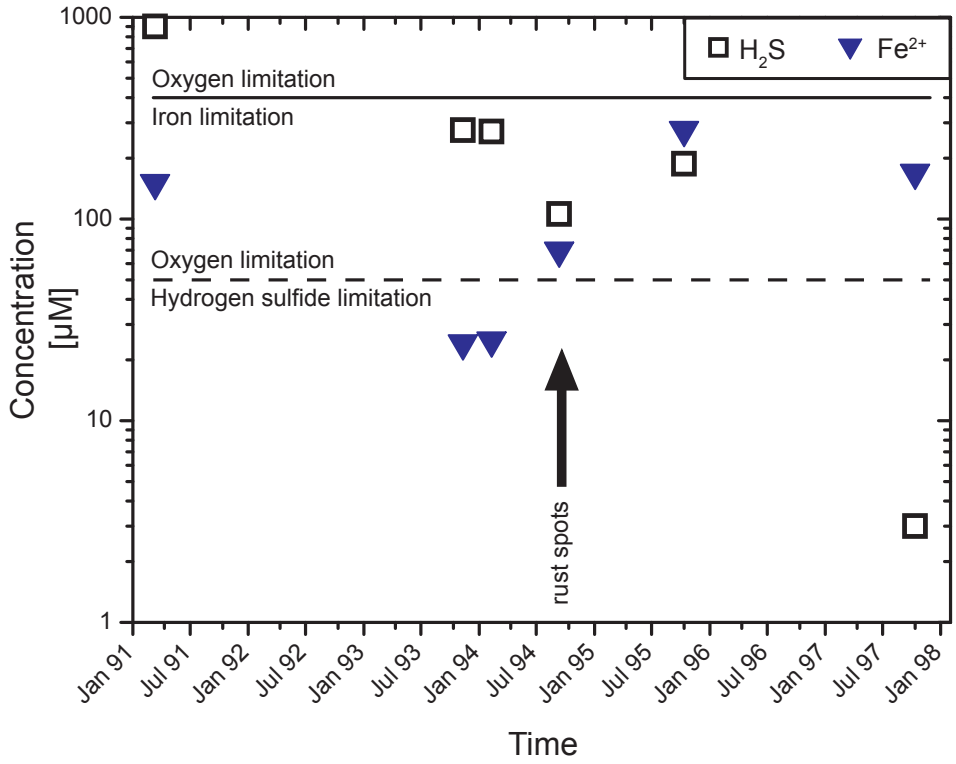

Figure 2-2: Temporal changes in concentrations of dissolved iron and hydrogen sulfide in diffuse fluids from the Bio9 area.
The increase in iron coincides with the appearance of rusty spots in the tubeworm colony (black arrow). The two horizontal lines represent the maximum concentrations of sulfide (dashed) and iron (continuous) that can be oxidized by seawater with an oxygen concentration of 100 µM. Iron is the limiting reactant over the whole time period, in contrast to sulfide, which is oxygen limited, except for the conditions in November 97.

We determined the affinities for both catabolic pathways for the time period of critical geochemical and ecological changes (1991-1997) to improve the understanding of the biological evolution of the vent ecosystems. The calculations make use of the measured concentrations of iron, H_2S and O_2. Unfortunately concentrations of O_2 and the pH for diffuse fluids are not available; therefore, these values are estimated from conservative mixing. Calculated pH values for the fluids show a narrow range of 5.3 to 5.7; likewise, small variations are predicted for O_2 concentrations (92 - 96 µM). Both pH and O_2 concentrations reflect the large fraction of seawater calculated from the silica mass balance. Depending on the mixing ratio of vent fluid and seawater, either one of the electron donors (Fe^{2+}, H_2S) or oxygen is the limiting reactant determining the amount of energy available per unit vent fluid based (Figure 2-2). Figure 2-2 shows the upper limit for iron and H_2S oxidation based on an O_2 concentration of the East Pacific bottom seawater of circa 100 µM O_2 (Betts and Holland, 1991). For

H_2S oxidation, O_2 is the limiting reactant, while Fe-oxidation is limited by the availability of iron. An exception is the fluid sampled last in the time series; it exhibits exceptionally low sulfide concentrations and H_2S is the compound limiting energy availability.

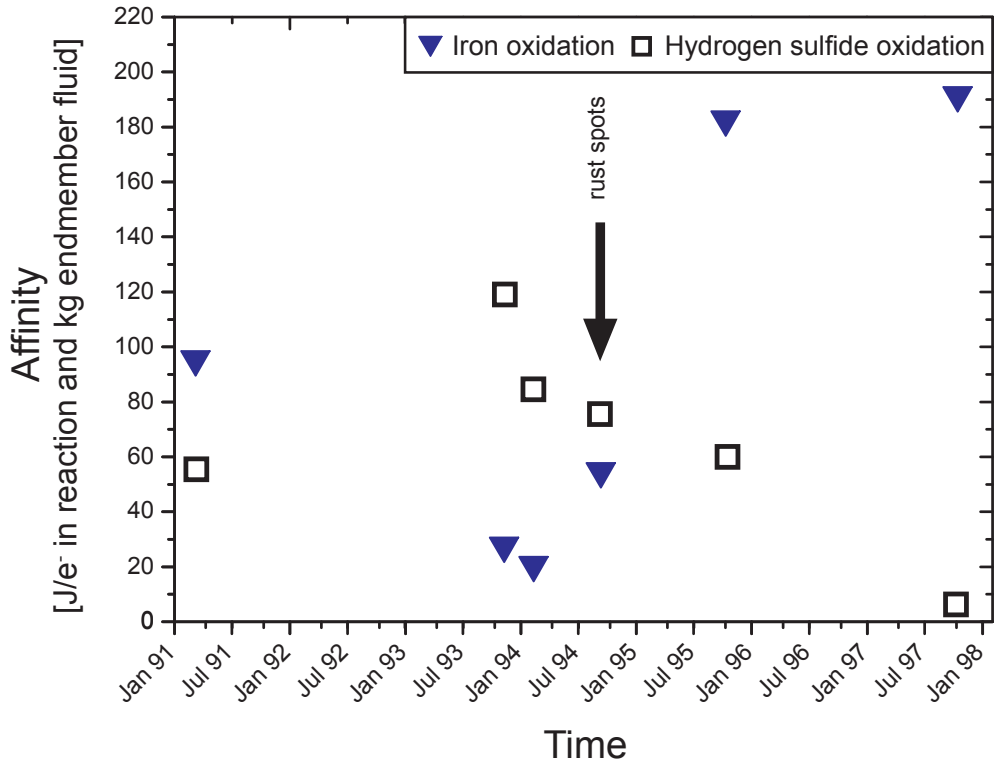

Figure 2-3: Normalized affinities for the oxidation of Fe^{2+} and H_2S in diffuse fluids from the Bio9 area during the period from April 1991 until November 1997. The generally high affinities for iron and hydrogen sulfide oxidation support life catabolizing these reactions. In October of 1994, affinities for both reactions are high, so that tubeworms (H_2S-oxidizers) and iron oxidizing microorganism (rusty staining) can grow simultaneously. The demise of the *Riftia* population in November of 1997 coincides with a sudden drop in the affinity of H_2S oxidation.

Figure 2-3 illustrates the normalized affinities for both reactions. It shows the consequence of limitation; sulfide oxidation has the highest affinity when the fraction of vent fluid in the mixture is lowest (Table 2-1), because then O_2 contents are greatest. In contrast, the normalized affinities for iron oxidation more closely mirror the iron concentration in the fluid. But affinities are also dependent on the vent fluid fraction, as increased pH favors ferric hydroxide precipitation from the mixed fluids.

The dynamic changes in the normalized affinities of sulfide and iron oxidation (Figure 2-3 and Table 2-3) can fully explain the ecological changes within the system. The incipient occurrence of rusty staining in November of 1994 correlates with an increased normalized affinity of iron oxidation, while the normalized affinity for sulfide oxidation remains at the same level. In November of 1995 a further increase in iron concentration in the fluid explains the continued spreading of the iron oxide staining. Tied to this change, the normalized affinity for Fe-oxidation almost quadrupled. The normalized affinity for hydrogen sulfide oxidation was only slightly decreased relative to 1994, which explains why the tubeworm colonies

Table 2-3: Normalized affinities for Aerobic sulfide oxidation and iron oxidation in J per e^- and kg Vent-fluid at the Northern Area (Bio9)

Northern Area	1 Aerobic sulfide oxidation	3 Aerobic iron oxidation
	Measured	Measured
April 1991	55.51	94.20
December 1993	27.31	119.13
March 1994	84.52	19.76
October 1994	75.59	53.79
November 1995	59.99	181.72
November 1997	6.319	190.04

were still thriving, despite the increased development of rusty staining. Apparently, both metabolic pathways were favorable and were being exploited at that stage of system evolution. After 1995, the normalized affinity for hydrogen sulfide oxidation dropped as a consequence of the strongly decreased sulfide concentration in the fluid. Because of this drop in the affinity of sulfide oxidation, the tubeworm population, relying on favorable energetics for H_2S oxidation, collapsed. Unlike sulfide oxidation, the normalized affinity for iron oxidation remains high, so organisms with the ability to gain energy from iron oxidation can still thrive. Since both reactions depend on oxygen, the reactions are in competition for that electron acceptor and the calculated affinities (Figure 2-3) are the predicted maxima.

The thermodynamic calculations presented here validate the interpretation by Von Damm and Lilley (2004) and confirm that the ecological changes are driven by changes in fluid composition.

Case study 2 – Tube Worm Pillar (TWP)

The fluid compositions of the diffuse fluids issuing in TWP area have been proposed to reveal insights in the redox reactions in the subseafloor (Von Damm and Lilley, 2004; Proskurowski et al., 2008). Increased methane concentrations in the diffuse fluids led Von Damm and Lilley (2004) to propose that hydrogenotrophic methanogenesis takes place in the subseafloor. Proskurowski et al. (2008) could confirm this interpretation through carbon stable isotope measurements of CH_4 and CO_2 demonstrating that the carbon isotope ratios are consistent with active microbial carbon cycling in this area.

The compositional changes of diffuse fluid compositions relative to the concentrations predicted from conservative mixing are depicted in Figure 2-4. Throughout the time series, H_2 concentrations are decreased by 1.5 to 2 orders of magnitude relative to the concentrations expected from conservative mixing (cf. Table 2-1). Methane, in contrast, is enriched by a factor of ten relative to the value predicted from conservative mixing in February-March of 1992. In October 1994 and November 1995 this enrichment is about 3-fold. By 2000, mea-

sured CH_4 corresponds to those predicted from conservative mixing, and no CH_4 excess can be observed (Figure 2-4). The methane excess in 1992-1995 is consistent with the decrease in hydrogen, and ratios of H_2 depletion to CH_4 excess between 3 and 6 are consistent with the stoichiometry of the hydrogenotrophic methanogenesis reaction, from which that ratio would be predicted to be 4. In 1997 and 2000, however, methane excess was minimal and

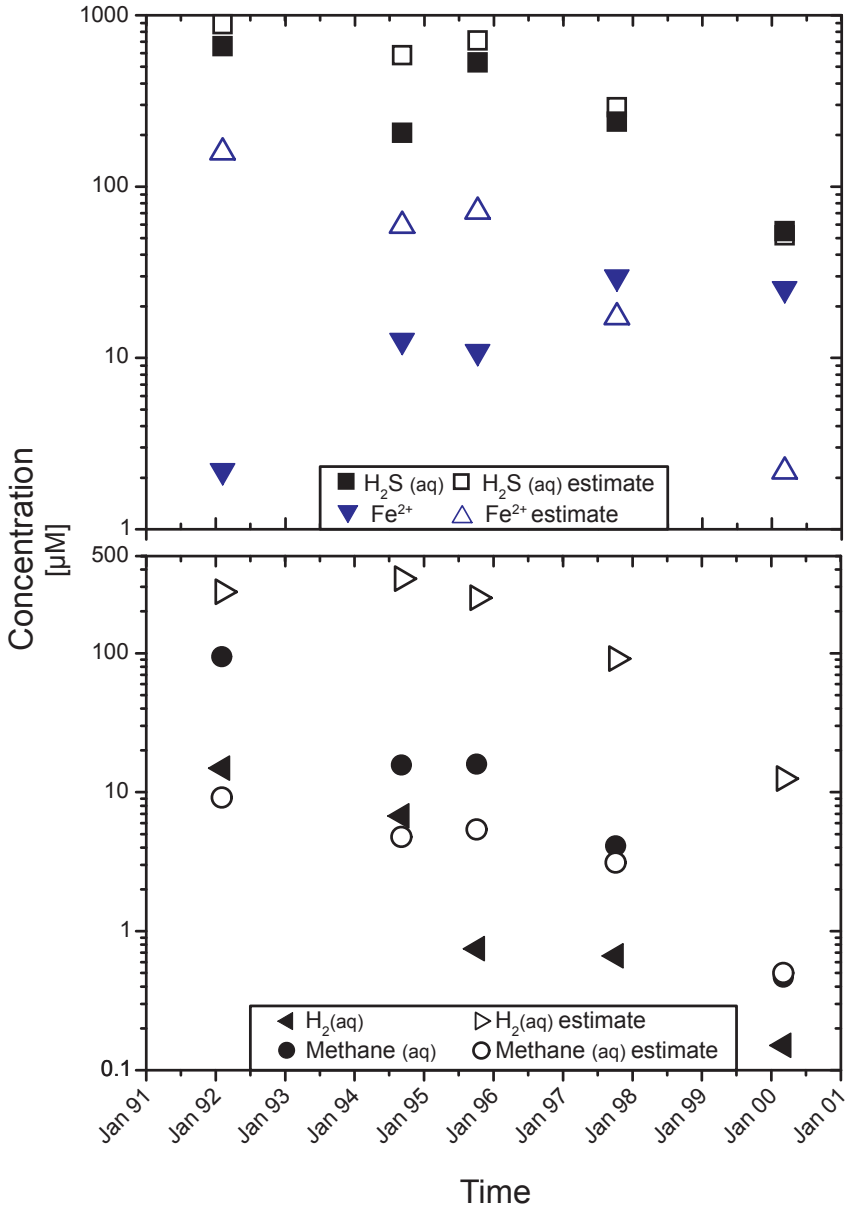

Figure 2-4: Predicted and measured concentrations of iron, hydrogen sulfide, hydrogen, and methane for diffuse fluids in the Tube Worm Pillar area. Hydrogen is strongly depleted over the entire period. Methane is enriched in the diffuse fluids, which may show methanogenesis in the subseafloor (Von Damm and Lilley, 2004). Until 1997, iron and H_2S concentrations are generally lower than predicted from conservative mixing. In November of 1997 predicted and measured concentration are similar to each other. In April of 2000 measured H_2S concentrations also correspond to the predictions from conservative mixing, but Fe-concentrations are higher than predicted in the diffuse fluid. Loss of Fe^{2+} and H_2S may be associated with precipitation of minerals. The surplus of measured Fe^{2+} in 2000 could indicate hydrogenotrophic iron reduction.

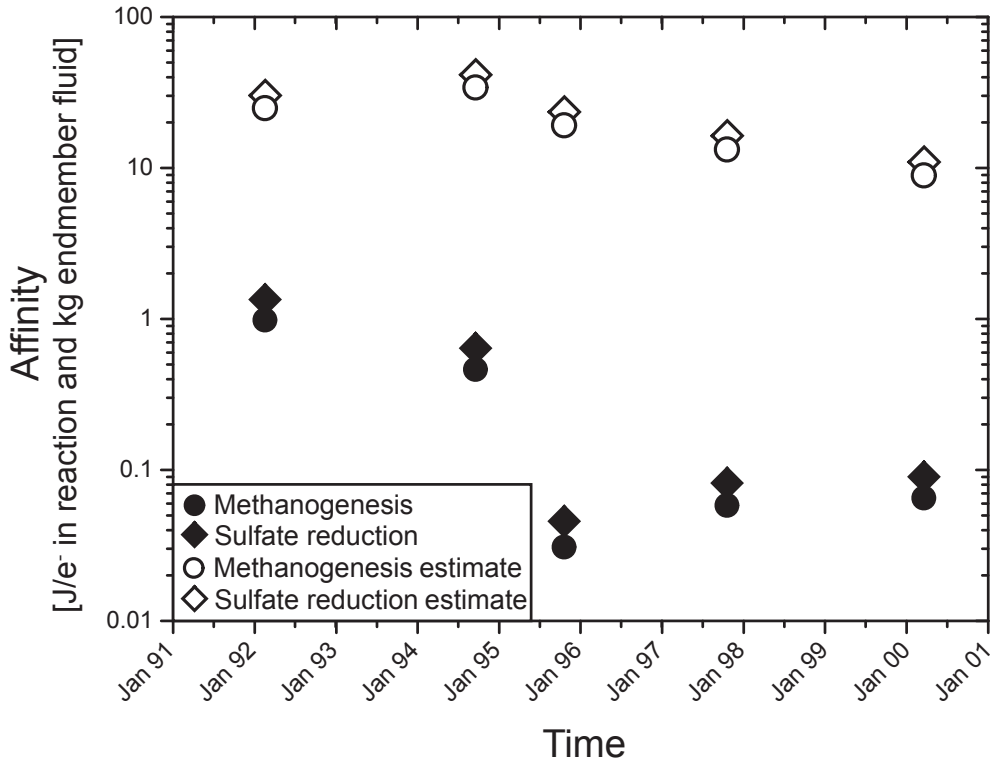

Figure 2-5: Normalized affinities for sulfate reduction and methanogenesis in the Tube Worm Pillar (TWP) area. Affinities are high in the hypothetical fluids calculated from conservative mixing of seawater and hydrothermal fluid. In the measured fluids the affinity is strongly decreased. Notably, affinities drop markedly in the first three years, which reflects the decrease in H_2 concentration in that time span (Figure 2-4). The removal of H_2 and the lowering of affinity reflect the exploitation of H_2 in fueling catabolic activity. During the last five years of the time series, normalized affinities had plateaued, possibly indicating a steady-state between hydrothermal energy supply and microbial utilization of energy.

H_2 depletion was still significant, suggesting that other hydrogen-consuming reactions may have also played a role.

While methane enrichment and depletion of hydrogen are indicators for methanogenesis, some of the methane may be metabolized shallower in the system prior to venting by aerobic or anaerobic respiration (Figure 2-1). There are indications from the Guaymas Basin that anaerobic oxidation of methane (AOM) may take place in vent settings and at temperatures >30°C (Schouten et al., 2003). Our calculations suggest that AOM is energetically feasible, so a loss of methane through AOM may be possible. If this reaction took place in the subseafloor, depletions of methane should be associated with increased hydrogen sulfide concentrations. This trend is not observed. AOM may still be taking place, but the rates are too small to affect the compositions of the diffuse fluids.

Affinity calculations for hydrogenotrophic methanogenesis and sulfate reduction in the modeled fluid (Figure 2-5) indicate strong driving forces for both reactions. The affinity for the reaction is strongly controlled by the hydrogen activity, which has a power of 4 in the relevant mass action equations. Hydrogen endmember concentrations increase from 6460 µM in February/March of 1992 to 8910 µM in March of 1994. Hydrogen concentrations then decrease in the following years to 2700 µM in April of 2000 (Table 2-1). Unfortunately, the

time series contains three points with data lacking for either the diffuse or endmember fluid. In March of 1994, the highest hydrogen concentration in the endmember fluid was measured, but no diffuse fluid was sampled. Hence, in our calculations, the sample collected in October of 1994 has the highest predicted hydrogen content (Figure 2-4) and also the highest normalized affinity for methanogenesis with 34.0 Joule per kg vent fluid and electron transferred in reaction (J/kg e^-) or of 41.5 J/kg e^- for sulfate reduction in the predicted diffuse fluid (Figure 2-5). The fluids sampled in April of 2000 have the smallest fraction of vent fluid and the lowest hydrogen endmember concentration of 12.5 µM, yielding normalized affinities for methanogenesis of 8.9 J/kg e^- and 11.0 J/kg e^- for sulfate reduction. In these diffuse fluids, hydrogen concentrations are still lower than predicted from conservative mixing and they do not correlate with the endmember concentration or extent of mixing with seawater.

Overall, hydrogen concentrations decrease linearly within the first four years of the time series from 14.9 to 0.7 µM. Hydrogen concentrations then remain fairly constant in the range of 0.7 to 0.2 µM until 2000. Figure 2-5 shows the affinities of these reactions per mol electrons in the reaction and normalized to kg of vent fluid. The normalized affinities of sulfate reduction decrease from 1.4 J/kg e^- to 0.05 J/kg e^- in 1995 and rebounds to 0.08-0.09 J/kg e^- in the following years. Hydrogenotrophic methanogenesis has an affinity of 1.0 J/kg e^- in 1992 and decreases to 0.05 to 0.06 J/kg e^- in 1995 – 2000 (Table 2-2).

The differences in the affinities (Table 2-2) reflect the variability in hydrogen concentrations, but the magnitude of these differences is quite small, because the intensive term ($\Delta_r G^o$) in the Gibbs energy calculation is very large for both reactions. The calculated affinities for methanogenesis and sulfate reduction (Table 2-2) lie above the estimated energy limit of microbial metabolism 10 kJ/8e^- (Hoehler, 2004). Minimum H_2 concentrations required for microbial harnessing of hydrogen at the temperatures of diffuse venting (11.9 to 24.7°C) is on the order of 10^{-8} M (Hoehler, 2004), which is considerably lower than the measured concentrations ($>2 \cdot 10^{-7}$ M). This result indicates that the microbial communities consume hydrogen but do not control its abundance. Apparently, hydrothermally driven influx of H_2 into the system is overall greater than the rate at which H_2 is metabolized. The constant hydrogen concentrations between 1995 and 2000 probably indicate some sort of steady-state between influx of hydrogen from below and hydrogen consumption in the subseafloor ecosystem. The early phase of decreasing hydrogen concentrations in the diffuse fluids is not related to changes in endmember compositions (steady between 250 and 350 µM), but may instead reflect the growth a hydrogenotrophic microbial community and increasing rates of consumption of H_2 advected into the system by hydrothermal flow. In that early stage, there was a relation between H_2 depletion and methane production, indicating that methanogenesis was responsible for both. In 1997 and 2000, H_2 was still consumed, but the methane excess had disappeared. Instead, there was excess Fe in the fluids, suggesting that Fe-reduction was taking place, perhaps because it requires lower H_2 activities than methanogenesis (Hoehler, 2004).

2.5 Conclusions

Thermodynamic calculations of energy yields of catabolic reactions from geochemical data of diffuse fluids facilitate an assessment of microbial metabolism in vent settings. This has been demonstrated in two case studies, both from the EPR 9°50'N region, where published geochemical data (Von Damm, 2004; Von Damm and Lilley, 2004) where used in systematic calculations of affinities of different catabolic reactions.

In the Bio9 area, affinities for sulfide oxidation strongly decrease, which is in accordance with the dying *Riftia* population. At the same time, an increase in the affinity for iron oxidation corresponds to a massive spread of red staining in the area, which is likely evidence for Fe-oxidizing bacteria. The results of the energy calculations verify the idea that the sudden change in vent fauna is a result of changes in fluid chemistry.

The example from the Bio9 area is more relevant to subseafloor processes. Enrichment of methane in diffuse fluids points to methanogenesis in the mixing and cooling zone. Our calculations confirm that hydrogenotrophic catabolic reactions have large energy yields throughout the duration of the time series (1992-2000). A large discrepancy in the amount of H_2 predicted from conservative mixing and the measured H_2 concentrations indicate effective scrubbing of H_2 by subseafloor hydrogenotrophic microorganisms. During the first three years of the time series, affinities for hydrogenotrophic reactions decreased despite continued high H_2 concentrations in the endmember fluids. This is interpreted to indicate the development of a hydrogenotrophic-based microbial ecosystem in the subseafloor. Between 1995 and 2000, the affinities remained constant and low (about an order of magnitude above the biological energy quantum). Apparently, influx of hydrogen from below and consumption of hydrogen within the subseafloor had reached a steady state. In 1997 and 2000, methane excesses were minimal, but the fluids showed pronounced enrichment of Fe relative to the concentrations predicted from conservative mixing. This finding may indicate a switch within the system from methanogenesis to Fe-reduction.

Our results show how thermodynamic calculations can be used to examine the relations between changes in fluid chemistry and seafloor biology. They are also a helpful tool in examining processes in the subseafloor and help highlight the tight relations and interdependencies between geochemistry and microbiology in vent systems.

2.6 Acknowledgements

We are grateful to two anonymous reviewers for numerous helpful comments and suggestions and to Greg Druschel for efficient editorial handling. This work was funded through the German Research Foundation (Grant BA1605/6-1). Prof. Dr. Wolfgang Bach acknowledges additional support through the University of Bremen and the MARUM Research Center and Cluster of Excellence

2.7 References

Amend, J.P., McCollom, T.M., Hentscher, M., Bach, W., 2011. Catabolic and anabolic energy for chemolithoautotrophs in deep-sea hydrothermal systems hosted in different rock types. Geochimica et Cosmochimica Acta 75, 5736-5748.

Amend, J.P., Shock, E.L., 2001. Energetics of overall metabolic reactions of thermophilic and hyperthermophilic Archaea and Bacteria. FEMS Microbiology Reviews 25, 175-243.

Bethke, C., 1996. Geochemical reaction modeling: Concepts and applications. Oxford University Press, USA.

Betts, J.N., Holland, H.D., 1991. The oxygen content of ocean bottom waters, the burial efficiency of organic carbon, and the regulation of atmospheric oxygen. Palaeogeography, Palaeoclimatology, Palaeoecology 97, 5-18.

Carroll, S., Mroczek, E., Alai, M., Ebert, M., 1998. Amorphous silica precipitation (60 to 120°C): comparison of laboratory and field rates. Geochimica et Cosmochimica Acta 62, 1379-1396.

Cavanaugh, C.M., 1983. Symbiotic chemoautotrophic bacteria in marine invertebrates from sulphide-rich habitats. Nature 302, 58-61.

Dick, J.M., 2008. Calculation of the relative metastabilities of proteins using the CHNOSZ software package. Geochemical Transactions 9, 10.

Drummond, S.E., 1981. Boiling and mixing of hydrothermal fluids. University Microfilms Int., Ann Arbor, Mich., p. 397 S.

Edmond, J.M., Measures, C., McDuff, R.E., Chan, L.H., Collier, R., Grant, B., Gordon, L.I., Corliss, J.B., 1979. Ridge crest hydrothermal activity and the balances of the major and minor elements in the ocean: The Galapagos data. Earth and Planetary Science Letters 46, 1-18.

Fornari, D.J., Shank, T., Von Damm, K.L., Gregg, T.K.P., Lilley, M., Levai, G., Bray, A., Haymon, R.M., Perfit, M.R., Lutz, R., 1998. Time-series temperature measurements at high-temperature hydrothermal vents, East Pacific Rise 9°49'-51'N: evidence for monitoring a crustal cracking event. Earth and Planetary Science Letters 160, 419-431.

Foustoukos, D.I., Houghton, J.L., Seyfried Jr, W.E., Sievert, S.M., Cody, G.D., 2011. Kinetics of H2–O2–H2O redox equilibria and formation of metastable H2O2 under low temperature hydrothermal conditions. Geochimica et Cosmochimica Acta 75, 1594-1607.

Helgeson, H.C., 1979. Mass transfer among minerals and hydrothermal solutions. Geochemistry of hydrothermal ore deposits 2, 568-610.

Hoehler, T.M., 2004. Biological energy requirements as quantitative boundary conditions for life in the subsurface. Geobiology 2, 205-215.

Houghton, J.L., Seyfried Jr, W.E., 2010. An experimental and theoretical approach to determining linkages between geochemical variability and microbial biodiversity in seafloor hydrothermal chimneys. Geobiology 8, 457-470.

Huber, J.A., Butterfield, D.A., Baross, J.A., 2003. Bacterial diversity in a subseafloor habitat following a deep-sea volcanic eruption. FEMS Microbiology Ecology 43, 393-409.

Jannasch, H.W., 1995. Microbial interactions with hydrothermal fluids, in: Humphris, S.E., Zierenberg, R.A., Mullineaux, L.S., Thomson, R.E. (Eds.), Seafloor hydrothermal systems: physical, chemical, biological, and geological interactions. AGU, Washington, DC, pp. 273-296.

Johnson, J.W., Oelkers, E.H., Helgeson, H.C., 1992. SUPCRT92: A software package for calculating the standard molal thermodynamic properties of minerals, gases, aqueous species, and reactions from 1 to 5000 bar and 0 to 1000°C. Computers & Geosciences 18, 899-947.

Kormas, K.A., Tivey, M.K., Von Damm, K., Teske, A., 2006. Bacterial and archaeal phylotypes associated with distinct mineralogical layers of a white smoker spire from a deep-sea hydrothermal vent site (9°N, East Pacific Rise). Environmental Microbiology 8, 909-920.

McCollom, T.M., 2007. Geochemical Constraints on Sources of Metabolic Energy for Chemolithoautotrophy in Ultramafic-Hosted Deep-Sea Hydrothermal Systems. Astrobiology 7, 933-950.

McCollom, T.M., Shock, E.L., 1997. Geochemical constraints on chemolithoautotrophic metabolism by microorganisms in seafloor hydrothermal systems. Geochimica et Cosmochimica Acta 61, 4375-4391.

Perner, M., Bach, W., Hentscher, M., Koschinsky, A., Garbe-Schönberg, D., Streit, W.R., Strauss, H., 2009. Short-term microbial and physico-chemical variability in low-temperature hydrothermal fluids near 5°S on the Mid-Atlantic Ridge. Environmental Microbiology 11, 2526-2541.

Petersen, J.M., Zielinski, F.U., Pape, T., Seifert, R., Moraru, C., Amann, R., Hourdez, S., Girguis, P.R., Wankel, S.D., Barbe, V., Pelletier, E., Fink, D., Borowski, C., Bach, W., Dubilier, N., 2011. Hydrogen is an energy source for hydrothermal vent symbioses. Nature 476, 176-180.

Proskurowski, G., Lilley, M.D., Olson, E.J., 2008. Stable isotopic evidence in support of active microbial methane cycling in low-temperature diffuse flow vents at 9°50'N East Pacific Rise. Geochimica et Cosmochimica Acta 72, 2005-2023.

Reysenbach, A.-L., Liu, Y., Banta, A.B., Beveridge, T.J., Kirshtein, J.D., Schouten, S., Tivey, M.K., Von Damm, K.L., Voytek, M.A., 2006. A ubiquitous thermoacidophilic archaeon from deep-sea hydrothermal vents. Nature 442, 444-447.

Schouten, S., Wakeham, S.G., Hopmans, E.C., Sinninghe Damste, J.S., 2003. Biogeochemical Evidence that Thermophilic Archaea Mediate the Anaerobic Oxidation of Methane. Applied and Environmental Microbiology 69, 1680-1686.

Shank, T.M., Fornari, D.J., Von Damm, K.L., Lilley, M.D., Haymon, R.M., Lutz, R.A., 1998. Temporal and spatial patterns of biological community development at nascent deep-sea hydrothermal vents (9°50'N, East Pacific Rise). Deep Sea Research Part II: Topical Studies in Oceanography 45, 465-515.

Shock, E., Holland, M.E., 2004. Geochemical energy sources that support the subsurface biosphere, in: Wilcock, W.S.D., DeLong, E.F., Kelley, D.S., Baross, J.A., Cary, S.C. (Eds.), The Subseafloor Biosphere at Mid-Ocean Ridges. American Geophysical Union, Washington, DC, pp. 153-165.

Sohn, R.A., Fornari, D.J., Von Damm, K.L., Hildebrand, J.A., Webb, S.C., 1998. Seismic and hydrothermal evidence for a cracking event on the East Pacific Rise crest at 9° 50' N. Nature 396, 159-161.

Tivey, M.K., Humphris, S.E., Thompson, G., Hannington, M.D., Rona, P.A., 1995. Deducing patterns of fluid flow and mixing within the TAG active hydrothermal mound using mineralogical and geochemical data. J. Geophys. Res. 100, 12527-12555.

Toner, B.M., Santelli, C.M., Marcus, M.A., Wirth, R., Chan, C.S., McCollom, T., Bach, W., Edwards, K.J., 2009. Biogenic iron oxyhydroxide formation at mid-ocean ridge hydrothermal vents: Juan de Fuca Ridge. Geochimica et Cosmochimica Acta 73, 388-403.

Von Damm, K.L., 2004. Evolution of the hydrothermal system at East Pacific Rise 9 50'N: Geochemical evidence for changes in the upper oceanic crust, in: German, C.R., Lin, J., Parson, L.M. (Eds.), Mid-Ocean Ridges: Hydrothermal Interactions between the Lithosphere and Oceans. American Geophysical Union, Washington, DC, pp. 285-304.

Von Damm, K.L., Lilley, M.D., 2004. Diffuse Flow Hydrothermal Fluids from 9 50'N East Pacific Rise: Origin, Evolution and Biogeochemical Controls, in: Wilcock, W.S.D., DeLong, E.F., Kelley, D.S., Baross, J.A., Cary, S.C. (Eds.), The Subseafloor Biosphere at Mid-Ocean Ridges. American Geophysical Union Washington, DC, pp. 245-268

Wolery, T., Jove-Colon, C., 2004. Qualification of thermodynamic data for geochemical modeling of mineral-water interactions in dilute systems. YMP (Yucca Mountain Project, Las Vegas, Nevada).

3. Geochemical modeling of CO_2 behavior in water-peridotite interactions: organic synthesis versus carbonate precipitation

Michael Hentscher[1§], Wolfgang Bach[1], Frieder Klein[2]

[1] *Department of Geoscience, University of Bremen, Klagenfurter Straße, 28359 Bremen, Germany*

[2] *Department of Geology and Geophysics, Woods Hole Oceanographic Institution, Woods Hole, MA 02543, USA*

[§]*Corresponding author: hentscher@uni-bremen.de*

wbach@uni-bremen.de

fklein@whoi.edu

3.1 Abstract

Dissolved CO_2 is reactive in serpentinization systems when conditions are alkaline and reducing. CO_2 may be reduced to organic carbon species or it may be sequestered in carbonates. Both, CO_2 reduction and carbonate precipitation are kinetically controlled. The relative stabilities of reduced dissolved carbon species versus carbonate minerals, however, have not been investigated systematically. We present geochemical models examining the energetics of the fate of CO_2 in serpentinization systems. We find that carbonate formation restricts the availability of dissolved inorganic carbon (DIC) for reduction to organic carbon species. Because the formation of methane is known to be particularly sluggish, we expect that and any carbonate precipitation will restrict methanogenesis. Organosynthesis reactions to methanol have been shown to proceed much faster, and we propose that they compete with carbonate precipitation. The model calculations predict that carbonate precipitation is thermodynamically favored over CO_2 reduction to methanol at water-to-rock mass ratios (W/R) <4-5.

These results imply that in fluids from the Lost City vent field methane formation may have taken place at W/R greater than those proposed for the reaction zone (W/R = 2-4). Our calculation suggest that the organosynthesis there does likely take place in the lower part of the recharge zone and that the fate of CO_2 in the rock-buffered reaction zone of the system in its current state should be the formation of carbonate.

3.2 Introduction

Hydrothermal systems are generally known as high temperature vents on the seafloor, heated by a magmatic process and issuing slightly acidic fluids. The emitting fluids are results of different processes during seawater circulation through the oceanic crust. Seawater enters the oceanic crust in a recharge zone, is heated and undergoes chemical exchange with the host rock in the reaction zone. Further modifications can occur such as phase separation and enrichment of magmatic gases like CO_2. Fluid compositions vary with the host rock they are interacting with. Compared with fluids venting from basalt-hosted hydrothermal systems fluids in peridotite-hosted hydrothermal systems, i.e. serpentinization fluids are characterized by high concentrations of hydrogen and methane, but low concentrations of dissolved hydrogen sulfide and dissolved silica (Charlou et al., 2002). Hydrogen is generated in substantial amounts because ferrous iron originally contained in olivine and orthopyroxene is oxidized by water to ferric iron in magnetite and serpentine. The high hydrogen concentrations along with elevated concentrations of CO_2 have been associated with the abiotic synthesis of carbohydrates (Berndt et al., 1996; Holm and Charlou, 2001; McCollom and Seewald, 2001; Schulte et al., 2006).

For a number of reasons early earth analogs of the recently discovered off-axis Lost City hydrothermal field (Kelley et al., 2001) have been considered to represent a possible venue for the origin of Life (Huber and Wächtershäuser, 2003; Martin et al., 2008; Russell and Hall, 2009). Lost City is evidently dominated by serpentinization reactions because its moderately warm (< 90°C), fluids are strongly alkaline, low in silica and reveal high concentrations of dissolved hydrogen, methane and calcium. The hydrogen concentrations are comparable with other high-temperature mafic-ultramafic hosted systems, such as Logatchev and Rainbow (Charlou et al., 2002), all of which are located at the Mid-Atlantic-Ridge. Isotopic evidence for abundant abiotic reduction of CO_2 to low-molecular-weight hydrocarbons at Lost City (Proskurowski et al., 2008; Lang et al., 2010) appears to be in contrast with the hypothesis that mixing of alkaline, Ca-rich serpentinization fluid with seawater causes the precipitation of abundant carbonate. Low concentrations of dissolved inorganic carbon (DIC) in the vent fluids (Proskurowski et al., 2008), the formation of carbonate chimneys (Ludwig et al., 2006), and ophicarbonate discovered close to the hydrothermal field (Boschi et al., 2006; Karson et al., 2006) demonstrate that carbonate precipitation is possibly a favored, but evidently a competitive process for the abiotic reduction of CO_2. The circumstances under which the abiotic reduction of CO_2 outranks the precipitation as carbonate are of great interest not only for researchers interested in the putative origin of life at early Earth Lost City analogs; they are key to furthering our understanding of the global carbon cycle and the habitability of the seafloor.

Here we present the results of equilibrium calculations to evaluate the environmental conditions under which either process – carbonate precipitation or abiotic reduction of CO_2 – is favored; our calculations are intended to be of particular relevance for low to moderate temperature serpentinization systems such as Lost City. Furthermore, we systematically studied the influence of organic C1 and C2 components to evaluate their contributions to the Lost City fluid chemistry. For these purposes we modified the models of Klein et al.(2009) to

calculate the equilibrium conditions in dependence of the water-to-rock mass (W/R) ratio and temperature. Details about the modeling procedure are presented in the following section.

3.3 Methods

Reaction path models were calculated to simulate the reaction of one kg of seawater with variable amounts harzburgite, consisting of 75 vol.% olivine, 20 vol.% orthopyroxene and 5 vol.% clinopyroxene (Table 3-1). Calculations were carried out using a batch titration model with the computer code EQ3/6, version 8.0 (Wolery, 1992b, a; Wolery and Jarek, 2003). In a first step, the composition of seawater (Table 3-2) was speciated at 25°C and 50 MPa using EQ3NR (Wolery, 1992b). In a second step, the speciated seawater was heated to the defined temperature using EQ6 (Wolery et al., 1992). In the third step the harzburgite was added in small increments until the defined W/R (in our model W/R = 1kg of water/ mass of harzburgite reacted) is reached. This approach can be understood as the recharge of seawater into the reaction zone. The seawater is heated and is not modified by reactions with the surrounding rock. In a natural system, this model would correspond to a fast fluid transport into the recharge zone along cracks and veins that have already been altered. The altered layer acts as a more or less inert coating preventing the equilibration of the fluid with the surrounding un-altered rock. Stepwise addition of rock simulates fluid-rock interaction in the reaction zone. On the basis of boron and strontium concentrations, as well as $\delta^{18}O$ and $^{87}Sr/^{86}Sr$ ratios of the hydrothermal fluid, the temperature of the reaction zone is inferred to range between 150 and 250°C at W/R = 2 - 4 (Foustoukos et al., 2008). To cover the range between measured temperatures at the vent sites and predicted temperature of the Lost City reaction zone, the model temperatures are chosen to be 100°C, 150°C, 200°C and 250°C.

Table 3-1: Mineral composition of the harzburgite used in reaction path models

Atoms	Olivine	Orthopyroxene	Clinopyroxene
SiO_2	1.00	1.98	1.985
Al_2O_3	0.00	0.04	0.03
FeO	0.20	0.19	0.0925
MgO	1.80	1.75	0.885
CaO	0.00	0.04	1.0075
X_{Mg}	0.90	0.902	0.905

Water-rock reactions are described by an improved serpentinization model of Klein et al. (2009). The adopted solid-solution model for the serpentinite consists of the mineral endmembers kaolinite, greenalite, cronstedtite and chrysotile and enhances the prediction for hydrogen produced in mineral reactions. Furthermore, solid-solutions for clinopyroxene (diopside, hedenbergite), chlorite (clinochlore-14A, daphnite-14A) and brucite (Fe-brucite, brucite) are considered in the database. Hydrogen is produced by the oxidation of Fe(II) in olivine and orthopyroxene to Fe(III) in magnetite and serpentine. Oxidation of two moles Fe(II) generates one mole H_2. Changes in serpentinite mineralogy during the reaction has a direct impact on the hydrogen content and finally on the reduction capacity of the fluid.

Dilution effects or trapping of hydrogen that might occur in a natural system, is not considered in our closed batch titration model.

Table 3-2: Seawater composition at 25°C (mMol/kg)

Cl^-	550
Na^+	441
Mg^{2+}	52.7
SO_4^{2-}	28.2
Ca^{2+}	10.7
K^+	9.80
HCO_3^-	2.34
SiO_2(aq)	0.130
Al^{3+}	0.000037
Fe^{2+}	0.0000015
O_2(aq)	0.119
pH	8.20

Thermodynamic calculations with the EQ3/6 computer code are done with an extended database after Klein et al., (2009). It covers the temperature range of 0-400°C in 25°C increments at 50 MPa pressure. Uncertainties of the calculation for lower pressure serpentinite systems are negligible, because the pressure effects on the equilibration constants are small in comparison with temperature effects. For example, a pressure decrease of 20 MPa can be compensated by a temperature decrease of a few degrees Celsius. The database was extended with equilibrium constants for organic C1 (methane, methanol, formaldehyde and formic acid) and C2 (ethane, ethanol, acetaldehyde, acetic acid, ethene and ethyne) compounds that were calculated with SUPCRT92 (Johnson et al., 1992) and the OBIGT database after Dick (2008). Organic metal complexation constants were excluded from the model due to substantial uncertainties at higher temperatures. Activity constants for dissolved organic and inorganic charged species are calculated with the B-dot equation. Hard-core diameters, B-dot and Debye-Hückel parameters for the equations are obtained from Wolery and Jove-Colon (2004). Activity constants for neutral species are assumed to be unity and for aqueous non-polar gases are adopted from CO_2 (Drummond, 1981).

In each step of the model EQ3/6 calculates the energy minimum of the system. In this state all phases (minerals, fluid, and gas) are in equilibrium. To evaluate the possible formation of metastable organic compounds, the dominating organic species in the model was suppressed and the model was recalculated.

Reported concentrations of aqueous species correspond to their concentration in one kg of the start reaction fluid. This calculation was established to avoid apparent increase of carbon content at low water rock ratios due to the loss of water by the formation of hydrous minerals.

Carbonate minerals like calcite, magnesite and dolomite are permitted in the system. This adjustment has the advantage that it can be distinguished whether the reduction capacity of the system is large enough to form organic molecules from carbonates or not.

The reducing conditions during serpentinization promote not only the formation of organic compounds, but also the reduction of sulfate. We decided that sulfate reduction is not allowed in the present calculations for the following reasons: Sulfate reduction and reduction of inorganic carbon to organic molecules are competitive reactions for the hydrogen source. Both reactions are kinetically hampered at low temperatures. Furthermore, anhydrite precipitates at higher temperatures from seawater, which lowers the sulfate and calcium concentration in the reaction fluid. If sulfate reduction in the closed system is permitted, hydrogen sulfide (H_2S) is produced, which causes a decrease in the predicted amount of anhydrite and an increase in dissolved calcium concentrations. In addition the increase of H_2S in the fluid leads to precipitation of iron sulfides.

3.4 Results

3.4.1 Predicted mineral assemblages

The predicted sequences and abundances of alteration phases are illustrated in Figure 3-1. From high to low W/R, the sequence of minerals precipitated includes serpentine, magnetite, chlorite, brucite and secondary clinopyroxene. With decreasing W/R, chlorite becomes stable and its abundance increases to a constant value. Brucite formation follows that of chlorite and its abundance increases with reaction progress. At 250°C, the increase in abundance is not as obvious as at lower temperatures because brucite is formed at higher W/R (not plotted).

Mg-Ca exchange equilibria between fluids and minerals strongly influence the pH. The assemblage brucite and serpentine buffers the in situ pH between 7.2 at 100°C and 5.5 at 200°C (Klein et al., 2009). Concentrations of dissolved Ca are high during serpentinization, because only trace amounts can be accommodated in serpentine, brucite, and chlorite. Secondary clinopyroxene, the main host of Ca, becomes stable at low W/R and is close to endmember diopside in composition. The appearance of secondary clinopyroxene is associated with an increase of pH from 7.2 to 9.8 at 100°C and from 5.5 to 7.5 at 250°C (Figure 3-2). The increase in pH indicates the change from brucite-serpentine-buffer (Brc-Srp) to the secondary clinopyroxene-brucite-serpentine-buffer (Cpx-Brc-Srp) (Klein et al., 2009).

If CO_2 reduction is suppressed or the reduction potential of the system is too low, then carbonate is predicted to form. The sequence of carbonate precipitation is determined by the fluid composition. At 100°C and high W/R the concentrations of magnesium and calcium are close to those of seawater (Figure 3-2). Here dolomite is predicted to be the dominant carbonate mineral. With increasing temperature, anhydrite precipitates from seawater. This will lower the Ca activity in the fluid and cause magnesite precipitation. Precipitation of serpentine and brucite consumes most of the dissolved magnesium with decreasing W/R. Calcium is released by the alteration of pyroxene. The increase in Ca and decrease in Mg concentrations goes along with the dissolution of magnesite and precipitation of dolomite.

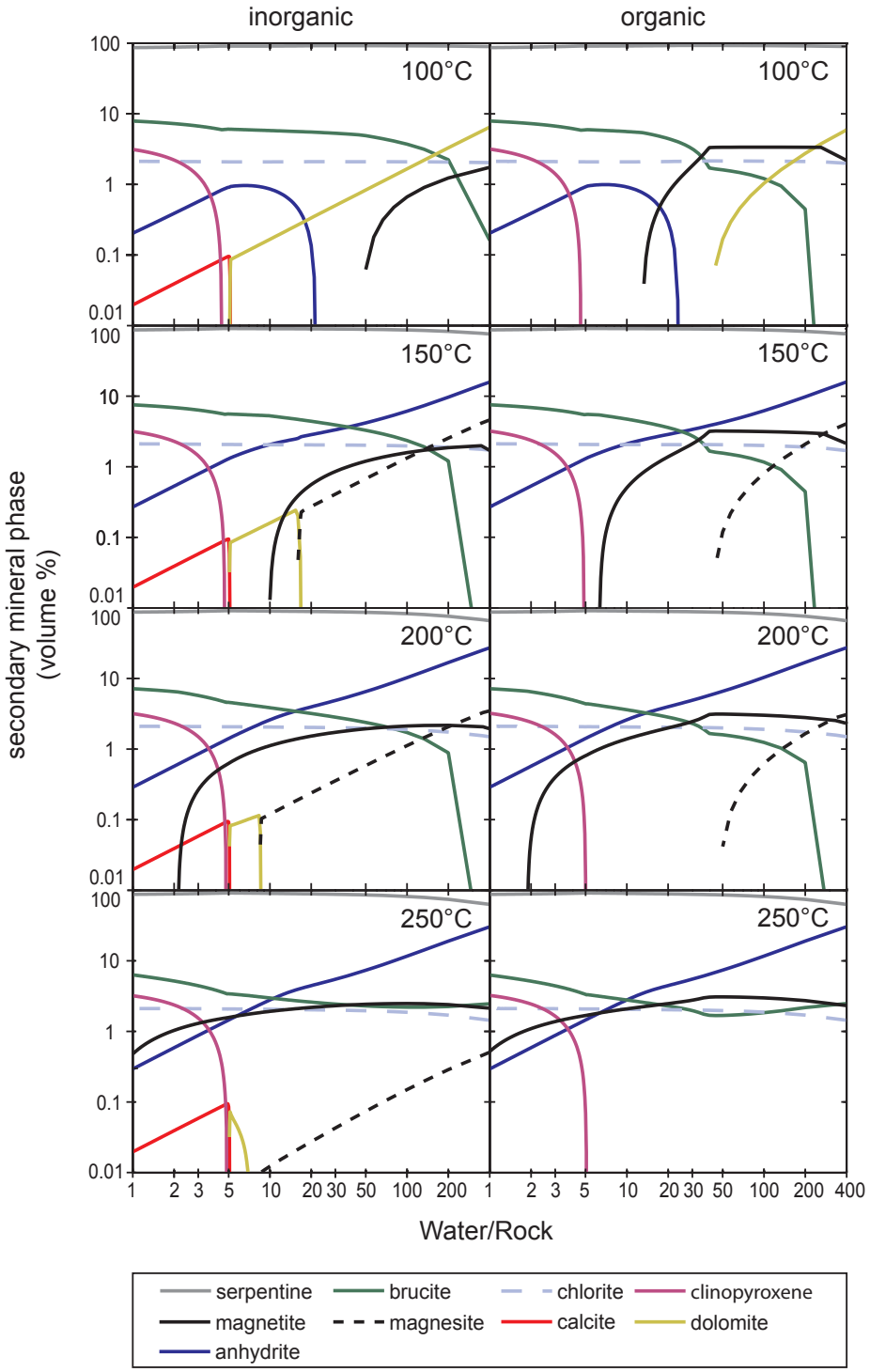

Figure 3-1: Mineral abundances of the alterated rock with allowed reduction of CO_2 to organic compounds (labeled "organic") and suppressed reduction of CO_2 ("inorganic").
Carbonate minerals are stable over the entire W/R range in the inorganic model. Magnesite, dolomite and calcite form from large to small W/R. Magnesite formation at large W/R is facilitated by the precipitation of anhydrite, which lowers the Ca activity of the fluid relative to Mg. Calcite occurs together with clinopyroxene which is indicative of a brucite-serpentine-clinopyroxene-buffer at Lost City rather than serpentine-brucite.
In the "organic" model, carbonates are only stable at high W/R, which is related to the reduction of CO_2. Magnetite abundance correlates with increasing temperatures and enhance its appearance towards smaller W/R. It appears that the stability of magnetite is influenced by the reduction of CO_2 because the magnetite amounts are increased in comparison with the "inorganic" model.

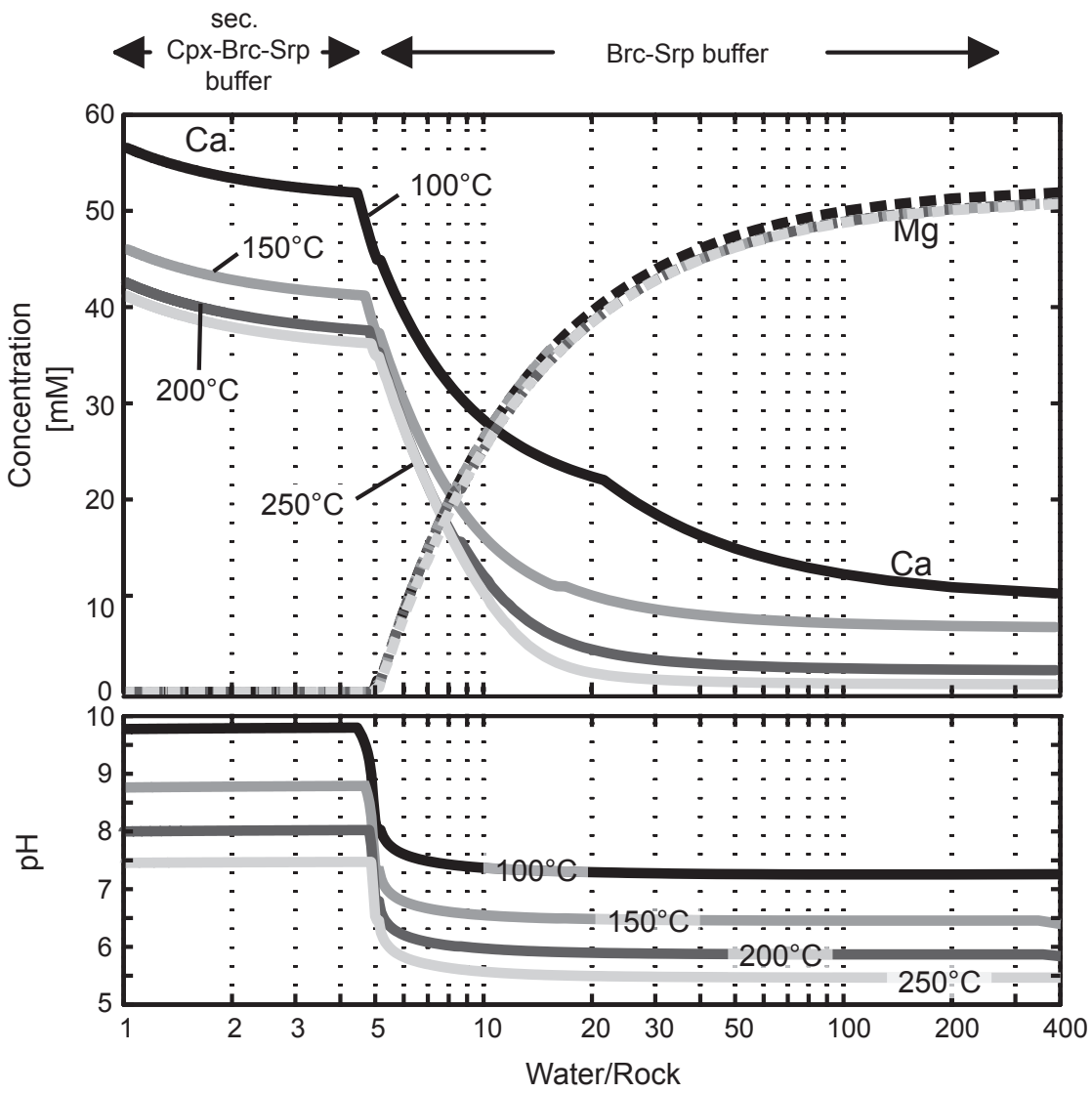

Figure 3-2: Mg and Ca concentrations (mM) as a function of W/R and temperature. Ca concentrations increase with decreasing W/R due to the alteration of Ca-bearing harzburgite and they plateau in the Cpx-Brc-Srp buffered domain. In contrast, concentrations of dissolved Mg decrease with decreasing W/R because Mg is incorporated in serpentine and brucite. The decrease of Mg marks the transition from the Brc-Srp to the Cpx-Brc-Srp buffer that coincides with an increase in pH.

Further decrease of Mg with decreasing W/R causes dissolution of dolomite while calcite precipitates. Calcite precipitation is facilitated by an increasing pH, which is buffered by Cpx-Brc-Srp (Figure 3-2).

While magnetite formation is predicted in all model calculations at temperatures <250°C magnetite is not part of the equilibrium mineral assemblage at small W/R (Figure 3-1). However, significant differences in the abundance of magnetite are predicted when CO_2 reduction is suppressed. In the model with CO_2 reduction (labeled "organic" in Figure 3-1) the predicted abundance of magnetite is greater than in models with suppressed CO_2 (labeled "inorganic" in Figure 3-1) reduction. Furthermore, both trends differ slightly as a function of W/R. Models allowing CO_2 reduction promote magnetite to lower W/R. These predictions illustrate how the formation of magnetite is linked to the redox behavior of carbon.

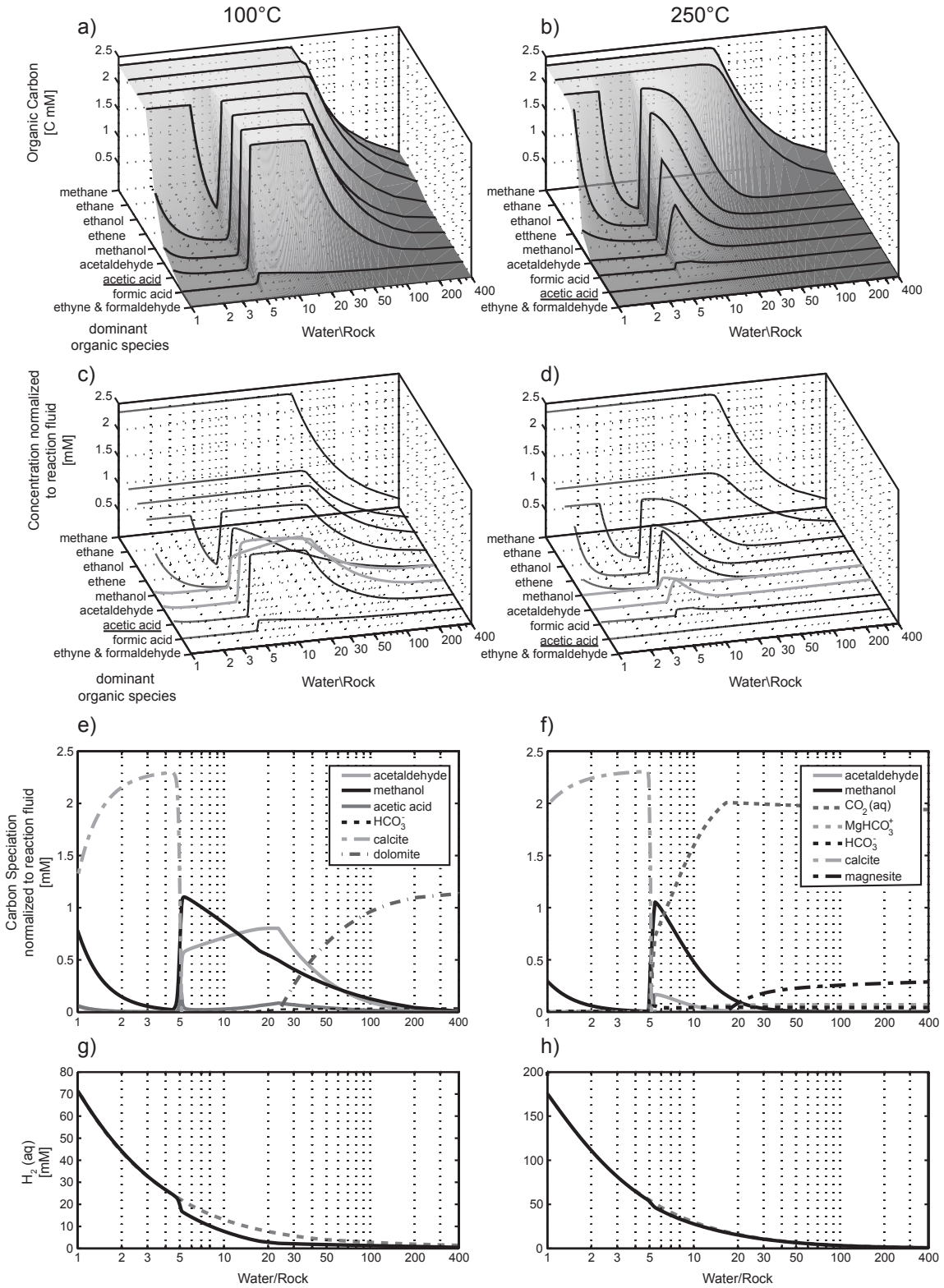

Figure 3-3:(a) and (b) evaluates the concentration of carbon bound in organic compounds as a function of W/R and the dominant organic species in a sequence of suppressing the most favored (reduced) organic species. If all organic species are permitted, methane predominates. Ethane marks the suppressing of methane, ethanol the suppressing of methane and ethane, and so on.

The comparison of a) and (b) shows that the formation of organic compounds is more favored at lower temperatures than at high temperatures. The decreasing concentrations of organic carbon to ethyne and formaldehyde indicate that increasing amounts of carbon are bound as inorganically such as in carbonate. The comparison of

(a) and (b) highlights the temperature dependence of the equilibrium constant and the change of formic acid and acetic acid in the suppressing sequence. At high temperatures formic acid is favored over acetic acid.
(c) and (d) illustrate the concentration of the dominant organic species normalized to the reaction fluid.
(e) and (f) show the methanol step of the modeling. At 100°C (e) methanol and acetaldehyde are the favored species. Acetaldehyde is more favored at lower W/R and methanol at high W/R. Both components drop in concentration when the reaction path of decreasing W/R crosses into the zone of Cpx-Brc-Srp buffering where calcite is stable. However, at lower W/R predicted methanol concentration increase again. At high temperatures (f) acetaldehyde concentrations are lower than at low temperatures (e). The much lower concentration of acetaldehyde at high temperature shows that smaller molecules like methanol are favored at higher temperatures. Likewise the transition from formic acid to acetic acid in the reduction sequence can be explained that way. (g) and h) show the predicted H_2 concentrations for the paths (e) and (f). The dashed line indicates the H_2 concentration predicted if the formation of organic compounds is suppressed.

3.4.2 Predictions of organic carbon stability

Equilibrium calculations for organic carbon during the serpentinization process show that methane is the dominant species (Figure 3-3). Even at high W/R ratios, the reduction potential of the system is sufficient to reduce CO_2 to methane. Other organic species are predicted to be present only in very low concentrations (< 30nM). Ethane is predicted to be the most abundant organic species when methane is suppressed. Like methane, if ethane is present it 'prevents' other organic species to form. If the formation of both alkanes is suppressed ethanol is predicted to form. In the sequence of increasing oxidation of carbon compounds, ethanol is the first species that shows a marked dependence on W/R and temperature. While in the temperature interval from 100 to 150°C there is no obvious difference to the alkanes, it exhibits a sharp decrease in concentration between 200 and 250°C and a W/R = 5. The drop in ethanol concentration coincides with a pronounced increase in calcite abundance. When the formation of ethanol is suppressed, the models predict that ethene is the dominant dissolved carbon species. If the formation of ethanol is suppressed the abundance of calcite is predicted to be increased over the entire temperature range. The concentrations of carbonates and inorganic species, mainly CO_2, increase with increasing W/R, whereas the concentration of organic species increases with decreasing W/R. By suppressing ethene the formation of other organic carbon compounds is limited. Methanol and acetaldehyde are predicted to form in an interval bound by the stability fields of inorganic carbon species (Figure 3-3). Higher temperatures and lower W/R promote the formation of methanol. Acetaldehyde in contrast is predicted to form preferentially at lower temperatures and concentrations of hydrogen. If the formation of methanol is suppressed, the stability of organic species is further reduced. At 250°C, there is only a small range of W/R where organic species are present. Acetaldehyde is the main predicted organic species. Suppressing acetaldehyde leads to a temperature dependent change of the predicted organic compounds. Low temperatures promote acetic acid formation while formic acid is predicted to dominate at higher temperature. Suppressing of both acids shows that neither ethyne nor formaldehyde is formed in considerable concentrations.

3.5 Discussion

3.5.1 Organic synthesis

Equilibrium thermodynamic calculations for hydrothermal fluids show that the dominating carbon compound should be methane (CH_4) and dissolved inorganic carbon (DIC). Methane is predicted to form at elevated H_2 activities and the reaction is favorable then because of the strong driving force generated from H_2 (power of 4 in the corresponding mass action equation):

$$CO_2 + 4\,H_2(aq) = CH_4(aq) + 2\,H_2O \qquad \text{(eq. 1)}$$

Equilibrium between CO_2, H_2, and CH_4 is not common in seafloor hydrothermal fluids. McCollom and Seewald (2007) show that there is an excess of CH_4 (i.e. affinity for the reaction to proceed from right to left) in basalt-hosted systems, while there is drive for methanogenesis in ultramafic hosted systems. Shock (1992) and Welhan (1988) proposed that temperatures >500°C are required to reach the equilibrium state. At lower temperatures, the methanogenesis reaction is kinetically sluggish. Shock (1992) proposed that, since the system does not reach equilibrium, reaction kinetics for intermediate aqueous organic compounds may be adequate to attain metastable equilibria. The driving force to attain metastable equilibria depends on the activity of H_2, i.e. the reducing capacity of the system. Shock (1992) assumed that FMQ (fayalite-magnetite-quartz), PPM (pyrite-pyrrhotite-magnetite) and HM (hematite-magnetite) control the H_2 activity in seafloor hydrothermal systems. These buffer curves are plotted in Figure 3-4 along with the H_2 activity of CO_2-CH_4 equilibrium for different ratios of CO_2 and CH_4. Shock (1992) argued that the FMQ buffer curve may be representative of H_2 activities in ultramafic rock-hosted systems and the gray area in Figure 3-4 marks the domain in which there is thermodynamic drive for organic synthesis. It is evident that the stability of organics decreases as the buffers become less reducing from FMQ (ultramafic) to PPM (basaltic) to HM (granitic) mineral assemblages. From a thermodynamic point of view Shock (1992) concluded that organic synthesis is most likely to happen in ultramafic-hosted hydrothermal systems. It is important to note that chemical data of vent fluids from ultramafic-hosted hydrothermal systems were not available when Shock wrote his seminal paper. Since then a number of field studies have generated a wealth of data making it possible to compare prediction and reality. Figure 3-4 compares the H_2 activity calculated on the basis of measured CH_4 and CO_2 activities with the measured H_2 activity at the venting temperature for two Lost City hydrothermal field (LCHF) samples (Proskurowski et al., 2008; Lang et al., 2010) and one high temperature fluid from the peridotite hosted Logatchev hydrothermal field (Charlou et al., 2002). It is evident that LCHF samples are far from equilibrium, while the higher temperature Logatchev fluids are closer to equilibrium. This is exactly what Shock (1992) had predicted, indicating that the basic concept of the approach is valid.

We have tried to contribute to this theoretical framework by adding temperature-dependent H_2 activities for actual serpentinization reactions rather than idealized mineral buffers. Figure 3-4 shows the calculated H_2 activity for additional buffers: the

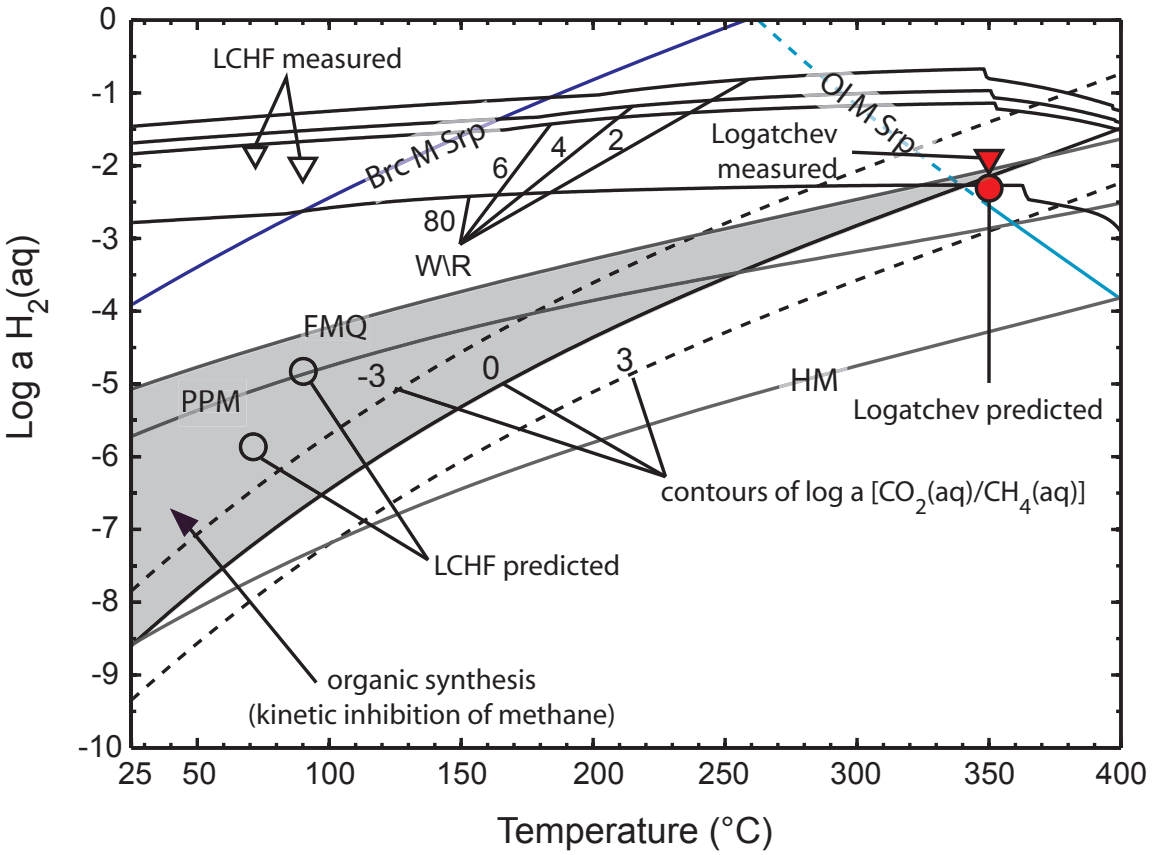

Figure 3-4: Plot of log a H_2(aq) against temperature modified after (Shock, 1992). Shown are the log a H_2(aq) buffered by the FMQ (fayalite-magnetite-quartz), PPM (pyrite-pyrrhotite-magnetite), HM (hematite-magnetite), SBM (serpentine (X_{Mg}0.95)-brucite (X_{Mg}0.9)-magnetite) and OSM (olivine(X_{Mg}0.9)-serpentine (X_{Mg}0.95)-magnetite) mineral assemblages as function of temperature. In addition, contours of log a (CO_2(aq)/CH_4(aq)) equal to 3, 0 and -3 and associated computed log a H_2(aq) at W/R 80, 6, 4 and 2 are shown as function of temperature. Circles indicate the predicted log a H_2(aq) for the methanogenesis equilibrium for Lost City hydrothermal fluids (LCHF) and Logatchev vent fluids (red) at the respective venting temperatures and estimated from the respective CH_4(aq) and CO_2(aq) activities. Triangles show the measured log a H_2(aq). The equilibrium of this reaction is not attained for the range of temperatures considered. This is apparent from the large differences between measured and predicted log a H_2(aq). Only higher temperatures show a tendency to reach equilibrium (Logatchev). Because of the disequilibrium, it is assumed that metastable equilibria for aqueous organic compounds may control the fate of carbon. The gray area corresponds to the region where metastable aqueous organic compounds may be expected (Shock, 1992). The discrepancies to idealized buffers indicate that comprehensive reaction path models are better guides to hydrogen production, which drives organic synthesis.

SBM (serpentine(X_{Mg}0.95)-brucite(X_{Mg}0.9)-magnetite) and OSM (olivine(X_{Mg}0.9)-serpentine (X_{Mg}0.95)-magnetite) assemblages. The OSM assemblage is predicted to replace the SBM assemblage with increasing temperatures (see cross-over in Figure 3-4). These two buffer curves indicate that H_2 yields should have a maximum around 300°C and H_2 activities should be considerably higher than FMQ at temperatures <350°C. However, H_2 activities associated with the OSM buffer may be smaller than those corresponding to the FMQ buffer at T>350°C. The SBM and OSM buffer lines will shift considerably if the Fe-contents of olivine, serpentine, and brucite change. These contents are not fixed and depend on temperature, rock composition, and water-to-rock ratio (W/R). Reaction path modeling provides

means of tracking all these parameter and predicts H_2 activities for a range of serpentinization fluids. Figure 3-4 shows the H_2 activity for harzburgite seawater reactions at the W/R 80, 6, 4 and 2 over a range of temperatures. Predicted hydrogen activities exceed those calculated from any fixed-composition buffer throughout most of the temperature range. This analysis indicates that serpentinization reactions create more driving force for organic synthesis than originally assumed by Shock (1992).

Several studies estimating the thermodynamic driving force of the abiotic synthesis of organic compounds under hydrothermal conditions suggest that decreasing temperatures facilitate their formation (Shock, 1992; Shock and Schulte, 1998; Amend and McCollom, 2009; Shock and Canovas, 2010; Amend et al., 2011). This can also be seen in Figure 3-3 a) and b). The predicted amount of organic carbon for metastable states at 100°C is larger than at 250°C. However, slow the abiotic reaction rates at low temperatures then it is likely that that organic synthesis reactions are inhibited. Adequate conditions for organic syntheses require sufficient driving force, reaction rate, and retention time of the fluid in the reaction zone.

While thermodynamic drive for methanogenesis is dissipating, metastable organic intermediates may accumulate in hydrothermal fluids. Seewald et al. (2006) investigated the reduction from CO_2 to methane with formic acid/formate, formaldehyde, and methanol as intermediates. Each reduction step consumes one mol of H_2 for one mol of reactant. Crucial for this reduction sequence is the first step with equilibration of the water-gas shift reaction:

$$CO(aq) + H_2O \rightarrow CO_2(aq) + H_2(aq)$$

Once this equilibrium is attained CO equilibrates rapidly with H_2O to formic acid. Seewald et al. (2006) could determine kinetic data for the overall reaction, indicating that the half-life of the reaction slows down from 2.3h at 250°C to 3y at 100°C. Thus, at temperatures >200-250°C, formic acid (or formate, respectively) reacts with CO_2 and H_2 fast enough to reach equilibrium in hydrothermal systems. Seewald et al. (2006) also showed that measurable amounts of methanol were formed during the runtime of the experiment whereas formaldehyde concentrations were below the limit of detection of their method. The driving force to form formaldehyde is low under hydrothermal conditions, as seen in Figure 3-3 a) and b). So that Seewald et al. (2006) proposed that formaldehyde due to its reactivity and low driving force is reduced nearly to methanol as soon as it is formed.

3.5.2 Methanogenesis versus carbonate precipitation

Since methanol forms relatively fast, its further reduction to methane may be the rate-limiting step in the overall methanogenesis reaction. Figure 3-3 shows where methanol and formate are stable at 100 and 250°C as a function of W/R. The results indicate that these organics are stable in a narrow W/R range. Towards higher and lower W/R both DIC and carbonate predominate. With the transition from Brc-Srp to Cpx-Brc-Srp buffer at low W/R calcite becomes more stable than the intermediate organic compounds, which is a conse-

quence of the increased pH and Ca content of the fluid. Despite the high H_2 activities at low W/R, only more reduced organic species, such as methane and ethane, are stable because of the large driving force (H_2 activity has a power of 3 or 4 in the relevant mass action equations). At high W/R (approximating seawater composition) the stability of formate and methanol is determined by the minimum H_2 activity required to reduce DIC to the organic compound. Another important parameter is temperature, which increases the stability of $CO_2 + H_2$ relative to that of hydrocarbons.

The results presented in Figure 3-3 imply that the formation of organic compounds is favored in a relatively small range of W/R. Although formate/formic acid is predicted to be in equilibrium at high temperatures, the expected concentrations under these conditions are low. Further reduction of formate and formic acid to formaldehyde and methanol, respectively, is favored as W/R decreases. This is because elevated H_2 facilitates methanol formation (Figure 3-3). Slow reaction kinetics will limit the amount of methanol, but methanol forms much more rapidly than methane (Seewald et al., 2006). It is therefore likely that the last step in reduction to methane is inhibited by a kinetic barrier, which leads to an enrichment in methanol. As seen in Figure 3-3 methanol is more abundant than formic acid. Methanol shows the same behavior as formic acid when the system changes to the secondary Cpx-Brc-Srp buffer. If methanol forms at higher W/R and the system evolves further to lower W/R, methanol concentrations are predicted to decrease by oxidation and carbonate precipitation. Methane is stable throughout the entire range of W/R, so that methanol may also react to methane, in which case it is not available to form carbonate. It is likely that calcite precipitation is kinetically faster than the reduction of methanol to methane. Hence, the bulk of the methane in the LCHF fluids must have formed at elevated W/R, when methanol concentrations can increase outside of the stability field of carbonates. The formation of formate strongly depends on temperature. At high temperatures, formate will become less abundant because of the fast kinetic of the water-gas shift reaction and to keep the equilibrium stable. At lower temperatures the formate equilibrium is kinetically sluggish this implies that the formate can still be present in higher concentrations, as it is predicted for small W/R.

The formation of carbonates hence has a strong impact on abiotic organosynthesis. If the system reaches calcite saturation only low concentrations of inorganic carbon are available for reduction by H_2. Although methane formation is still predicted to take place, its precursor (methanol) is not expected to build up in the system, so that the kinetics of methane formation are probably very slow. In addition, it is critical how much inorganic carbon is lost in the recharge zone by precipitation of magnesite or dolomite. The model shows that at low temperatures their precipitation is predicted. Experimental evidence suggests that magnesite precipitation rates increases with temperature (Saldi et al. 2012). Giammar et al.(2005) suggest that a saturation index (SI) between 0.25 and 1.14 is necessary at 95°C to precipitate magnesite. The predicted SI of magnesite ranges between 0.1 and 0.75 in our models. Hence, it is questionable if the system is sufficiently saturated for magnesite precipitation. These results imply that in cases of low supersaturation, higher concentrations of dissolved carbon can be expected and this may facilitate the transport of CO_2 to the most reducing part of the reaction zone. Higher temperatures are unlikely to promote precipitation of significant

amounts of magnesite because aqueous CO_2 becomes increasingly stable with temperature (Figure 3-3 f). Thus it remains unclear whether carbonate will limit the formation of organic compounds in the reaction zone of Lost City .

The formation of organic compounds has further implications for the mineralogical composition of serpentinite. Magnetite abundance increases if organic carbon species are allowed to form. Figure 3-5 shows how much the magnetite abundance is influenced by the different organic species at 100°C. Methane has the highest driving force and can buffer the hydrogen concentration (reduction potential) in the system to the lowest value, which facilitates the formation of magnetite. Increased hydrogen concentrations cause a decrease in magnetite abundance. Consequently, Fe is incorporated in serpentine and brucite.

The stoichiometry of the serpentine-brucite-magnetite buffer:

$$3\,Fe(OH)_2 + 3\,Mg(OH)_2 + Fe_3Si_2O_5(OH)_4 = 2\,Fe_3O_4 + Mg_3Si_2O_5(OH)_4 + 4\,H_2O + 2\,H_2(aq)$$

3 Fe-brucite + 3 brucite + greenalite = 2 magnetite + chrysotile + 4 water + 2 hydrogen

illustrates this relation. As $H_2(aq)$ is consumed in the reduction of CO_2, equilibrium will shift to the right and more magnetite will form.

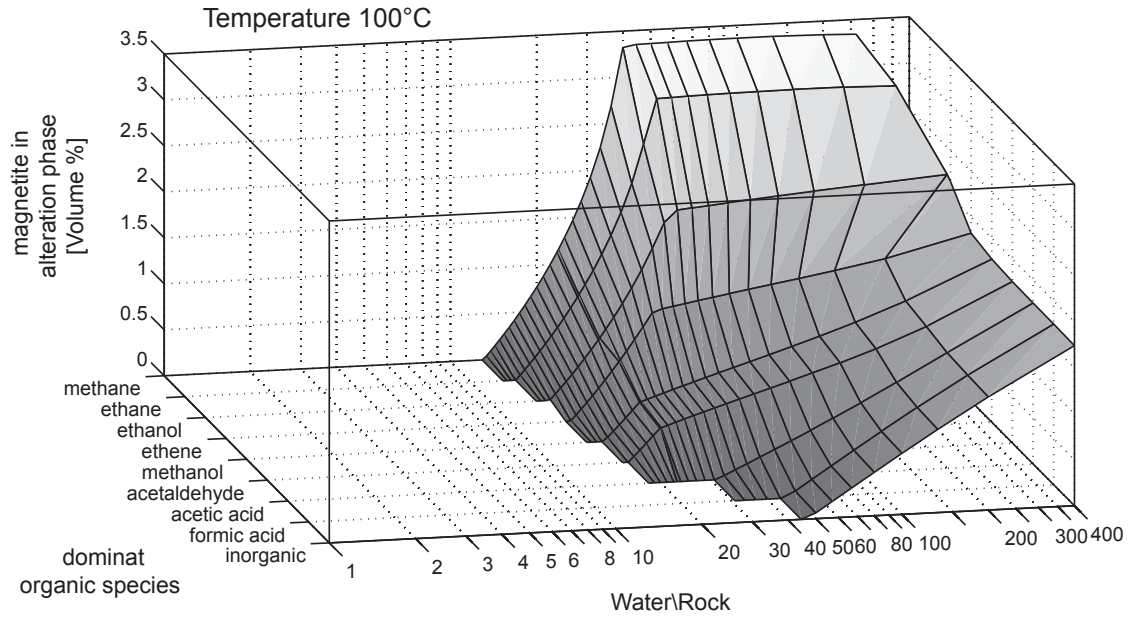

Figure 3-5: Magnetite abundance relative to the dominant organic species and W/R at 100°C. Methane dominates if all organic species are allowed to form. The formation of methane has a large positive effect on the predicted magnetite. This effect is decreases with suppression of methane and subsequent dominant species and results from the buffered hydrogen concentration when organic species formation is allowed. Each organic species has another thermodynamic driving force and buffers the hydrogen to a different concentration until the equilibrium is reached. Low hydrogen concentrations favor the formation of magnetite.

3.5.3 Implications for Lost City

Lost City vent fluid compositions have been suggested to indicate temperatures around 250°C and W/R of 2 to 4 in the root zone (Allen and Seyfried, 2004; Foustoukos et al., 2008). Our model calculations suggest that, under these temperatures and W/R conditions the fluids should be Cpx-Brc-Srp buffered and CO_2 should be reduced to methane or else should precipitate calcite if methane formation is inhibited. Analyses of fluids from Lost City indeed show very low concentrations of inorganic carbon (Proskurowski et al., 2008), are calcite saturated, and show high concentrations of methane and other organic compounds (Proskurowski et al., 2008; Konn et al., 2009; Lang et al., 2010).

Methane concentrations between 0.9 and 2.0 mM (Proskurowski et al., 2008) indicate that methane formation by CO_2 reduction takes place, but not all the CO_2 sourced from recharging seawater and magmatic degassing is reduced to methane in the reaction zone.

Isotopic evidence suggests that Fischer-Tropsch-Type (FFT) abiotic organosynthesis reactions causes the formation of C2-C4 alkanes at Lost City (Proskurowski et al., 2008). FFT synthesis (Fischer, 1935; Anderson et al., 1984) is an industrial process in which a mixture of CO and H_2 gases reacts to form hydrocarbons and is frequently proposed for organic formation in hydrothermal systems (McCollom et al., 1999; McCollom and Seewald, 2001; Rushdi and Simoneit, 2001, 2005; Rushdi and Simoneit, 2006; Seewald et al., 2006; Konn et al., 2009). However, methane is more enriched in the industrial FTT products than it is the case at Lost City (i.e., methane / ethane ratios are much higher than expected for FTT processes). This discrepancy tentatively indicates that Sabatier-type synthesis causes methane generation (McCollom and Seewald, 2007) rather than FTT.

The CH_4, CO_2, and H_2 concentrations in the Lost City vent fluids suggest ample thermodynamic drive to make more methane than has been actually measured. Hence, organosynthesis at Lost City is possible (Figure 3-4). It is worthwhile to compare predicted with observed concentrations of intermediate C1 components. Lang et al. (2010) measured formic acid concentrations in the Lost City hydrothermal fluids that range between 36 and 158 µM. Thermodynamic calculations from Lang et al. (2010) show that there is an excess of formic acid relative to what would be expected from equilibrium with CO_2 and H_2. Lang et al (2010) discuss the formation of formic acid from DOC (dissolved organic carbon) but the carbon isotopic composition of the formic acid shows no evidence for this hypothesis.

A comparison of the measured vent fluid and the modeled fluid reveals that H_2 concentrations in the model are up to ten times higher than the measured concentrations (Table 3-3). The lowest modeled H_2 concentration is 20.1 mM at 175°C and a WR of 10, the highest measured concentration reported by Lang et al.(2010) is 12.3 mM. Increasing temperatures enhance this difference because more hydrogen is predicted at these conditions (Figure 3-3 g) and h)).

The measured venting temperatures are between 43 and 90°C, and model temperatures on the basis of the H_2-H_2O D/H isotope thermometer (Horibe and Craig, 1995) are only slightly higher (55 to 106°C; Horibe and Craig, 1995; Proskurowski et al., 2006). These temperatures are substantially lower than the ones calculated from fluid composition by Allen and Seyfried (2004) and Foustoukos et al (2008) indicating conductive cooling of the fluids from the reaction zone to the discharge zone. The temperatures of venting are sufficiently

low to allow microbial life. Indeed, there is ample evidence for hydrogenotrophic metabolic pathways (methanotrophy, sulfate reduction) from microbiological investigations (Schrenk et al., 2004; Brazelton et al., 2006). The venting fluid is therefore most likely already depleted in hydrogen by microbial respiration. Indeed, vent fluids with low concentration of hydrogen were suggested to be altered by sulfate reduction (Proskurowski et al., 2006).

Table 3-3: Formic acid concentration in the model. Highest concentration and WR 5, 4 and 2.

Temperature (°C)	Water/Rock	HCO_3^- (μM)	H^2(aq) (mM)	Formic acid (μM)	*In situ* pH
100	5.13	17.7	21.7	205	8.0
100	4.00	0.279	26.6	4.01	9.8
100	2.00	0.269	44.6	6.79	9.8
150	5.06	33.6	27.8	191	7.3
150	4.00	1.07	33.9	7.52	8.8
150	2.00	1.04	58.3	13.1	8.8
175	10	68.4	20.1	180	6.2
175	5.06	41.0	31.4	171	7.0
175	4.00	1.77	37.5	8.89	8.4
175	2.00	1.71	65.2	15.7	8.4
200	8.33	70.8	27.5	172	6.0
200	5.12	47.2	39.5	165	6.8
200	4.00	2.71	46.9	11.4	8.0
200	2.00	2.62	72.1	17.7	8.0
250	6.90	72.2	40.7	130	5.7
250	5.06	57.2	53.0	129	6.5
250	4.00	5.42	64.7	15.0	7.5
250	2.00	5.24	111	26.1	7.5

In our model calculations, the highest concentrations of formic acid are predicted at high W/R and within the Brc-Srp buffered region. Within the predicted W/R range of 2 to 4 (Foustoukos et al., 2008) the model calculations predict low formic acid concentrations in the range of 4 to 26 μM, but distinctly higher concentration of hydrogen than what is measured (Table 3-3). Clearly, the formation of carbonate predicted to take place under Cpx-Brc-Srp buffered conditions is responsible for the decreased formic acid concentrations. Carbonate precipitation competes with the reduction of CO_2 to formic acid and is a critical limiting factor for transforming CO_2 to organic species in the model.

3.6 Conclusions

A probable scenario to describe the generation of Lost City fluids might be that seawater is heated rapidly. This will avoid the loss of CO_2 by precipitation of magnesite or dolomite because the carbon can be kept in solution through the enhanced stability of CO_2. This state would also allow the addition of CO_2 from a magmatic source as proposed from Proskurowski et al. (2008) on the basis of high ^3He fluxes. Higher temperatures increase the reaction rate for rock alteration and abiotic organic synthesis. With increasing temperatures and decreasing W/R along the fluid flow path, H_2 production is enhanced and there is ample drive for the formation of methane as well as other organic compounds. Methanol forms reasonably fast and may be a critical precursor in the formation of methane. Because of the high concentrations of methane, which forms slowly from methanol, the fluids have dwelled in the region of metastable methanol formation (e.g., W/R >5, 200-250°C. Under these conditions, predicted metastable formic acid concentrations are also similar to what is measured in the vent fluids. Further reaction with rock (lower W/R) would lead to carbonate precipitation and methanol and formic acid concentrations are predicted to decrease by reduction to methane or re-oxidation to CO_2 before the fluids vent at the seafloor. Crucial here is that the formation of carbonates is kinetically faster than the reduction methane. Formic acid formation is faster and may proceed in the reaction zone. The high levels of formic acid formed during that stage were apparently preserved in the fluids. One possibility is that formic acid did not react in the course of discharge and cooling because decreasing temperatures slowed down the reaction kinetics enough to stabilize it.

3.7 References

Allen, D.E., Seyfried, J.W.E., 2004. Serpentinization and heat generation: constraints from Lost City and Rainbow hydrothermal systems. Geochimica et Cosmochimica Acta 68, 1347-1354.

Amend, J.P., McCollom, T.M., 2009. Energetics of Biomolecule Synthesis on Early Earth, Chemical Evolution II: From the Origins of Life to Modern Society. American Chemical Society, pp. 63-94.

Amend, J.P., McCollom, T.M., Hentscher, M., Bach, W., 2011. Catabolic and anabolic energy for chemolithoautotrophs in deep-sea hydrothermal systems hosted in different rock types. Geochimica et Cosmochimica Acta 75, 5736-5748.

Anderson, R.B., Kölbel, H., Rálek, M., 1984. The Fischer-Tropsch synthesis. Academic Press.

Berndt, M.E., Allen, D.E., Seyfried, W.E., 1996. Reduction of CO_2 during serpentinization of olivine at 300°C and 500 bar. Geology 24, 351-354.

Boschi, C., Früh-Green, G.L., Delacour, A., Karson, J.A., Kelley, D.S., 2006. Mass transfer and fluid flow during detachment faulting and development of an oceanic core complex, Atlantis Massif (MAR 30°N). Geochemistry, Geophysics, Geosystems 7, Q01004.

Brazelton, W.J., Schrenk, M.O., Kelley, D.S., Baross, J.A., 2006. Methane- and Sulfur-Metabolizing Microbial Communities Dominate the Lost City Hydrothermal Field Ecosystem. Applied and Environmental Microbiology 72, 6257-6270.

Charlou, J.L., Donval, J.P., Fouquet, Y., Jean-Baptiste, P., Holm, N., 2002. Geochemistry of high H2 and CH4 vent fluids issuing from ultramafic rocks at the Rainbow hydrothermal field (36°14'N, MAR). Chemical Geology 191, 345-359.

Dick, J.M., 2008. Calculation of the relative metastabilities of proteins using the CHNOSZ software package. Geochemical Transactions 9, 10.

Drummond, S.E., 1981. Boiling and mixing of hydrothermal fluids. University Microfilms Int., Ann Arbor, Mich., p. 397 S.

Fischer, F., 1935. Die Synthese der Treibstoffe (Kogasin) und Schmieröle aus Kohlenoxyd und Wasserstoff bei gewöhnlichen Druck. Brennstoff-Chemie 16, 1-11.

Foustoukos, D.I., Savov, I.P., Janecky, D.R., 2008. Chemical and isotopic constraints on water/rock interactions at the Lost City hydrothermal field, 30°N Mid-Atlantic Ridge. Geochimica et Cosmochimica Acta 72, 5457-5474.

Giammar, D.E., Bruant Jr, R.G., Peters, C.A., 2005. Forsterite dissolution and magnesite precipitation at conditions relevant for deep saline aquifer storage and sequestration of carbon dioxide. Chemical Geology 217, 257-276.

Holm, N.G., Charlou, J.L., 2001. Initial indications of abiotic formation of hydrocarbons in the Rainbow ultramafic hydrothermal system, Mid-Atlantic Ridge. Earth and Planetary Science Letters 191, 1-8.

Horibe, Y., Craig, H., 1995. D/H fractionation in the system methane-hydrogen-water. Geochimica et Cosmochimica Acta 59, 5209-5217.

Huber, C., Wächtershäuser, G., 2003. Primordial reductive amination revisited. Tetrahedron Letters 44, 1695-1697.

Johnson, J.W., Oelkers, E.H., Helgeson, H.C., 1992. SUPCRT92: A software package for calculating the standard molal thermodynamic properties of minerals, gases, aqueous species, and reactions from 1 to 5000 bar and 0 to 1000°C. Computers & Geosciences 18, 899-947.

Karson, J.A., Früh-Green, G.L., Kelley, D.S., Williams, E.A., Yoerger, D.R., Jakuba, M., 2006. Detachment shear zone of the Atlantis Massif core complex, Mid-Atlantic Ridge, 30°N. Geochemistry, Geophysics, Geosystems 7, Q06016.

Kelley, D.S., Karson, J.A., Blackman, D.K., Fruh-Green, G.L., Butterfield, D.A., Lilley, M.D., Olson, E.J., Schrenk, M.O., Roe, K.K., Lebon, G.T., Rivizzigno, P., the, A.T.S.P., 2001. An off-axis hydrothermal vent field near the Mid-Atlantic Ridge at 30° N. Nature 412, 145-149.

Klein, F., Bach, W., Jöns, N., McCollom, T., Moskowitz, B., Berquó, T., 2009. Iron partitioning and hydrogen generation during serpentinization of abyssal peridotites from 15°N on the Mid-Atlantic Ridge. Geochimica et Cosmochimica Acta 73, 6868-6893.

Konn, C., Charlou, J.L., Donval, J.P., Holm, N.G., Dehairs, F., Bouillon, S., 2009. Hydrocarbons and oxidized organic compounds in hydrothermal fluids from Rainbow and Lost City ultramafic-hosted vents. Chemical Geology 258, 299-314.

Lang, S.Q., Butterfield, D.A., Schulte, M., Kelley, D.S., Lilley, M.D., 2010. Elevated concentrations of formate, acetate and dissolved organic carbon found at the Lost City hydrothermal field. Geochimica et Cosmochimica Acta 74, 941-952.

Ludwig, K.A., Kelley, D.S., Butterfield, D.A., Nelson, B.K., Früh-Green, G., 2006. Formation and evolution of carbonate chimneys at the Lost City Hydrothermal Field. Geochimica et Cosmochimica Acta 70, 3625-3645.

Martin, W., Baross, J., Kelley, D., Russell, M.J., 2008. Hydrothermal vents and the origin of life. Nature Reviews Microbiology 6, 805-814.

McCollom, T.M., Ritter, G., Simoneit, B.R.T., 1999. Lipid Synthesis Under Hydrothermal Conditions by Fischer- Tropsch-Type Reactions. Origins of Life and Evolution of Biospheres 29, 153-166.

McCollom, T.M., Seewald, J.S., 2001. A reassessment of the potential for reduction of dissolved CO_2 to hydrocarbons during serpentinization of olivine. Geochimica et Cosmochimica Acta 65, 3769-3778.

McCollom, T.M., Seewald, J.S., 2007. Abiotic Synthesis of Organic Compounds in Deep-Sea Hydrothermal Environments. Chem. Rev. 107, 382-401.

Proskurowski, G., Lilley, M.D., Kelley, D.S., Olson, E.J., 2006. Low temperature volatile production at the Lost City Hydrothermal Field, evidence from a hydrogen stable isotope geothermometer. Chemical Geology 229, 331-343.

Proskurowski, G., Lilley, M.D., Seewald, J.S., Früh-Green, G.L., Olson, E.J., Lupton, J.E., Sylva, S.P., Kelley, D.S., 2008. Abiogenic Hydrocarbon Production at Lost City Hydrothermal Field. Science 319, 604-607.

Rushdi, A., Simoneit, B., 2006. Abiotic Condensation Synthesis of Glyceride Lipids and Wax Esters Under Simulated Hydrothermal Conditions. Origins of Life and Evolution of Biospheres 36, 93-108.

Rushdi, A.I., Simoneit, B.R.T., 2001. Lipid Formation by Aqueous Fischer-Tropsch-Type Synthesis over a Temperature Range of 100 to 400 °C. Origins of Life and Evolution of Biospheres 31, 103-118.

Rushdi, A.I., Simoneit, B.R.T., 2005. Abiotic Synthesis of Organic Compounds from Carbon Disulfide Under Hydrothermal Conditions. Astrobiology 5, 749-769.

Russell, M., J., Hall, A., J., 2009. The Hydrothermal Source of Energy and Materials at the Origin of Life, Chemical Evolution II: From the Origins of Life to Modern Society. American Chemical Society, pp. 45-62.

Saldi, G.D., Schott, J., Pokrovsky, O.S., Gautier, Q., Oelkers, E.H., 2012. An experimental study of magnesite precipitation rates at neutral to alkaline conditions and 100–200°C as a function of pH, aqueous solution composition and chemical affinity. Geochimica et Cosmochimica Acta 83, 93-109.

Schrenk, M.O., Kelley, D.S., Bolton, S.A., Baross, J.A., 2004. Low archaeal diversity linked to subseafloor geochemical processes at the Lost City Hydrothermal Field, Mid-Atlantic Ridge. Environmental Microbiology 6, 1086-1095.

Schulte, M., Blake, D., Hoehler, T., McCollom, T., 2006. Serpentinization and Its Implications for Life on the Early Earth and Mars. Astrobiology 6, 364-376.

Seewald, J.S., Zolotov, M.Y., McCollom, T., 2006. Experimental investigation of single carbon compounds under hydrothermal conditions. Geochimica et Cosmochimica Acta 70, 446-460.

Shock, E., Canovas, P., 2010. The potential for abiotic organic synthesis and biosynthesis at seafloor hydrothermal systems. Geofluids 10, 161-192.

Shock, E.L., 1992. Chapter 5 Chemical environments of submarine hydrothermal systems. Origins of Life and Evolution of Biospheres (Formerly Origins of Life and Evolution of the Biosphere) 22, 67-107.

Shock, E.L., Schulte, M.D., 1998. Organic synthesis during fluid mixing in hydrothermal systems. Journal of Geophysical Research 103, 28513-28528.

Welhan, J.A., 1988. Origins of methane in hydrothermal systems. Chemical Geology 71, 183-198.

Wolery, T., Jarek, R., 2003. EQ3/6, Version 8.0, Software User's Manual. Civilian Radioactive Waste Management System, Management & Operating Contractor. Sandia National Laboratories, Albuquerque, New Mexico.

Wolery, T., Jove-Colon, C., 2004. Qualification of thermodynamic data for geochemical modeling of mineral-water interactions in dilute systems. YMP (Yucca Mountain Project, Las Vegas, Nevada).

Wolery, T.J., 1992a. EQ3/6: A software package for geochemical modeling of aqueous systems: package overview and installation guide (version 7.0). Lawrence Livermore National Laboratory.

Wolery, T.J., 1992b. EQ3NR, a computer program for geochemical aqueous speciation-solubility calculations: theoretical manual, user's guide, and related documentation (version 7.0). Lawrence Livermore National Laboratory, Livermore, California.

Wolery, T.J., Daveler, S.A., Laboratory, L.L., 1992. EQ6, a computer program for reaction path modeling of aqueous geochemical systems: theoretical manual, user's guide and related documentation (Version 7.0). Lawrence Livermore Laboratory, University of California.

4. Thermodynamic assessment of catabolic and anabolic energetics in submarine hydrothermal systems

4.1 Summary

This chapter presents a comprehensive and systematic assessment of energetics of chemolithoautotrophs in the deep-sea. Submarine hydrothermal vent systems are generally accompanied by high microbial activity forming the base of a food-web that often include higher organisms. The primary production of biomass is boosted by redox disequilibrium that serves as energy source for chemolithoautotrophic microbial life. The redox disequilibrium is generated by (1) mixing of chemical reduced hydrothermal vent fluids with ambient seawater, (2) interaction of seawater with basement, (3) volcanic degassing, or interplays of these processes. I conducted computational simulations of these processes and calculated associated affinities of catabolic (energy-harvesting) and anabolic (biosynthesis) reactions along widely variable reaction paths. These computations are aimed at mapping out what metabolic strategies may be exploited in different environments and how much biomass may be produced. This approach has been used to asses the catabolic energy demands and catabolic energy yields in a range of hydrothermal vents in different rock type and geotectonic settings (Amend et al., 2011). Furthermore, from the difference between predicted and observed concentrations of non-conservative species in diffuse fluids, energetically feasible catabolic pathways will be identified and provide insights into subseafloor microbial metabolism. Examples from combined microbiological and thermodynamic studies of diffuse fluids from Mid-Atlantic Ridge 5°S and 9°S hydrothermal vent sites demonstrate the strong control of fluid composition on microbial community compositions (Perner et al., 2009; Perner et al., 2011). A borehole incubation study in ridge flank hydrothermal systems (Orcutt et al., 2011) has revealed temporal changes in microbial community composition from Fe(II) oxidizer dominated in the first period to a stage of microbial nitrogen and sulfur cycling after the borehole had attained its natural state. That shift in the prevailing microbial metabolism can be explained by radical changes in the affinities of the different catabolic reactions calculated from geochemical data of the borehole fluids.

4.2 Introduction

The hot spots of life in the deep sea are associated with hydrothermal vent systems, where reduced, metal- and sulfide-rich fluids are generated by water-rock reactions and magmatic degassing. Where these fluids mix with oxygenated seawater, large redox disequilibria develop that can support chemolithoautotrophic microorganisms. Those microorganisms form the base of a unique foodweb that is independent of sunlight and strongly dependent on geological and geochemical processes supplying the energy in the form of

electron donors to the seafloor. The basic concept of chemotrophy is coupling an exergonic (energy yielding) catabolic reaction to an endergonic anabolic reaction such that the overall metabolic reaction can take place (Figure 4-1). The biomass yield (Y) is a function of the relative rates of anabolic and catabolic reactions and is always <1. This is a consequence of the fact that irreversible processes, such as cellular growth, will always take place at a loss of free energy (and an increase of entropy, here in form of release of heat and small molecules) (Schrodinger, 1944).

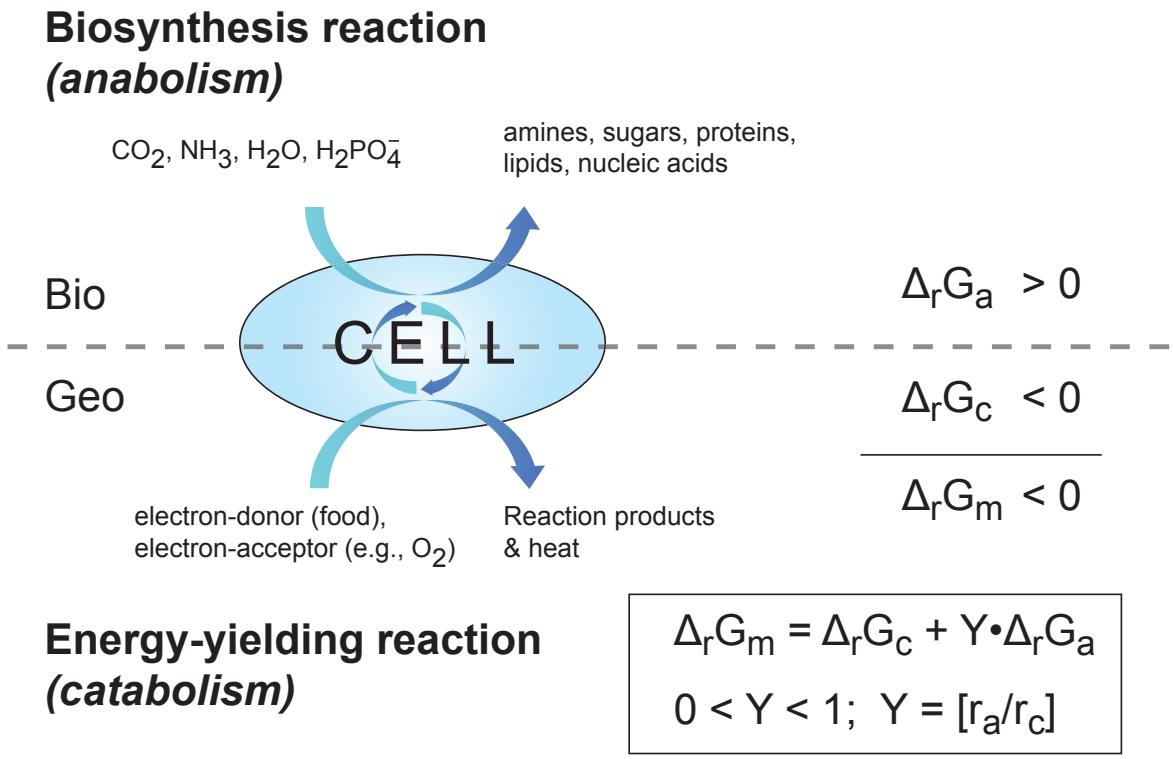

Figure 4-1: Cellular coupling of catabolic and anabolic reactions, by which a "payload" anabolic reaction is facilitated by a "driving" catabolic reaction in the overall metabolic framework. Redrawn after von Stockar et al.(2008)

A number of fundamentally different habitats have been identified where chemolitho-autotrophic primary production may take place (Jannasch, 1995; McCollom and Shock, 1997; McCollom, 2000; Kelley et al., 2001; Bach and Edwards, 2003; Mottl et al., 2003; Edwards et al., 2005; Kelley et al., 2005). One is in the direct vicinity of hydrothermal venting of 350 to 400°C hot fluids (Figure 4-2). Mixing of vent fluids and cold, oxygenated seawater will make conditions of moderate temperatures and abundance of chemical species that represent redox-couples known to be catalyzed by microbial enzymatic activity. The classic example is the aerobic oxidation of H_2S, but anaerobic reactions using sulfate, Fe(III) minerals or even CO_2 are also possible in many environments (Karl et al., 1980; Jannasch and Mottl, 1985; Jannasch, 1995). Mixing takes place in a turbulent regime in hydrothermal plumes, where the hydrothermal input is diluted by 5 to 6 orders of magnitude even within the buoyant part of the plume. Nonetheless, electron donors brought into the system by hydrothermal venting plume (e.g., H_2, CH_4, Mn) are still many orders of magnitude enriched in a dilute plume relative to background seawater and can support microbial life within the plume (Cowen et

al., 1986; Baker et al., 1995; McCollom 2000). It has been shown that biomass production relative to methane venting is high, as about 25% of the amount of methane-bound carbon influx gets fixed by aerobic methane oxidizers (de Angelis et al., 1993).

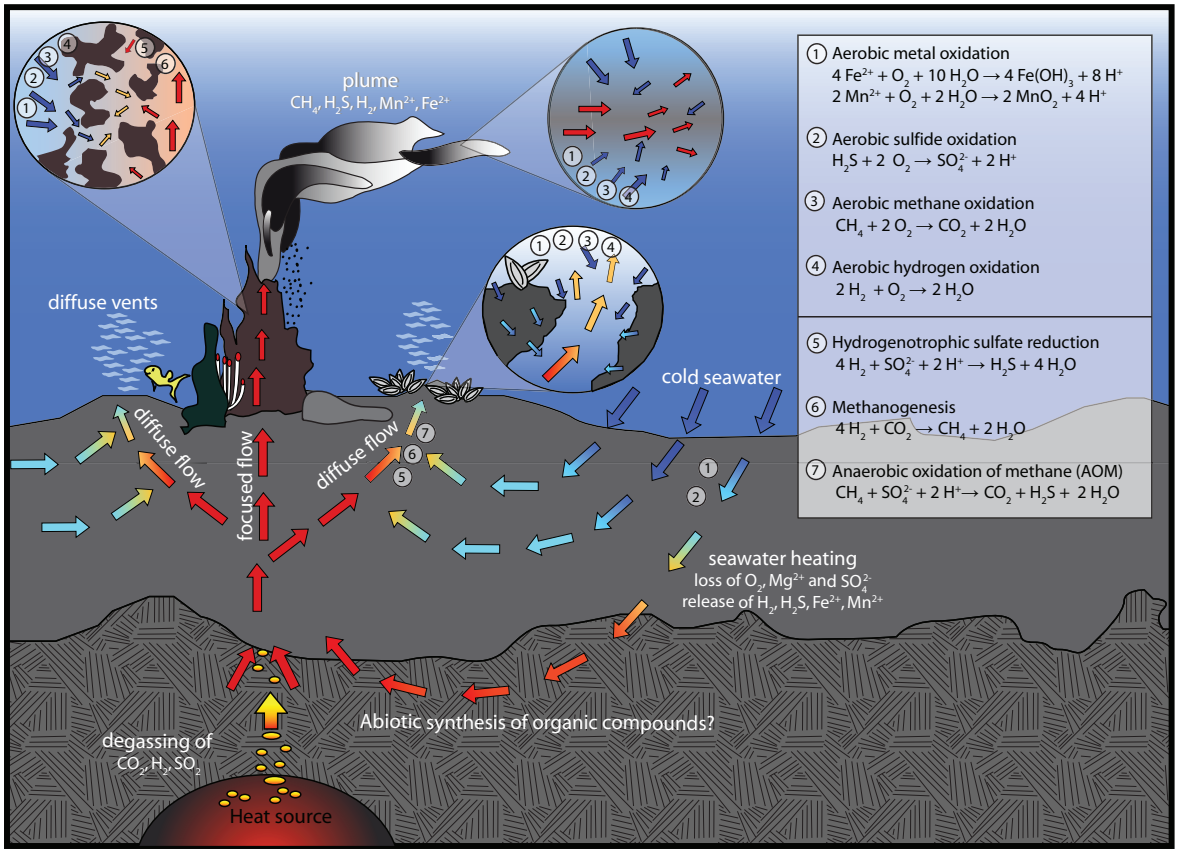

Figure 4-2: Sketch of a hydrothermal vent site and some of the catabolic reactions that can support chemolithoautotrophic life in the different compartments of the system.

Another habitat for microorganisms in vent sites is the wall of the black smoker sulfide chimneys, where microorganisms thrive in steep gradients of temperature, pH, and redox conditions (McCollom and Shock, 1997; Kormas et al., 2006; Pagé et al., 2008). Besides hydrothermal plumes and sulfide chimney walls, a likely habitat for microorganisms is the subseafloor, where upwelling vent fluids and cold seawater mix and form low-temperature hydrothermal fluids that slowly seep out of the seafloor (diffuse fluids) (Schultz and Elderfield, 1997; Butterfield et al., 2004). Areas of diffuse venting are extremely common in submarine hydrothermal vent fields around the world. In terms of transport of heat and solutes, the diffuse fluid flow can be more important that the focused venting through black smokers by up to a factor of 10 (Rona and Trivett, 1992; Schultz et al., 1992). Indeed, microbiological (Holden et al., 1998; Huber et al., 2003) and geochemical (Von Damm and Lilley, 2004; Proskurowski et al., 2008) investigations provide strong support for microbial activity within this subseafloor mixing zone. A much more common environment where microbial life can thrive is in hydrologically active ocean crust, comprising about 50% of all seafloor (Stein et al., 1995; Elderfield and Schultz, 1996). How much microbial biomass can be supported

in these systems is still largely unknown, but the numbers are potentially large and could be significant relative to subseafloor life in marine sediments (Bach and Edwards, 2003).

Microbial biomass production can be assessed by linking energy availability directly to ATP production (Thauer et al., 1977; LaRowe and Helgeson, 2006a, b), or by using empirical Gibbs energy dissipation approaches (Heijnen and Van Dijken, 1992; Tijhuis et al., 1993). Bioenergetic approaches have also been used to calculate minimal substrate concentrations required for survival, maintenance, and growth of microorganisms (Harder, 1997; Hoehler, 2004).

In many thermodynamic treatments of growth, only standard Gibbs energies have been used assuming that concentration-dependent terms will not modify the calculation results significantly (von Stockar and van der Wielen, 1997; Battley, 1998). Environmental conditions, however, range so strongly in some environments that substrate and product concentrations and speciation matter (Conrad et al., 1986). This is particularly true for hydrothermal settings, where (1) pressure and temperature conditions are different from standard state and (2) the free energies for catabolic reactions often differ radically from molality (McCollom and Shock, 1997).

The physicochemical conditions in hydrothermal systems are extremely variable (in terms of redox, metal and sulfur contents, pH), which affects not only the energetics of the catabolic (energy-yielding) reactions but also that of anabolic (biosynthesis) reactions. It has long been recognized that there may be an energetic advantage to autotrophic growth in anaerobic environments arising from the smaller amount of energy required for synthesis of biomolecules under reducing conditions (Morowitz, 1968). This advantage is apparently reflected in the lower energy requirements for some metabolic pathways in anaerobes relative to analogous pathways in aerobes, and in higher biomass yields per unit energy input for anaerobes compared to aerobes. Assessments of growth yields indicate that autotrophic anaerobes such as methanogens require ~30-40 kJ to produce each g (dry wt.) of biomass, whereas aerobic autotrophs (including sulfide-, thiosulfate-, iron-, ammonium-, and nitrite-oxidizers) require between 80 and 170 kJ per gram of biomass (Heijnen and Van Dijken, 1992). McCollom and Amend (2005) used thermodynamic calculations to demonstrate that synthesis of cellular biomass by autotrophs should require less energy in anaerobic than aerobic environments and evaluated this effect quantitatively. Specifically, computations based on the thermodynamic properties of individual cellular components (amino acids, nucleotides, etc.) were used to quantify and compare the relative energetic costs of cellular biomass synthesis under aerobic and anaerobic conditions. The results indicate that aerobic organisms require up to 17 $kJ \cdot (g\ cells)^{-1}$ more energy than anaerobes to synthesize the same amount of biomass. This advantage may help explain why anaerobic organisms appear to yield greater biomass per unit energy input than aerobic organisms in laboratory growth studies, and why anaerobic microbes can exist where the energy yield from catabolism is extremely low. Microbial habitability of submarine hydrothermal environments must therefore be examined by coupled investigations of energy supply and demand in a specific setting.

The following three sections of this chapter summarize thermodynamic modelling contributions to research papers I have published jointly with various collaborators. In collaboration with Jan P. Amend, Tom M. McCollom and Wolfgang Bach I assessed the thermo-

dynamic potential for chemolithoautotrophic microbial life fueled by geochemical energy in different hydrothermal vents (subseafloor mixing zones and plumes (Amend et al., 2011)). I employed geochemical reaction path models for assessing the catabolic energy availability in these different settings and the catabolic energy requirement for synthesis of biomolecules. This work is summarized in section 4.4.1 of this chapter. I also conducted thermodynamic modeling in two other collaborative projects: Juan de Fuca Ridge flank (Orcutt et al., 2011) and Mid-Atlantic Ridge hydrothermal systems (Perner et al., 2009; Perner et al., 2011). In each of these joint projects I conducted all the thermodynamic calculations, helped with their interpretation and wrote parts of the methods and results sections. These contributions are summarized in this thesis chapter.

4.2.1 Hydrothermal systems

A plethora of submarine hydrothermal systems spans a wide variety of temperature, pressure, fluid and rock compositions, precipitate type and abundance (Figure 4-3). Settings range from mid-ocean ridges with axial high-temperature venting (Von Damm, 1990) to moderate temperature circulation systems in young ridge flanks either in basaltic basement (Mottl et al., 1998; Wheat and Mottl, 2000) or oceanic core complexes, where the lithospheric mantle is exhumed by detachment faulting (Tucholke et al., 1998; Kelley et al., 2001), to cold ridge flank circulation, often facilitated by the presence of seamounts (Fisher et al., 2003). In convergent margin settings, yet other types of hydrothermal systems are developed that are extremely acidic (pH 1-3) due to influx of CO_2 and/or SO_2 (sulfur dioxid) from degassing of volatile-rich magmas generated in supra-subduction zones. We provide a rigorous thermodynamic assessment of the catabolic and anabolic energy constraints in representatives of these different settings, using both geochemical reaction path models and chemical analyses of vent fluids and rocks.

Mid-ocean ridge sites

Areas suitable for the proposed studies are those for which chemical data are available for fluids. These include vents hosted in basalt occurring in the East Pacific Rise 21°N area (Von Damm, 1990), at the Endeavour vent field (Seewald et al., 2003; Seyfried et al., 2003), the Lucky Strike and Menez Gwen vent field (Charlou et al., 1998; Charlou et al., 2000), Trans-Atlantic Geotraverse (TAG) hydrothermal vent field (Charlou et al., 1996; Charlou et al., 1998), the Edmond Vent Field, Central Indian Ridge (Gallant and Von Damm, 2006) and peridotite-hosted vent fields like the Lost City (Kelley et al., 2005; Proskurowski et al., 2006) as well as the Logatchev and Rainbow vent fields (Charlou et al., 1998; Charlou et al., 2002; Douville et al., 2002). In addition, the Kairei vent filed (Gallant and Von Damm, 2006) which is located in troctolites and basalts, is included.

Back-arc basin / island-arc systems

Intra-oceanic arc and associated back-arc basin hydrothermal systems are represented by two vent sites: the Brothers vent field (Takai et al., 2008; Takai et al., 2009) located at the NW caldera of the Brothers volcano at the Kermadec Arc, and the Mariner hydrothermal

field at the crest of the Valu Fa Ridge in the Lau Basin (Takai et al., 2008). Both hydrothermal fields are variably influenced by carbonic acid and present the lowest pH conditions in this study. Because of combined biological and chemical studies at these vent sites, they presents the most comprehensive geochemical dataset for bioenergetic calculations.

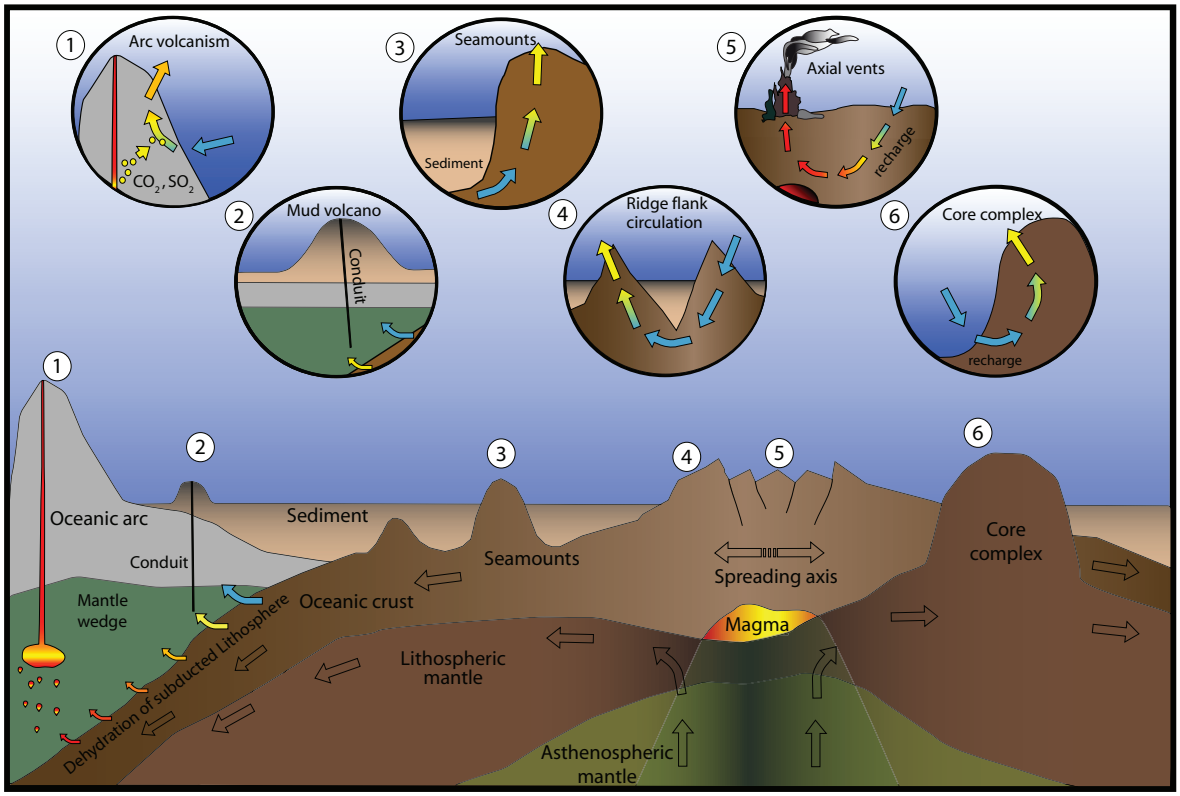

Figure 4-3: Schematic overview of the different types and styles of fluid flow systems in the submarine realm.

4.3 Methods

Thermodynamic calculations of free energies ($\Delta_r G$) of catabolic reactions were conducted using the relation $\Delta_r G = RT \cdot 2.303 \cdot (\log Q - \log K)$, where log Q is the sum of log activities of reaction products subtracted by the sum of log activities of the reactants, and log K is the equilibrium constant of reactions at seafloor conditions. Log K values were calculated using SUPCRT92 (Johnson et al., 1992) and a database that has all updates for inorganic and organic aqueous species (Dick, 2008). This database is frequently updated and extended by the author in collaboration with Tom McCollom and Jan Amend.

In computations of log Q by the program SpecE8, which is part of Geochemist's Workbench® (GWB) version 7.0.2 (Bethke, 1996), an extended Debye–Hückel equation (Helgeson, 1969) is used to calculate activity coefficients, with B–dot extended parameters and hard core diameters for each species taken from (Wolery, 2004). Dissolved neutral species are assigned an activity coefficient of one, except for non–polar species for which CO_2 activity coefficients were used (Drummond, 1981). Geochemical mixing calculations were carried out using the program REACT (GWB 7.0.2) and a thermodynamic database calculated by SUPCRT92 (Johnson et al., 1992). The data base consists of standard-state thermodynamic parameters, Maier-Kelley coefficients, and equation of state parameters for minerals and

aqueous species that are used to compute equilibrium constants for temperatures and pressures up to 1000°C and 500 MPa. In the mixing calculations, mineral precipitation and redox reactions were suppressed. This constraint allows predicting species distributions prior to mineral precipitation, acknowledging that these reactions can significantly affect fluid pH, redox, and aqueous species concentrations. The mixing calculations provide estimates of the quantity of free energy available if the diffuse fluids were simple mixtures of the high-temperature hydrothermal vent fluid and cold seawater. Discrepancies between free energies predicted from the mixing model and the actual free energies of redox reactions calculated for the diffuse fluid compositions provide insights into the kind of redox (i.e. potential catabolic) reactions taking place in the system. For instance, if the predicted free energy is equal to the actual free energy for a particular catabolic reaction, then that particular reaction is obviously not exploited by the microbial consortium. If, on the other hand, the calculated free energy is considerably lower than the predicted free energies, the redox reaction does proceed in the environment, likely catalyzed by microbial activity. This is particularly evident in reactions that have free energies close to the biological energy quantum of 10-20 kJ per mol reaction (Hoehler, 2004).

We calculated the Gibbs energies of catabolic and anabolic reactions for >20 catabolic and >60 anabolic reactions. Table 4-1 shows how different the apparent Gibbs energies are in a hydrothermal mixing environment from those at standard conditions. The numbers indicate that for many reactions thermodynamic calculations based on standard properties will be highly compromised. The results of these calculations allow estimations of (1) energy availability for microbial growth and maintenance and (2) energy demand for biosynthesis. The latter was accomplished by weighing the specific Gibbs energies of the individual biosynthesis reactions to reflect the actual composition of a microorganism (e.g., McCollom and Amend, 2005; Amend and McCollom, 2009). These results are evaluated against temperature-dependent energy demands for fixing and maintaining microbial biomass (Harder, 1997; Hoehler, 2004). Moreover, energy-balances in microbial biomass production from the view-point of Gibbs energy dissipation and related approaches popular in biochemical engineering (Heijnen and Van Dijken, 1992; Tijhuis et al., 1993; von Stockar and van der Wielen, 1997; von Stockar et al., 2006) were used in assessing biomass production.

Thermodynamic affinity of various redox reactions that may have occurred within the ridge flank observatory environment at Hole 1301A was also explored (Orcutt et al., 2011). This was done by calculating water-rock reaction path models (using GWB) for temperatures between 2 and 65°C and by simulating the interaction of 30 g of rock with 1 kg of seawater. The used a rock composition of 3.0 g olivine (Fo_{70}), 15.6 g plagioclase (An_{80}), 11.4 g clinopyroxene ($Wo_{50}En_{40}Fs_{10}$), and 0.05 g MnO, which corresponds to average Mid-Ocean Ridge basalt composition. Seawater composition represents deep sea water from near Hole 1301A (Wheat and Mottl, 2000). In the model, all redox couples (except H_2/H^+) were suppressed. A GWB thermodynamic database was constructed for 250 bars and temperatures from 2-65°C using SUPCRT92 databases mentioned above.

Table 4-1: Difference between standard Gibbs energy (25°C, 1bar, molal quantities) and apparent Gibbs energy calculated for a conservative mixture of 350°C vent fluid from the Logatchev hydrothermal field with seawater (25°C, 300bar, calculated activities). All numbers are in kJ/mol reaction.

	$\Delta_r G^o$	$\Delta_r G$	Reaction
H_2S oxidation	-751.78	-774.02	$H_2S(aq) + 2\,O_2(aq) = SO_4^{2-} + 2\,H^+$
Methanotrophy	-824.30	-815.08	$CH_4(aq) + 2\,O_2(aq) = CO_2(aq) + 2\,H_2O$
Fe(II) oxidation	-115.66	-293.70	$Fe^{2+} + 0.25\,O_2(aq) + 2.5\,H_2O = Fe(OH)_3 + 2\,H^+$
Knallgas reaction	-527.18	-471.73	$2\,H_2(aq) + O_2(aq) = 2\,H_2O$
Methanogenesis	-230.51	-128.84	$CO_2(aq) + 4\,H_2(aq) = CH_4(aq) + 2\,H_2O$
Sulfate reduction	-303.22	-170.07	$SO_4^{2-} + 4\,H_2(aq) + 2\,H^+ = H_2S(aq) + 4\,H_2O$
AOM	-72.71	-41.24	$CH_4(aq) + SO_4^{2-} + 2\,H^+ = H_2S(aq) + CO_2(aq) + 2\,H_2O$
Amino acids			
Alanine	52.45	-91.22	$3\,HCO_3^- + NH_4^+ + 6\,H_2(aq) + 2\,H^+ = C_3H_7NO_2 + 7\,H_2O$
Cysteine	37.08	5.32	$3\,HCO_3^- + NH_4^+ + H_2S + 5\,H_2(aq) + 2\,H^+ = C_3H_7NO_2S + 7\,H_2O$
Leucine	142.93	-289.45	$6\,HCO_3^- + NH_4^+ + 15\,H_2(aq) + 5\,H^+ = C_6H_{13}NO_2 + 16\,H_2O$
Serine	33.50	-0.39	$3\,HCO_3^- + NH_4^+ + 5\,H_2(aq) + 12\,H^+ = C_3H_7NO_3 + 6\,H_2O$
Valine	112.48	-221.71	$5\,HCO_3^- + NH_4^+ + 12\,H_2(aq) + 4\,H^+ = C_5H_{11}NO_2 + 13\,H_2O$
Nucleic acids			
AMP^{2-}	61.53	465.04	$10\,HCO_3^- + 5\,NH_4^{+} + HPO_4^{2-} + 15\,H_2(aq) + 5\,H^+ = C_{10}H_{12}N_5O_7P^{2-} + 27\,H_2O$
GMP^{2-}	60.15	455.62	$10\,HCO_3^- + 5\,NH_4^+ + HPO_4^{2-} + 14\,H_2(aq) + 5\,H^+ = C_{10}H_{12}N_5O_8P^{2-} + 26\,H_2O$
Fatty acids			
Palmiate	453.37	-1031.29	$16\,HCO_3^- + 46\,H_2(aq) + 15\,H^+ = C_{16}H_{31}O_2^- + 46\,H_2O$
Oleate	494.69	-1072.34	$18\,HCO_3^- + 51\,H_2(aq) + 17\,H^+ = C_{18}H_{33}O_2^- + 52\,H_2O$
Sugars			
Glycerol	48.45	-61.53	$3\,HCO_3^- + 7\,H_2(aq) + 3\,H^+ = C_3H_8O_3 + 6\,H_2O$
Glucose	79.93	7.65	$6\,HCO_3^- + 12\,H_2(aq) + 6\,H^+ = C_6H_{12}O_6 + 12\,H_2O$
N-acetylglucoamine	122.61	-48.06	$8\,HCO_3^- + NH_4^+ + 16\,H_2(aq) + 9\,H^+ = C_8H_{15}NO_6 + 18\,H_2O$
N-acetylmuramic acid	185.92	-143.23	$11\,HCO_3^- + NH_4^+ + 22\,H_2(aq) + 10\,H^+ = C_{11}H_{19}NO_8 + 25\,H_2O$
Amines			
Ethnolamine	28.13	-23.80	$2\,HCO_3^- + NH_4^+ + 5\,H_2(aq) + H^+ = C_2H_7NO + 5\,H_2O$
Diaminopilemic acid	115.59	-86.22	$7\,HCO_3^- + 2\,NH_4^+ + 14\,H_2(aq) + 5\,H^+ = C_7H_{14}N_2O_4 + 17\,H_2O$

4.4 Results and discussion

4.4.1 Bioenergetics in hydrothermal vents

The calculation of the available catabolic energy for mixtures of the seawater with hydrothermal fluid from 12 vent fields indicates distinct differences between the hosted rock types (Figure 4-4). In basalt-hosted and felsic rock-hosted systems, sulfide oxidation is clearly the dominant energy source followed by noticeable amounts of energy from methane and iron oxidation. Peridotite-hosted systems are characterized by a much larger diversity of catabolic energy sources and by a relatively low energy yield from sulfide oxidation. The high hydrogen content of these fluids generates drive for hydrogenotrophic catabolic reactions, like methanogenesis or sulfate reduction as well as hydrogen oxidation. These reactions are commonly endergonic in basalt-hosted systems; they increase the variability of energy sources in peridotite-hosted systems. The troctolite-basalt hybrid at Kairei seems to be an intermediate between the basalt and felsic rock-hosted systems on one side and the peridotite-hosted system on the other side.

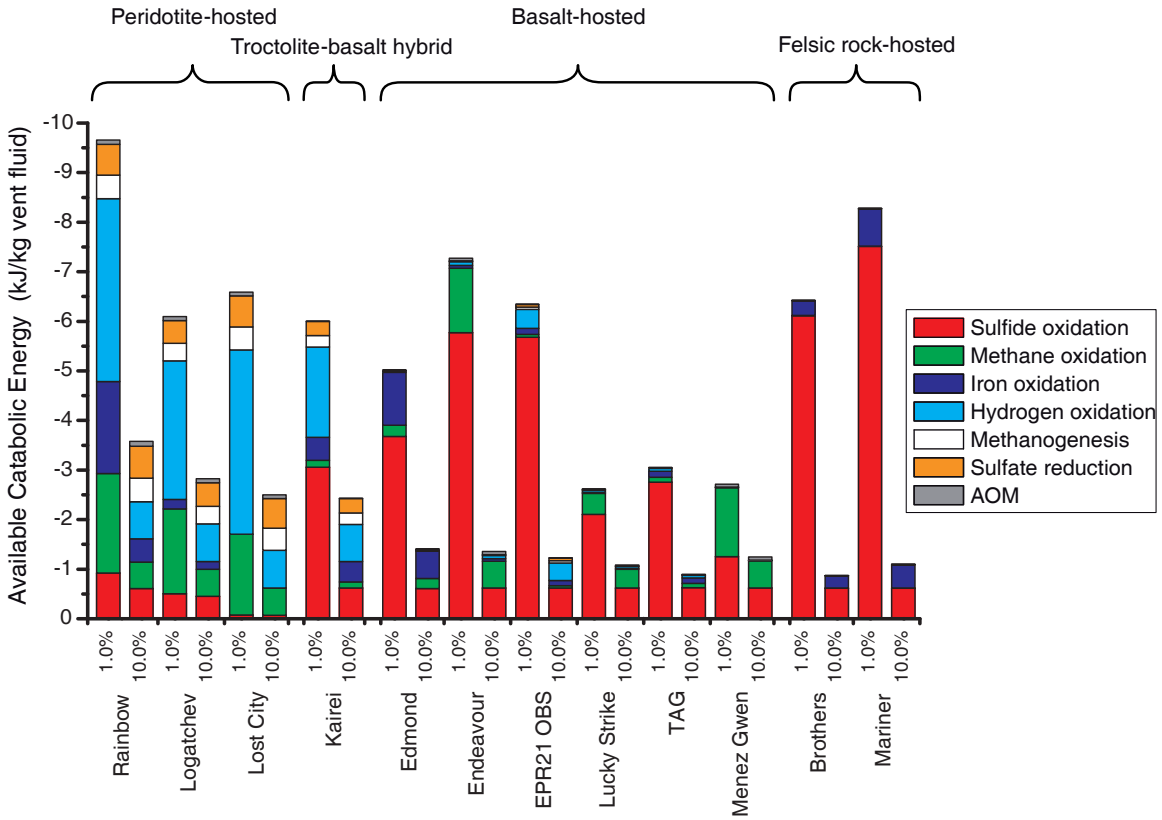

Figure 4-4: Catabolic energies (in kJ per kg vent fluid) available from seven different redox reactions in 12 hydrothermal systems hosted in peridotite, troctolite-basalt hybrid, basalt, and felsic rock. Values are computed at 1% and 10% hydrothermal fluid contribution to the mixed solutions.

Figure 4-5 depicts the consequence of the fluid composition for one example from each rock type. Energy yields are greatest at low temperatures with high seawater fractions for all systems. With increasing temperature (lower seawater fraction) the Gibbs energy values decrease rapidly. At Rainbow (peridotite-hosted), a fundamental transformation occurs

around. 45°C: two anaerobic processes (sulfate reduction and methanogenesis) become more exergonic than aerobic reactions. Both reactions remain strongly exergonic over the considered range of temperatures, while the affinities for aerobic processes decline with increasing temperature.

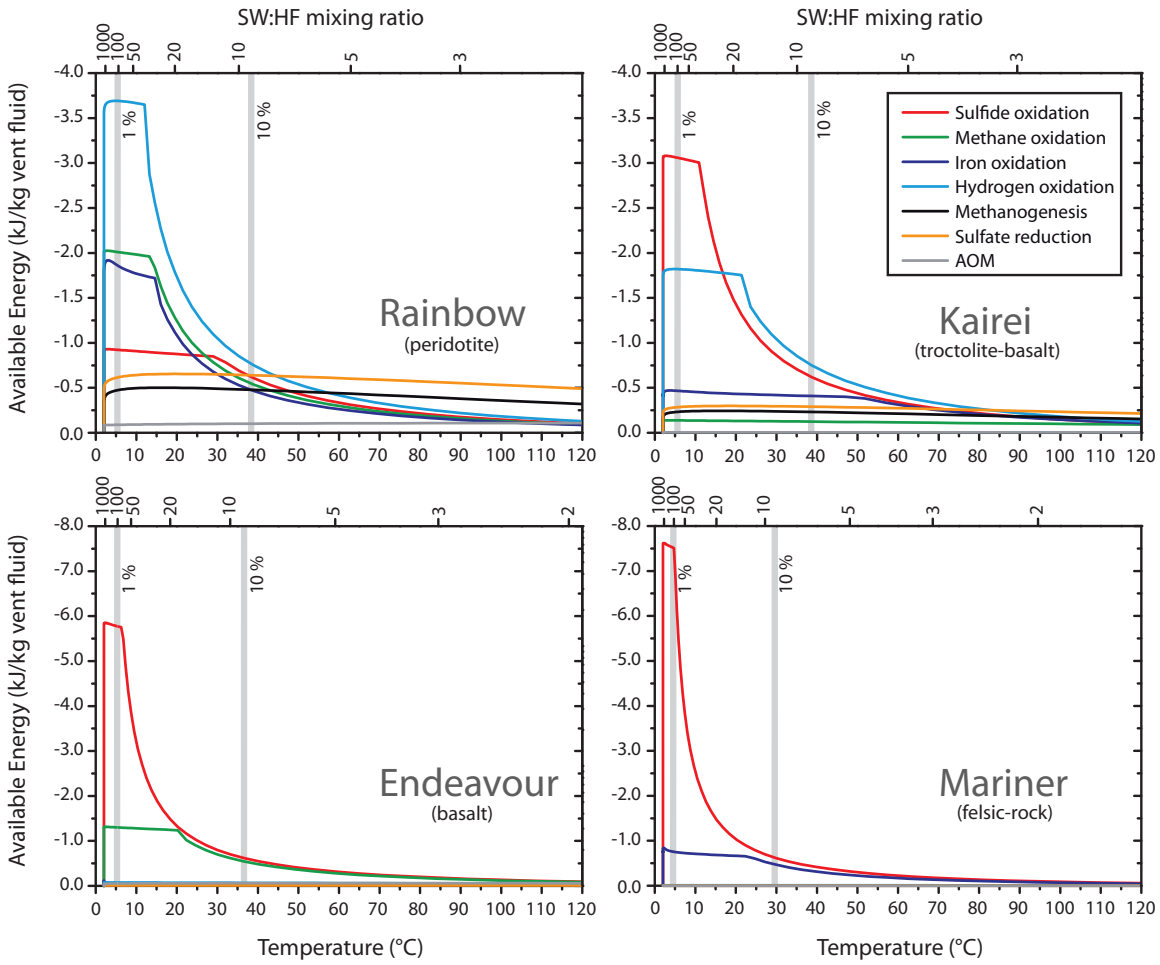

Figure 4-5: Catabolic energies (in kJ per kg vent fluid) available from seven different redox reactions as a function of temperature and seawater:hydrothermal fluid (SW:HF) mixing ratio in four different vent systems. The 1% and 10% hydrothermal fluid contribution to the mixed solutions are indicated for context. Owing to different vent fluid temperatures, the scales for the SW:HF mixing ratio are slightly different in the four sub-figures.

The variability in geochemical energy sources at different vent sites may govern significant variations in metabolic and phylogenetic diversities of microbial communities that inhabit the different systems. Energy modeling can guide the exploration of these communities by predicting which strategies might be dominant and which are likely rare. If the catabolic energy availability dictates microbial community in mixing zones, then Rainbow will be dominated at low temperatures by aerobes, especially hydrogen oxidizers, and at high temperatures anaerobe sulfate reducers and methanogens should prevail. Consistent with this prediction, endosymbionts in the vent mussel *Bathymodiolus* from the Logatchev hydrothermal vent field, which is similar in composition to the Rainbow system, have been shown to use aerobic oxidation of hydrogen as a main energy source (Petersen et al., 2011).

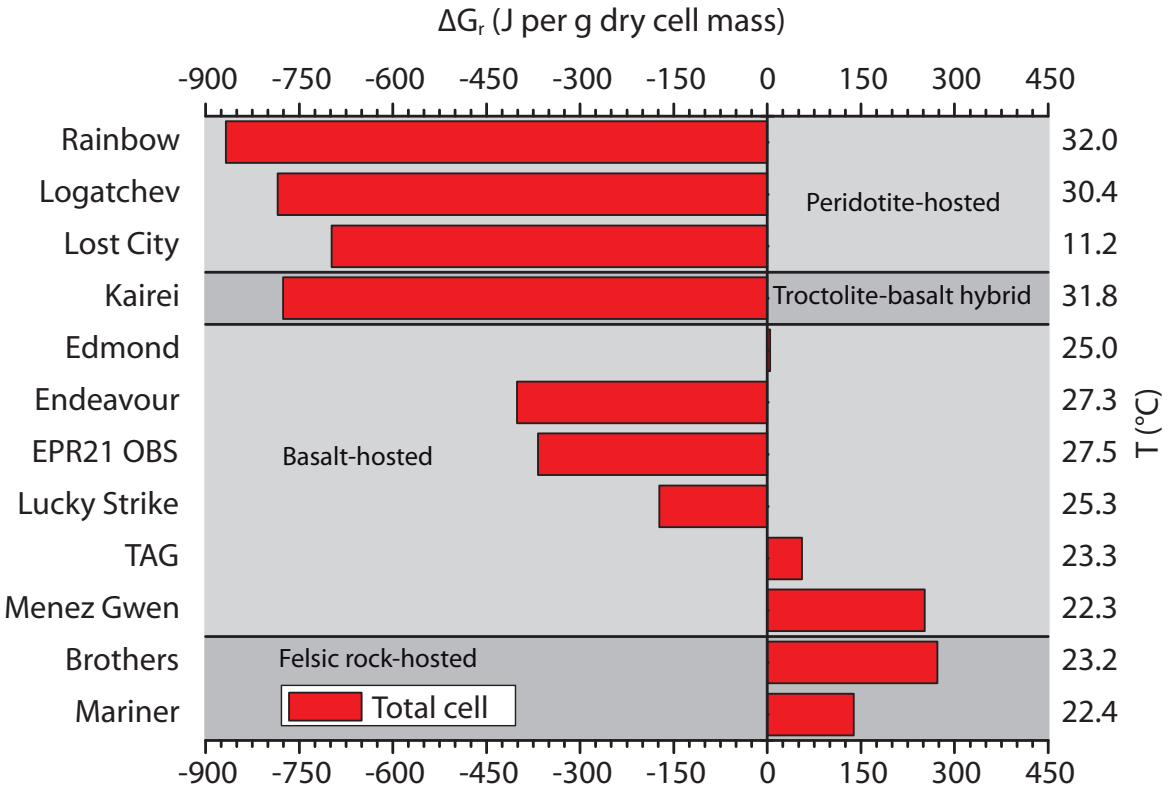

Figure 4-6: Gibbs energies (in J per g dry cell mass) of the sum total of the anabolic reactions in the 12 hydrothermal systems calculated at the energetically most favorable SW:HF mixing ratio (between 5.8% and 8.3% hydrothermal fluid). The temperatures to which these ratios correspond are given on the right hand side.

Figure 4-6 shows ΔG_r values for the synthesis of all monomers needed to construct 1g of dry cell weight for the most favorable temperature (at batch mixing conditions). Peridotite and troctolite-basalt hybrid hosted vent systems are strongly exergonic and this may significantly reduce the ATP requirement of growing cells or shunt the extra ATP to unfavorable biomass synthesis, including polymerization reactions. Biosynthesis in basalt-hosted systems, by comparison, is less favorable and, in some biosynthesis is endergonic like in felsic rock-hosted systems.

The standard view of biological energy flow holds that catabolic processes drive the generation of ATP, which is used as energy carrier to enable anabolic processes. This implies that anabolic processes are endergonic, requiring external energy to proceed. Our investigations show that under common geochemical conditions in deep-sea hydrothermal systems, some biomass synthesis reactions can be accompanied by a net energy gain. Under these circumstances, the net amount of amino acid and fatty acid synthesis reactions is exergonic while synthesis of nucleotides is always endergonic (Amend et al., 2011).

The scrutiny of catabolic and anabolic reaction energetics shows a clear biogeochemical distinction between peridotite-hosted and basalt-hosted systems. The distinction for catabolic reactions is demonstrated by the most exergonic reactions: hydrogen oxidation in peridotite and sulfide oxidation in basalt. In anabolic reactions the amount of released energy is high in peridotite-hosted system and low in basalt-hosted systems. All these results are pointing to hydrogen concentrations as the most influential geochemical factor determining

the sum of anabolic and catabolic reaction energetics in the wide spectrum of hydrothermal systems. The overall dominant role of hydrogen is also a function of reaction stoichiometric in catabolism and anabolism, where its stoichiometric reaction coefficient is in general greater than that of other species.

4.4.2 Potential for ridge flank microbial processes

Thermodynamic and bioenergetic calculations were used by Bach and Edwards, 2003 to estimate the potential chemolithoautotrophic microbial biomass production within ridge flanks. Compilations of Fe_2O_3, FeO, and S concentrations from DSDP/ODP drill core samples representing upper basaltic ocean crust led to an estimation of annual oxidation rates of $1.7\pm1.2\cdot10^{12}$ mol Fe and $1.1\pm0.7\cdot10^{11}$ mol S. They estimated that 50% of Fe oxidation may be attributed to hydrolysis, producing $4.5\pm3.0\cdot10^{11}$ mol H_2/yr.

Combined, aerobic and anaerobic Fe and S oxidation may support production of up to $48\pm21\cdot10^{10}$ g cellular carbon (C). Hydrogen-consuming reactions may support production of a similar or larger amount of microbial biomass if iron reduction, nitrate reduction, or hydrogen oxidation by O_2(aq) are the prevailing metabolic reactions. If autotrophic sulfate reduction or methanogenesis prevail, the potential biomass production is $9\pm7\cdot10^{10}$ g C/yr and $3\pm2\cdot10^{10}$ g C/yr, respectively. Combined primary production of up to 10^{12} g C/yr should be similar to biomass production fueled by anaerobic oxidation of organic matter in deep-seated heterotrophic systems. These estimates suggest that water-rock reactions may support significant microbial life within ridge flank hydrothermal systems.

A case study from the Juan de Fuca Ridge (Orcutt et al., 2011) reveals the importance of rocks and minerals as energy sources under certain physical and chemical conditions. For this purpose colonization experiments consisting of polished minerals chips were deployed in boreholes within young oceanic crust and sealed by CORK observatories (‘Circulation Obviation Retrofit Kit’, Davis et al., 1992; Becker and Davis, 2005). CORKs allow the formation of subsections in boreholes and monitoring of distinct physical and chemical parameter in each section. During the experimental time of four years the measured physical and chemical data indicate a transition from seawater conditions (caused by the drilling process) to natural conditions in the oceanic crust. Indicators for this shift are a decrease in oxic compounds like sulfate and nitrate (seawater) and an increase of reduced compounds for example manganese and ammonia (basement fluid). Also, the temperature increased from 2 to 65°C. Investigations of the mineral surfaces show traces of microbial population quite similar to that produced by microaerophilic, neutrophilic, and iron oxidizing bacteria. The abundance of colonization shows a preference for the pyrite/magnetite chip (64±4% surface covering) followed by basalt (20±5%), dunite (13±5%) and biotite chip (9±4%), which can be explained with the accessibility and abundance of iron. However, the oxidation of iron is largely favored under oxic conditions and drops down at reducing conditions that lead to the extinction of this population with establishing the natural conditions of this aquifer. Under natural conditions, Firmicutes dominate the bacterial community. The metabolic potential of Firmicutes is unknown but may involve N or S cycling. This short time experiment is per-

haps an analogue for the use of potential energy sources at certain condition in the oceanic crust and shows how fast the microbial community can respond to the change of conditions.

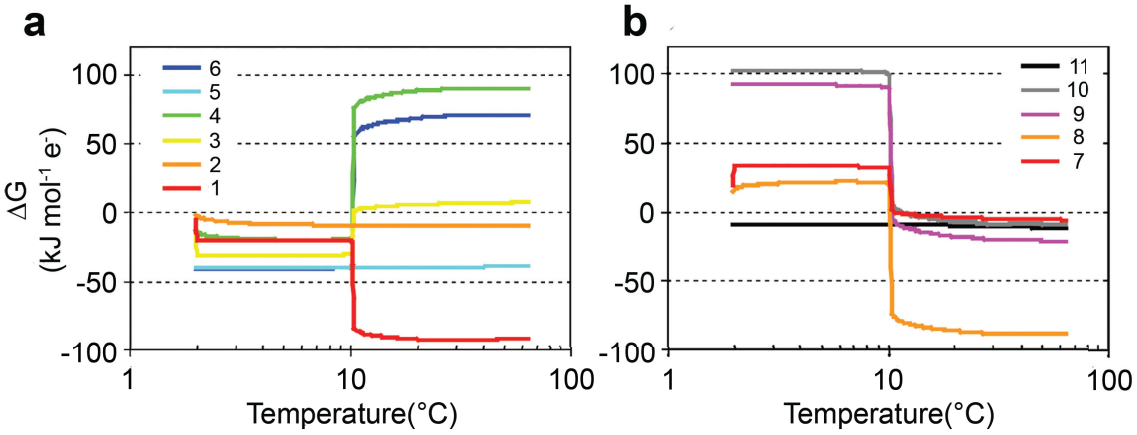

Figure 4-7: Free energy yields of reactions (in kJ/mol e^-) calculated by from a rock-seawater reaction model at temperatures ranging from 2-65°C. Reactions considered include:

1	$5\,Fe^{2+} + NO_3^- + 7\,H_2O \rightarrow 5\,FeOOH + 0.5\,N_2 + 9\,H^+$
2	$5\,Mn^{2+} + 2\,NO_3^- + 4\,H_2O \rightarrow 5\,MnO_2 + N_2 + 8\,H^+$
3	$Fe^{2+} + 0.25\,O_2 + 1.5\,H_2O \rightarrow FeOOH + 2\,H^+$
4	$Mn^{2+} + 0.5\,O_2 + H_2O \rightarrow MnO_2 + 2\,H^+$
5	$3\,NO_3^- + 5\,NH_4^+ \rightarrow 4\,N_2 + 9\,H_2O + 2\,H^+$
6	$NH_4^+ + 2\,O_2 \rightarrow NO_3^- + 2\,H^+ + H_2O$
7	$FeOOH + 0.5\,H_2 + 2\,H^+ \rightarrow Fe^{2+} + 2\,H_2O$
8	$MnO_2 + H_2 + 2\,H^+ \rightarrow Mn^{2+} + 2\,H_2O$
9	$SO_4^{2-} + 4\,H_2 + 2\,H^+ \rightarrow H_2S + 4\,H_2O$
10	$HCO_3^- + 4\,H_2 + H^+ \rightarrow CH_4 + 3\,H_2O$
11	$SO_4^{2-} + CH_4 + H^+ \rightarrow H_2S + HCO_3^- + H_2O$

The results of the rock-water reaction path model indicate that Fe(II) oxidation with oxygen would be favorable (i.e. negative $\Delta_r G$) during the cooler initial periods of the experiment. Fe(II) oxidation becomes unfavorable as temperatures increased (Figure 4-7), after the period of rebound to natural state in Hole 1301A. The switch to unfavorable conditions is related to the removal of oxygen from the reaction environment. The oxidation of Mn(II) and NH_4^+ with oxygen also changes the conditions from thermodynamically favorable to unfavorable as temperatures increase. The temperature of the transition from favorable to unfavorable conditions is dependent on the quantity of rock considered to have reacted in the model. In contrast, Fe(II), Mn(II), and NH_4^+ oxidation with nitrate would be thermodynamically favorable reactions at all temperatures considered. Hydrogen-driven reduction of iron-oxyhydroxides, manganese oxide, sulfate, and bicarbonate only become thermodynamically favorable at elevated temperatures and in an anaerobic environment. These results indicate that iron oxidation would have been a possible reaction in the early, cooler periods of the observatory experiment (Figure 4-3), and support the hypothesis of early colonization of the experimental minerals by iron oxidizing bacteria. The calculations also indicate that Fe(II) oxidation was not a viable catabolic reaction after the borehole turned around to its

natural state. The model results can explain why microbial groups forming the twisted stalk particles, died out, leaving only the stalk particles as fossil evidence of their former presence.

4.4.3 Vent fluid chemistry as a guide to microbial metabolism

Diffuse fluids have been used as a window to the subseafloor biosphere. They bring microbes from the subseafloor habitat to the seafloor (e.g., Huber et al., 2006) and they allow inferences about microbial metabolism from compositional parameters (e.g., Hentscher and Bach, 2012). Diffuse fluids from selected Mid-Atlantic Ridge hydrothermal sites were also examined to understand subseafloor microbial metabolism. Perner et al., (2009) report on 8°C warm diffuse fluids from the Mid-Atlantic Ridge at 5°S that differ substantially from compositions calculated for conservative mixing of a 400°C endmember fluid and 2°C seawater. Most notable are depletions in hydrogen by three to four orders of magnitude. An obvious interpretation of the lower-than-expected hydrogen concentrations is that it behaves strongly non-conservative, likely because it is utilized as energy source in the subseafloor. Indeed, all catabolic reactions using hydrogen as electron donor are strongly exergonic in the model fluid composition. Even in the sampled fluid, energy yields for aerobic oxidation of hydrogen are still extremely high. Similarly, the oxidation of methane, Fe(II) and hydrogen sulfide has uniformly high free energies. These observations indicate insufficient scrubbing of electron donors (H_2, H_2S, iron, methane) entering the turbulent mixing environment at the seafloor at high flux rates typical for advective regimes. Below the seafloor, oxygen concentrations are likely much reduced, so that electron acceptors other than oxygen are being respired. Thermodynamic drive for methanogenesis is great in the hypothetical fluid of the mixing model (110 kJ/mol methane). In the sampled fluids, however, the free energy of methanogenesis is much lower. Likewise, the free energies for hydrogenotrophy using sulfate and sulfur as electron acceptor are also lowered relative to the conservative mixing model, while the free energy of reaction for AOM (anaerobic oxidation of methane) is not reduced. These results suggest that oxidation of hydrogen by carbon dioxide, sulfur and sulfate is taking place in the subseafloor-mixing zone underlying the vent field. While hydrogen is efficiently removed, other electron donors – H_2S, Fe(II), and methane – are not. An obvious explanation is that these compounds can be produced in hydrogenotrophic metabolic reactions (methanogenesis, Fe-reduction, as well as sulfate and sulfur reduction). The fluid compositions hence provide indirect evidence for active cycling of carbon, iron and sulfur in the subseafloor.

In a follow-up study, Perner et al., (2011) demonstrated that diffuse vents reflect the microbial community within the associated fluid path and mixing regime by combining biological and thermodynamic methods. Two diffuse fluids from different basalt-hosted vent fields with proposed different permeability were investigated. Diffuse fluids at both sites contain large fractions of seawater but differ in concentration of redox sensitive species. The Desperate (5°S Mid-Atlantic Ridge [MAR]) fluid contains elevated concentrations of H_2S and O_2, but H_2 was barely detectable. In contrast, Lilliput vent fluids (9°S MAR) are enriched in reduced species as well as H_2 but have much lower concentrations of O_2. Ther-

modynamic calculations for the vents (Figure 4-8) show that, at Desperate, only hydrogen sulfide oxidation is favored, while Lilliput also favors hydrogen and methane oxidation. The higher energy availability at Lilliput has consequences for the microbial ecosystems there. In fluid incubation experiments all provided energy sources were used, indicating physiologically versatile microbial communities and growth under nearly all conditions. However, in fluids from Desperate only amendments with H_2S led to CO_2 fixation in the experiments. Desperate fluids seem to represent a habitat which is already limited by H_2, but not by sulfide and electrochemically positive electron acceptors. *Thiomicrospira* dominates the microbial community at Desperate. Survival in the subsurface of Lilliput seems to depend on the competition for less positive electron acceptors due to the less O_2 availability. These

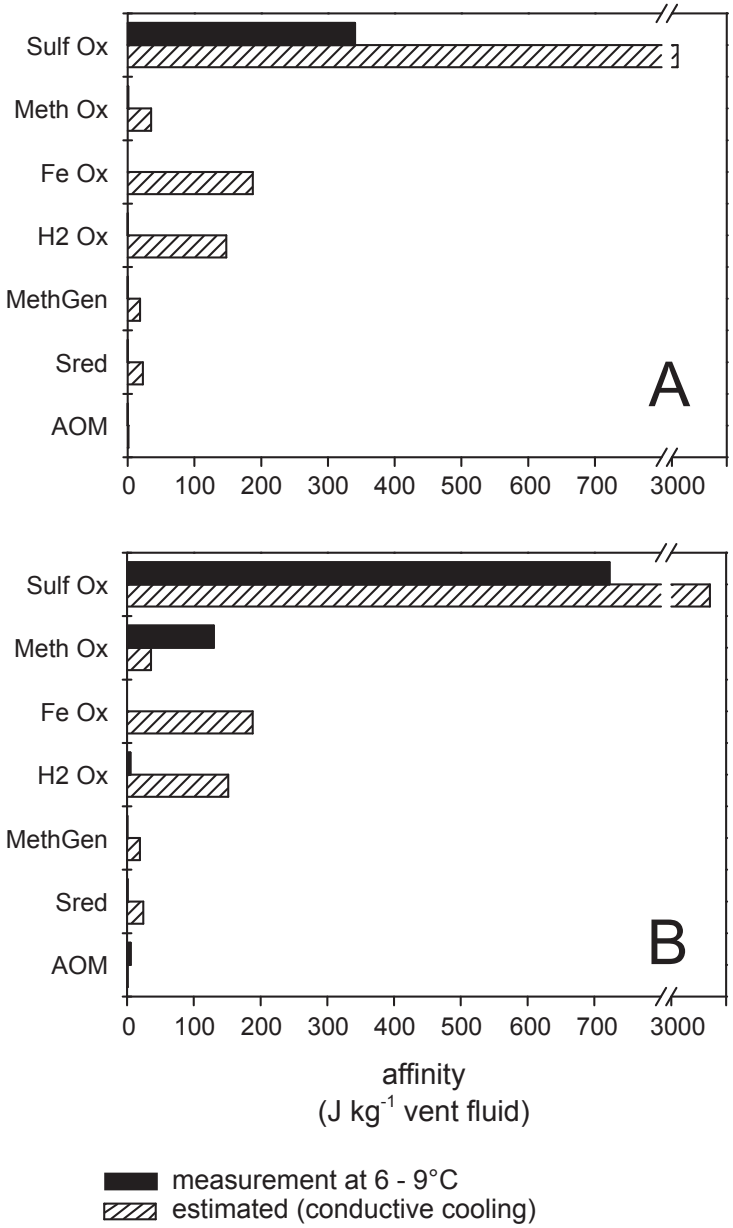

Figure 4-8: Calculated affinities of metabolic reactions for the near surface region (based on average measured concentrations) and estimated from conservative mixing and conductive cooling. Measured temperatures were 6°C for Desperate (A) and 9°C for Lilliput (B). Endmember percentages used for the conductive cooling model were 2.3% and 3.8%, respectively, for Desperate and Lilliput.
SulfOx = Aerobic sulfide oxidation
Meth Ox = aerobic methane oxidation
H_2 Ox = aerobic hydrogen oxidation
Fe Ox = aerobic iron oxidation
MethGen = methanogenesis
Sred = sulfur reduction
AOM = anaerobic oxidation of methane.

microaerophilic or anaerobic habitats seem to favor growth of Epsilonproteobacteria, which are the prevailing group of microorganisms in these fluids. The degree of seawater admixed to the endmember fluids of these systems, appears to be one major force acting on the local microbial community structure.

4.5 Summary and conclusion

This chapter demonstrated the use of thermodynamic calculations in assessing anabolic energy requirements and catabolic energy availability in a range of submarine hydrothermal systems. Geochemical reaction path models have been successfully employed to compute the affinities of catabolic (energy-harvesting) and anabolic (biosynthesis) reactions along trajectories of batch mixing between vent fluids and 2°C seawater. These calculations reveal what metabolic reaction has the highest energy-yield for chemolithotrophic catabolism in different hydrothermal systems occurring in different geotectonic settings (mid-ocean ridges, back-arcs, arcs, ridge flanks). They allow us to map out what metabolic strategies may succeed in the various system and under certain circumstances. Calculations of catabolic energy yields show that the dominant reactions in serpentinite-hosted vents, for example at Rainbow, Logatchev, or Lost City, are the oxidation of H_2, Fe(II) and methane. In contrast, basalt-hosted systems, such as TAG and 21°N EPR uniformly indicate H_2S oxidation to be the catabolically dominant reaction over the entire microbial-relevant temperature range. Affinities have also been calculated for the formation of individual cellular building blocks from inorganic reactants (H_2, CO_2, NH_4^+, HPO_4^{2-}, etc.). These include amino acids, sugars, amines, nucleic acids, and fatty acids. Again, ultramafic-hosted sites appear to be distinct from their volcanically-hosted counterparts in that biosynthesis reactions are much less energy-demanding. For a range of biosynthesis reactions, including the formation of proteins, vent systems like Lost City appear to have a fairly wide window of temperature (i.e., fluid mixing ratio) in which biosynthesis reactions are actually exergonic. These results will also have potential implications for the development of early life (Martin et al., 2008), as alkaline and reducing vent fluids generate an environment that appears to lower the energetic demands of biosynthesis reactions considerably.

A similar approach has been used by Perner et al., (2011), complemented by investigations of the actual microbial communities from DNA sequencing and culture experiments. It could be shown that diffuse fluids are affected by microbial metabolism and that the compositional changes in relation to what would be predicted from conservative mixing and conductive cooling is in line with the results of microbiological studies. The style of subseafloor mixing and the degree of conductive cooling apparently have a strong effect on the composition of microbial communities inhabiting subseafloor mixing zones near hydrothermal vents.

In summary, thermodynamic modeling can be used in varied ways to predict affinities and biomass yields for a range of processes in different geological settings (Figure 4-9). Future work should focus on combining thermodynamic calculation with kinetic constraints to assess the effect of kinetics on both the release of electron donors from the rock substrate and the growth of microorganisms (Jin and Bethke, 2007)

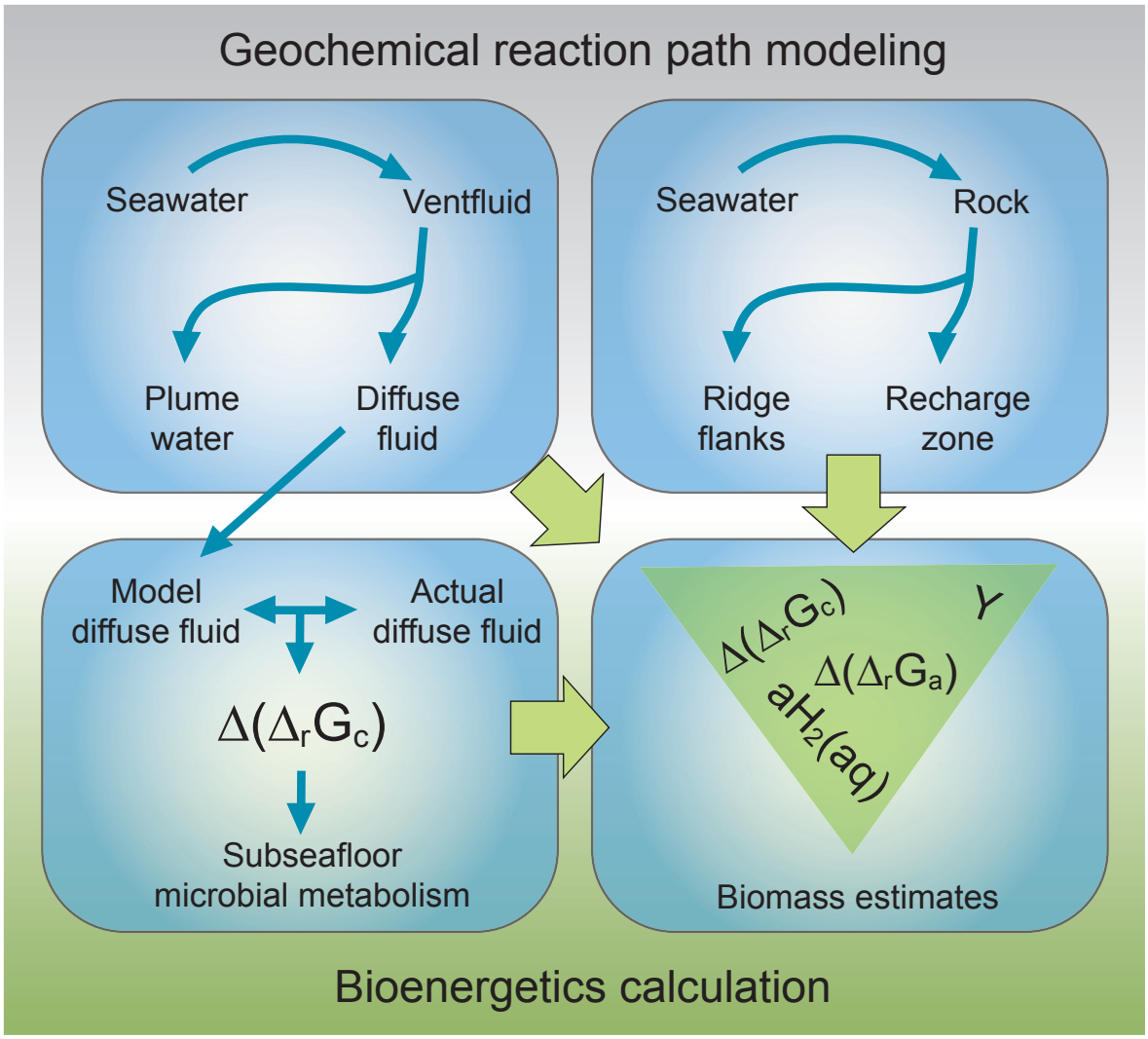

Figure 4-9: Illustration of the basic components of the proposed study and anticipated work/data flow. Geochemical reaction path models will be used to compute Gibbs energies and substrate activities, which are used in bioenergetics calculations aimed at examining possible microbial metabolism and biomass production.

4.6 References

Amend, J.P., McCollom, T.M., 2009. Energetics of Biomolecule Synthesis on Early Earth, Chemical Evolution II: From the Origins of Life to Modern Society. American Chemical Society, pp. 63-94.

Amend, J.P., McCollom, T.M., Hentscher, M., Bach, W., 2011. Catabolic and anabolic energy for chemolithoautotrophs in deep-sea hydrothermal systems hosted in different rock types. Geochimica et Cosmochimica Acta 75, 5736-5748.

Bach, W., Edwards, K.J., 2003. Iron and sulfide oxidation within the basaltic ocean crust: implications for chemolithoautotrophic microbial biomass production. Geochimica et Cosmochimica Acta 67, 3871-3887.

Baker, E.T., German, C.R., Elderfield, H., 1995. Hydrothermal plumes over spreading-center axes: global distribution and geological inferences, in: Humphris, S.E., Zierenberg, R.A., Mullineaux, L.S., Thomson, R.E. (Eds.), Seafloor hydrothermal systems. American Geophysical Union, Washington, DC.

Battley, E.H., 1998. The development of direct and indirect methods for the study of the thermodynamics of microbial growth. Thermochimica Acta 309, 17-37.

Becker, K., Davis, E.E., 2005. A review of CORK designs and operations during the Ocean Drilling Program, in: Fisher, A.T., Urabe, T., Klaus, A., Expedition 301 Scientists (Eds.), Proceedings of the IODP. Integrated Ocean Drilling Program Management International, Inc., College Station, pp. 1-28.

Bethke, C., 1996. Geochemical reaction modeling: Concepts and applications. Oxford University Press, USA.

Butterfield, D.A., Roe, K.K., Lilley, M.D., Huber, J.A., Baross, J.A., Embley, R.M., Massoth, G.J., 2004. Mixing, reaction and microbial activity in the sub-seafloor revealed by temporal and spatial variation in diffuse flow vents at Axial Volcano, in: Wilcock, W.S.D., DeLong, E.F., Kelley, D.S., Baross, J.A., Cary, S.C. (Eds.), The Subseafloor Biosphere at Mid-Ocean Ridges. American Geophysical Union, Washington, DC, pp. 269-289.

Charlou, J.L., Donaval, J.P., Jean-Baptiste, P., Dapoigny, A., Rona, P.A., 1996. Gases and helium isotopes in high temperature solutions sampled before and after ODP Leg 158 drilling at TAG hydrothermal field(26 °N, MAR): TAG. Geophysical research letters 23, 3491-3494.

Charlou, J.L., Donval, J.P., Douville, E., Jean-Baptiste, P., Radford-Knoery, J., Fouquet, Y., Dapoigny, A., Stievenard, M., 2000. Compared geochemical signatures and the evolution of Menez Gwen (37°50'N) and Lucky Strike (37°17'N) hydrothermal fluids, south of the Azores Triple Junction on the Mid-Atlantic Ridge. Chemical Geology 171, 49-75.

Charlou, J.L., Donval, J.P., Fouquet, Y., Jean-Baptiste, P., Holm, N., 2002. Geochemistry of high H_2 and CH_4 vent fluids issuing from ultramafic rocks at the Rainbow hydrothermal field (36°14'N, MAR). Chemical Geology 191, 345-359.

Charlou, J.L., Fouquet, Y., Bougault, H., Donval, J.P., Etoubleau, J., Jean-Baptiste, P., Dapoigny, A., Appriou, P., Rona, P.A., 1998. Intense CH_4 plumes generated by serpentinization of ultramafic rocks at the intersection of the 15°20'N fracture zone and the Mid-Atlantic Ridge. Geochimica et Cosmochimica Acta 62, 2323-2333.

Conrad, R., Schink, B., Phelps, T.J., 1986. Thermodynamics of H_2-consuming and H_2-producing metabolic reactions in diverse methanogenic environments under in situ conditions. FEMS Microbiology Letters 38, 353-360.

Cowen, J.P., Massoth, G.J., Baker, E.T., 1986. Bacterial scavenging of Mn and Fe in a mid- to far-field hydrothermal particle plume. Nature 322, 169-171.

Davis, E., Becker, K., Pettigrew, T., Carson, B., MacDonald, R., 1992. CORK: a hydrologie seal and downhole observatory for deep-ocean boreholes, Proc ODP Init Reports 139, pp. 43-54.

de Angelis, M.A., Lilley, M.D., Baross, J.A., 1993. Methane oxidation in deep-sea hydrothermal plumes of the endeavour segment of the Juan de Fuca Ridge. Deep Sea Research Part I: Oceanographic Research Papers 40, 1169-1186.

Dick, J.M., 2008. Calculation of the relative metastabilities of proteins using the CHNOSZ software package. Geochemical Transactions 9, 10.

Douville, E., Charlou, J.L., Oelkers, E.H., Bienvenu, P., Jove Colon, C.F., Donval, J.P., Fouquet, Y., Prieur, D., Appriou, P., 2002. The rainbow vent fluids (36°14'N, MAR): the influence of ultramafic rocks and phase separation on trace metal content in Mid-Atlantic Ridge hydrothermal fluids. Chemical Geology 184, 37-48.

Drummond, S.E., 1981. Boiling and mixing of hydrothermal fluids: chemical effects on mineral precipitation. Pennsylvania State University.

Edwards, K.J., Bach, W., McCollom, T.M., 2005. Geomicrobiology in oceanography: microbe–mineral interactions at and below the seafloor. Trends in Microbiology 13, 449-456.

Elderfield, H., Schultz, A., 1996. Mid-ocean ridge hydrothermal fluxes and the chemical composition of the ocean. Annual Review of Earth and Planetary Sciences 24, 191-224.

Fisher, A.T., Davis, E.E., Hutnak, M., Spiess, V., Zuhlsdorff, L., Cherkaoui, A., Christiansen, L., Edwards, K., Macdonald, R., Villinger, H., Mottl, M.J., Wheat, C.G., Becker, K., 2003. Hydrothermal recharge and discharge across 50 km guided by seamounts on a young ridge flank. Nature 421, 618-621.

Gallant, R.M., Von Damm, K.L., 2006. Geochemical controls on hydrothermal fluids from the Kairei and Edmond Vent Fields, 23°-25°S, Central Indian Ridge. Geochemistry, Geophysics, Geosystems 7, 1-24.

Harder, J., 1997. Species-independent maintenance energy and natural population sizes. FEMS Microbiology Ecology 23, 39-44.

Heijnen, J.J., Van Dijken, J.P., 1992. In search of a thermodynamic description of biomass yields for the chemotrophic growth of microorganisms. Biotechnology and Bioengineering 39, 833-858.

Helgeson, H.C., 1969. Thermodynamics of hydrothermal systems at elevated temperatures and pressures. American Journal of Science 267, 729-804.

Hentscher, M., Bach, W., 2012. Geochemically induced shifts in catabolic energy yields explain past ecological changes of diffuse vents in the East Pacific Rise 9°50'N area. Geochemical Transactions 13, 2.

Hoehler, T.M., 2004. Biological energy requirements as quantitative boundary conditions for life in the subsurface. Geobiology 2, 205-215.

Holden, J.F., Summit, M., Baross, J.A., 1998. Thermophilic and hyperthermophilic microorganisms in 3-30°C hydrothermal fluids following a deep-sea volcanic eruption. FEMS Microbiology Ecology 25, 33-41.

Huber, J.A., Butterfield, D.A., Baross, J.A., 2003. Bacterial diversity in a subseafloor habitat following a deep-sea volcanic eruption. FEMS Microbiology Ecology 43, 393-409.

Huber, J.A., Johnson, H.P., Butterfield, D.A., Baross, J.A., 2006. Microbial life in ridge flank crustal fluids. Environmental Microbiology 8, 88-99.

Jannasch, H.W., 1995. Microbial interactions with hydrothermal fluids, in: Humphris, S.E., Zierenberg, R.A., Mullineaux, L.S., Thomson, R.E. (Eds.), Seafloor hydrothermal systems: physical, chemical, biological, and geological interactions. AGU, Washington, DC, pp. 273-296.

Jannasch, H.W., Mottl, M.J., 1985. Geomicrobiology of Deep-Sea Hydrothermal Vents. Science 229, 717-725.

Jin, Q., Bethke, C.M., 2007. The Thermodynamic and Kinetic of Microbial Metabolism. American Journal of Science Volumes 307, 643-677.

Johnson, J.W., Oelkers, E.H., Helgeson, H.C., 1992. SUPCRT92: A software package for calculating the standard molal thermodynamic properties of minerals, gases, aqueous species, and reactions from 1 to 5000 bar and 0 to 1000°C. Computers & Geosciences 18, 899-947.

Karl, D.M., Wirsen, C.O., Jannasch, H.W., 1980. Deep-sea primary production at the Galapagos hydrothermal vents. Science 207, 1345-1347.

Kelley, D.S., Karson, J.A., Blackman, D.K., Fruh-Green, G.L., Butterfield, D.A., Lilley, M.D., Olson, E.J., Schrenk, M.O., Roe, K.K., Lebon, G.T., Rivizzigno, P., the, A.T.S.P., 2001. An off-axis hydrothermal vent field near the Mid-Atlantic Ridge at 30° N. Nature 412, 145-149.

Kelley, D.S., Karson, J.A., Fruh-Green, G.L., Yoerger, D.R., Shank, T.M., Butterfield, D.A., Hayes, J.M., Schrenk, M.O., Olson, E.J., Proskurowski, G., Jakuba, M., Bradley, A., Larson, B., Ludwig, K., Glickson, D., Buckman, K., Bradley, A.S., Brazelton, W.J., Roe, K., Elend, M.J., Delacour, A., Bernasconi, S.M., Lilley, M.D., Baross, J.A., Summons, R.E., Sylva, S.P., 2005. A Serpentinite-Hosted Ecosystem: The Lost City Hydrothermal Field. Science 307, 1428-1434.

Kormas, K.A., Tivey, M.K., Von Damm, K., Teske, A., 2006. Bacterial and archaeal phylotypes associated with distinct mineralogical layers of a white smoker spire from a deep-sea hydrothermal vent site (9°N, East Pacific Rise). Environmental Microbiology 8, 909-920.

LaRowe, D.E., Helgeson, H.C., 2006a. Biomolecules in hydrothermal systems: Calculation of the standard molal thermodynamic properties of nucleic-acid bases, nucleosides, and nucleotides at elevated temperatures and pressures. Geochimica et Cosmochimica Acta 70, 4680-4724.

LaRowe, D.E., Helgeson, H.C., 2006b. The energetics of metabolism in hydrothermal systems: Calculation of the standard molal thermodynamic properties of magnesium-complexed adenosine nucleotides and NAD and NADP at elevated temperatures and pressures. Thermochimica Acta 448, 82-106.

Martin, W., Baross, J., Kelley, D., Russell, M.J., 2008. Hydrothermal vents and the origin of life. Nature Reviews Microbiology 6, 805-814.

McCollom, T.M., 2000. Geochemical constraints on primary productivity in submarine hydrothermal vent plumes. Deep Sea Research Part I: Oceanographic Research Papers 47, 85-101.

McCollom, T.M., Amend, J.P., 2005. A thermodynamic assessment of energy requirements for biomass synthesis by chemolithoautotrophic micro-organisms in oxic and anoxic environments. Geobiology 3, 135-144.

McCollom, T.M., Shock, E.L., 1997. Geochemical constraints on chemolithoautotrophic metabolism by microorganisms in seafloor hydrothermal systems. Geochimica et Cosmochimica Acta 61, 4375-4391.

Morowitz, H.J., 1968. Energy flow in biology: biological organization as a problem in thermal physics. Academic Press, New York.

Mottl, M.J., Komor, S.C., Fryer, P., Moyer, C.L., 2003. Deep-slab fluids fuel extremophilic Archaea on a Mariana forearc serpentinite mud volcano: Ocean Drilling Program Leg 195. Geochemistry, Geophysics, Geosystems 4, 9009.

Mottl, M.J., Wheat, G., Baker, E., Becker, N., Davis, E., Feely, R., Grehan, A., Kadko, D., Lilley, M., Massoth, G., Moyer, C., Sansone, F., 1998. Warm springs discovered on 3.5 Ma oceanic crust, eastern flank of the Juan de Fuca Ridge. Geology 26, 51-54.

Orcutt, B.N., Bach, W., Becker, K., Fisher, A.T., Hentscher, M., Toner, B.M., Wheat, C.G., Edwards, K.J., 2011. Colonization of subsurface microbial observatories deployed in young ocean crust. ISME Journal 5, 692-703.

Pagé, A., Tivey, M.K., Stakes, D.S., Reysenbach, A.-L., 2008. Temporal and spatial archaeal colonization of hydrothermal vent deposits. Environmental Microbiology 10, 874-884.

Perner, M., Bach, W., Hentscher, M., Koschinsky, A., Garbe-Schönberg, D., Streit, W.R., Strauss, H., 2009. Short-term microbial and physico-chemical variability in low-temperature hydrothermal fluids near 5°S on the Mid-Atlantic Ridge. Environmental Microbiology 11, 2526-2541.

Perner, M., Hentscher, M., Rychlik, N., Seifert, R., Strauss, H., Bach, W., 2011. Driving forces behind the biotope structures in two low-temperature hydrothermal venting sites on the southern Mid-Atlantic Ridge. Environmental Microbiology Reports 3, 727-737.

Petersen, J.M., Zielinski, F.U., Pape, T., Seifert, R., Moraru, C., Amann, R., Hourdez, S., Girguis, P.R., Wankel, S.D., Barbe, V., Pelletier, E., Fink, D., Borowski, C., Bach, W., Dubilier, N., 2011. Hydrogen is an energy source for hydrothermal vent symbioses. Nature 476, 176-180.

Proskurowski, G., Lilley, M.D., Kelley, D.S., Olson, E.J., 2006. Low temperature volatile production at the Lost City Hydrothermal Field, evidence from a hydrogen stable isotope geothermometer. Chemical Geology 229, 331-343.

Proskurowski, G., Lilley, M.D., Olson, E.J., 2008. Stable isotopic evidence in support of active microbial methane cycling in low-temperature diffuse flow vents at 9°50'N East Pacific Rise. Geochimica et Cosmochimica Acta 72, 2005-2023.

Rona, P.A., Trivett, D.A., 1992. Discrete and diffuse heat transfer atashes vent field, Axial Volcano, Juan de Fuca Ridge. Earth and Planetary Science Letters 109, 57-71.

Schrodinger, E., 1944. What is life? The physical aspect of the living cell. Cambridge, Cambridge University Press

Schultz, A., Delaney, J.R., McDuff, R.E., 1992. On the Partitioning of Heat Flux Between Diffuse and Point Source Seafloor Venting. Journal of Geophysical Research 97, 12299-12314.

Schultz, A., Elderfield, H., 1997. Controls on the physics and chemistry of seafloor hydrothermal circulation. Philosophical Transactions of the Royal Society of London. Series A: Mathematical, Physical and Engineering Sciences 355, 387-425.

Seewald, J., Cruse, A., Saccocia, P., 2003. Aqueous volatiles in hydrothermal fluids from the Main Endeavour Field, northern Juan de Fuca Ridge: temporal variability following earthquake activity. Earth and Planetary Science Letters 216, 575-590.

Seyfried, W.E., Seewald, J.S., Berndt, M.E., Ding, K., Foustoukos, D.I., 2003. Chemistry of hydrothermal vent fluids from the Main Endeavour Field, northern Juan de Fuca Ridge: Geochemical controls in the aftermath of June 1999 seismic events. Journal of Geophysical Research 108.

Stein, C.A., Stein, S., Pelayo, A., 1995. Heat flow and hydrothermal circulation, in: Humphris, S.E., Zierenberg, R.A., Mullineaux, L.S., Thomson, R.E. (Eds.), Seafloor hydrothermal processes. American Geophysical Union, Washington, DC, pp. 425-445.

Takai, K., Nunoura, T., Horikoshi, K., Shibuya, T., Nakamura, K., Suzuki, Y., Stott, M., Massoth, G.J., Christenson, B.W., deRonde, C.E.J., Butterfield, D.A., Ishibashi, J.-i., Lupton, J.E., Evans, L.J., 2009. Variability in Microbial Communities in Black Smoker Chimneys at the NW Caldera Vent Field, Brothers Volcano, Kermadec Arc. Geomicrobiology Journal 26, 552-569.

Takai, K., Nunoura, T., Ishibashi, J.-i., Lupton, J., Suzuki, R., Hamasaki, H., Ueno, Y., Kawagucci, S., Gamo, T., Suzuki, Y., Hirayama, H., Horikoshi, K., 2008. Variability in the microbial communities and hydrothermal fluid chemistry at the newly discovered Mariner hydrothermal field, southern Lau Basin. J. Geophys. Res. 113, G02031.

Thauer, R.K., Jungermann, K., Decker, K., 1977. Energy conservation in chemotrophic anaerobic bacteria. Bacteriological Reviews 41, 100-180.

Tijhuis, L., Van Loosdrecht, M.C.M., Heijnen, J.J., 1993. A thermodynamically based correlation for maintenance Gibbs energy requirements in aerobic and anaerobic chemotrophic growth. Biotechnology and Bioengineering 42, 509-519.

Tucholke, B.E., Lin, J., Kleinrock, M.C., 1998. Megamullions and mullion structure defining oceanic metamorphic core complexes on the Mid-Atlantic Ridge. Journal of Geophysical Research 103, 9857-9866.

Von Damm, K.L., 1990. Seafloor Hydrothermal Activity: Black Smoker Chemistry and Chimneys. Annual Review of Earth and Planetary Sciences 18, 173-204.

Von Damm, K.L., Lilley, M.D., 2004. Diffuse Flow Hydrothermal Fluids from 9 50'N East Pacific Rise: Origin, Evolution and Biogeochemical Controls, in: Wilcock, W.S.D., DeLong, E.F., Kelley, D.S., Baross, J.A., Cary, S.C. (Eds.), The Subseafloor Biosphere at Mid-Ocean Ridges. American Geophysical Union Washington, DC, pp. 245-268

von Stockar, U., Maskow, T., Liu, J., Marison, I.W., Patiño, R., 2006. Thermodynamics of microbial growth and metabolism: An analysis of the current situation. Journal of Biotechnology 121, 517-533.

von Stockar, U., van der Wielen, L.A.M., 1997. Thermodynamics in biochemical engineering. Journal of Biotechnology 59, 25-37.

von Stockar, U., Vojinović, V., Maskow, T., Liu, J., 2008. Can microbial growth yield be estimated using simple thermodynamic analogies to technical processes? Chemical Engineering and Processing: Process Intensification 47, 980-990.

Wheat, C.G., Mottl, M.J., 2000. Composition of pore and spring waters from Baby Bare: global implications of geochemical fluxes from a ridge flank hydrothermal system. Geochimica et Cosmochimica Acta 64, 629-642.

Wolery, T.J., 2004. Qualification of Thermodynamic Data for Geochemical Modeling of Mineral-Water Interactions in Dilute Systems, in: Energy, U.S.D.o. (Ed.). Bechtel SAIC Company, LLC.

5. Synthesis and Outlook

5.1 Synthesis

Water-rock interactions and metabolic energy supply and demand in hydrothermal systems have been investigated by using thermodynamic computations. The studies presented in this thesis showed that there are tight relations between vent fluid chemistry and microbial community compositions. These relations are perhaps most obvious in an example from time series studies in the EPR 9°50'N vent area, where the demise of the *Riftia* population follows a sudden decrease in Gibbs energy of sulfide oxidation (Hentscher and Bach, 2012). At the same time, the Gibbs energy of iron oxidation increased and, predictably, massive red staining developed, which is evidence for the growths of Fe-oxidizing bacteria. It has also been demonstrated that it is possible to infer on microbial processes in the subseafloor by comparing concentrations and energy yields for diffuse vents with modeled conservatively mixed fluids. An example of diffuse fluids from another field of the EPR 9°50'N vent area were used to demonstrate the validity of this concept (Hentscher and Bach, 2012). The vents are enriched in methane and depleted in H_2 and there is isotopic evidence in the literature for methanogenesis. Thermodynamic calculations presented here, indicate that for several years in the aftermath of a volcanic eruption, affinities for hydrogenotrophic reactions in the diffuse fluids decreased despite uniformly high H_2 concentrations in the endmember fluids. This decrease is likely related to the growth of a hydrogenotrophic-based microbial ecosystem in the subseafloor. During later years, the influx of hydrogen from below and consumption of hydrogen within the subseafloor apparently had reached a steady state. Towards the end of the time series, methane excesses were small and the fluids showed a strong enrichment of Fe relative to the concentrations predicted from conservative mixing. This change in diffuse fluid composition may indicate a switch within the system from methanogenesis to Fe-reduction.

In similar studies microbiological and geochemical data and observations were combined through thermodynamic calculations and it could be shown that diffuse fluids reflect the metabolic processes driving microbial communities in the subseafloor (Perner et al., 2009; Perner et al., 2011). Again, differences between modeled and observed diffuse fluid compositions indicate the pathways which are microbially exploited in the subsurface. Fluids from Desperate (5°S Mid-Atlantic Ridge [MAR]) contain elevated concentrations of H_2S and O_2, but have very low H_2 contents. In contrast, Lilliput vent fluids (9°S MAR) are enriched in reduced species as well as H_2 but have much lower concentrations of O_2. Catabolic energy calculations reveal that only hydrogen sulfide oxidation is favorable at Desperate. At Lilliput, hydrogen and methane oxidation are also strongly exergonic. In line with these predictions, growth experiments and microbial analysis of these fluids show that the sulfur oxidizing bacteria *Thiomicrospira* dominates the microbial community at Desperate. Lilliput, on the other hand, is inhabited by Epsilonproteobacteria, which prefer microaerophilic or anaerobic conditions. Thermodynamic calculations were also used to explain the shift in microbial population in a borehole colonization experiment on the eastern flank of

the Juan de Fuca ridge (Orcutt et al., 2011). The recovered mineral chips from this experiment showed twisted FeOOH stalks overgrown by sulfides, indicative of an early colonization by iron oxidizing microorgansims and a subsequent change to sulfidic conditions. Fluid analyses reveal a shift from cold seawater composition to the actual basement fluid, which is strongly affected by exchange with the crust. Thermodynamic calculations reveal that iron oxidation would have been a possible reaction in the early, cooler periods of the observatory experiment and support the hypothesis of early colonization of the experimental minerals by iron oxidizing bacteria. The calculations also indicate that Fe(II) oxidation was not a viable catabolic reaction after the borehole turned around to its natural state.

All these studies showed how thermodynamic calculations can be used to examine the relations between changes in fluid chemistry and seafloor/subseafloor biology. Thermodynamic computations are also a helpful tool in examining processes in the subseafloor and help highlight the tight relations and interdependencies between geochemistry and microbiology in vent systems.

The predictive power of thermodynamic modeling was employed to examine possible catabolic reactions for chemoautotrophs for a range of hydrothermal vents in different rock type and geotectonic settings (Amend et al., 2011). These computations encompass batch mixing models for conservative mixing of seawater with hydrothermal endmember fluid and calculating the driving force for catabolic reaction in these estimated mixtures. The results imply distinct difference between peridotite and basalt hosted systems. Basalt hosted systems seem to be dominated by sulfide- and iron-oxidation while in peridotite hosted system more energy yielding catabolic reactions are possible. Especially hydrogenotrophic reactions are high in energy yield. In addition the driving force for anabolic reactions (formation of biomass components) was calculated. The results indicate that some of these reactions can be accompanied by a net energy gain under certain conditions, preferentially in peridotite-hosted systems. Hydrogen concentration is the most influential geochemical factor which determines the sum of anabolic and catabolic reaction energetics in the wide spectrum of hydrothermal systems.

Thermodynamic modeling was also used to understand the behavior of dissolved inorganic carbon (DIC) in serpentinization systems (Hentscher et al., in submission). The alkaline and reducing conditions during serpentinization may either lead to reduction of DIC to organic species or to CO_2 fixation as carbonate. Both pathways are kinetically controlled. Equilibrium thermodynamic modeling of peridotite–seawater interactions at different temperatures and water-to-rock ratios (W/R) showed that the formation of methane is largely favored, but methane formation is also known to be kinetically sluggish. Rapidly forming metastable organic compounds (e.g., methanol) likely play an important role. These intermediate compounds are predicted to form at W/R >4-5. At lower W/R, carbonate precipitation outcompetes DIC reduction, and organic synthesis is not predicted to take place. The computations indicate that carbonate precipitation severely restricts the availability of DIC for organosynthesis. Based on these results it is proposed that the formation of organics in fluids from the Lost City hydrothermal system have taken place at W/R greater than those

proposed for the reaction zone (W/R= 2-4). Furthermore, the calculation results indicate that the organosynthesis may take place in the lower part of the recharge zone, whereas the fate of CO_2 in the rock-buffered reaction zone of a Lost City type system is the formation of carbonate.

In conclusion, the research presented in this dissertation has shown that thermodynamic calculations can improve our understanding of the complex hydrothermal processes in the deep sea. The results of this study indicate that thermodynamic calculations can be used to examine the relations between changes in fluid chemistry and seafloor biology. They are also a helpful tool in examining processes in the subseafloor and help highlight the tight relations and interdependencies between geochemistry and microbiology in diffuse vent systems. Furthermore, thermodynamic reaction path models provide insight into water rock interaction in the ocean crust and identify sweet-spots for abiotic organosynthesis.

5.2 Outlook

Microbial habitability of submarine hydrothermal environments should be examined by coupled investigations of energy supply and demand in a specific setting. Temperature-dependencies for minimal substrate concentrations required for survival, maintenance, and growth of microorganisms (Hoehler, 2004) need to be fully considered. Also, energy-balances in investigating microbial biomass production from a the view-point of Gibbs energy dissipation and related approaches from biochemical engineering (Heijnen and Van Dijken, 1992; Tijhuis et al., 1993; von Stockar and van der Wielen, 1997; von Stockar et al., 2006) may be used more comprehensively in future studies. Other promising approaches link energy availability directly to ATP production (Thauer et al., 1977; LaRowe and Helgeson, 2006 a,b) in assessing potential biomass production.

Rigorously linking geology and biology, such computations can be used in mapping out what metabolic strategies may be exploited in different environments and how much biomass may be produced. Major new tools in this endeavour are sensors and mass spectrometers that measure *in situ* activities in hydrothermal vent fields with high spatial resolution. These data can be used to construct affinity contours for different metabolic reactions, against which insights from molecular and microbiological ecology could be compared.

The versatility of thermodynamic modeling can be improved to predict affinities and biomass yields for a range of processes in different geological settings. Future work should focus on combining thermodynamic calculations with kinetic constraints to assess the effect of kinetics on both the release of electron donors from the rock substrate and the growths of microorganisms (Jin and Bethke, 2007).

A range of biosynthesis reactions, including the formation of proteins, vent systems like Lost City appear to have a fairly wide window of temperature (i.e., fluid mixing ratio) in which biosynthesis reactions are actually exergonic. Curiously, this case would then consti-

tute a situation where life does NOT “feed on negative entropy”, which was postulated a trademark of life by Schrodinger (1944); (cf. von Stockar and Liu, 1999). These results warrant follow-up studies as there is potential implications for the development of early life (Martin et al., 2008), if alkaline and reducing vent fluids indeed generate an environment that appears to lower the energetic demands of biosynthesis reactions considerably.

5.3 References

Amend, J.P., McCollom, T.M., Hentscher, M., Bach, W., 2011. Catabolic and anabolic energy for chemolithoautotrophs in deep-sea hydrothermal systems hosted in different rock types. Geochimica et Cosmochimica Acta 75, 5736-5748.

Heijnen, J.J., Van Dijken, J.P., 1992. In search of a thermodynamic description of biomass yields for the chemotrophic growth of microorganisms. Biotechnology and Bioengineering 39, 833-858.

Hentscher, M., Bach, W., 2012. Geochemically induced shifts in catabolic energy yields explain past ecological changes of diffuse vents in the East Pacific Rise 9°50’N area. Geochemical Transactions 13, 2.

Hoehler, T.M., 2004. Biological energy requirements as quantitative boundary conditions for life in the subsurface. Geobiology 2, 205-215.

Jin, Q., Bethke, C.M., 2007. The Thermodynamic and Kinetic of Microbial Metabolism. American Journal of Science Volumes 307, 643-677.

LaRowe, D.E., Helgeson, H.C., 2006a. Biomolecules in hydrothermal systems: Calculation of the standard molal thermodynamic propertiesof nucleic-acid bases, nucleosides, and nucleotides at elevated temperatures and pressures. Geochim Cosmochim Acta 70, 4680-4724.

LaRowe, D.E., Helgeson, H.C., 2006b. The energetics of metabolism in hydrothermal systems: Calculation of the standard molal thermodynamic properties of magnesium-complexed adenosine nucleotides and NAD and NADP at elevated temperatures and pressures. Thermochimica Acta 448, 82-106.

Martin, W., Baross, J., Kelley, D.S., Russell, M.J., 2008. Hydrothermal vents and the origin of life. Nature Review Microbiology 6, 805-814.

Orcutt, B.N., Bach, W., Becker, K., Fisher, A.T., Hentscher, M., Toner, B.M., Wheat, C.G., Edwards, K.J., 2011. Colonization of subsurface microbial observatories deployed in young ocean crust. ISME Journal 5, 692-703.

Perner, M., Bach, W., Hentscher, M., Koschinsky, A., Garbe-Schönberg, D., Streit, W.R., Strauss, H., 2009. Short-term microbial and physico-chemical variability in low-temperature hydrothermal fluids near 5°S on the Mid-Atlantic Ridge. Environmental Microbiology 11, 2526-2541.

Appendix

Geochemical Transactions 2012, 13:2; doi:10.1186/1467-4866-13-2

6. Appendix-A: Geochemically induced shifts in catabolic energy yields explain past ecological changes of diffuse vents in the East Pacific Rise 9°50'N area

Michael Hentscher[1§], Wolfgang Bach [1]

[1] *Department of Geoscience, University of Bremen, Klagenfurter Straße, 28359 Bremen, Germany*

[§]*Corresponding author: hentscher@uni-bremen.de*

wbach@uni-bremen.de

6.1 Abstract

The East Pacific Rise (EPR) at 9°50'N hosts a hydrothermal vent field (Bio9) where the change in fluid chemistry is believed to have caused the demise of a tubeworm colony. We test this hypothesis and expand on it by providing a thermodynamic perspective in calculating free energies for a range of catabolic reactions from published compositional data. The energy calculations show that there was excess hydrogen sulfide (H_2S) in the fluids and that oxygen (O_2) was the limiting reactant from 1991 to 1997. Energy levels are generally high, although they declined in that time span. In 1997, sulfide availability decreased substantially and H_2S was the limiting reactant. Energy availability dropped by a factor of 10 to 20 from what it had been between 1991 and 1995. The perishing of the tubeworm colonies began in 1995 and coincided with the timing of energy decrease for sulfide oxidizers. In the same time interval, energy availability for iron oxidizers increased by a factor of 6 to 8, and, in 1997, there was 25 times more energy per transferred electron in iron oxidation than in sulfide oxidation. This change coincides with a massive spread of red staining (putative colonization by Fe-oxidizing bacteria) between 1995 and 1997.

For a different cluster of vents from the EPR 9°50'N area (Tube Worm Pillar), thermodynamic modeling is used to examine changes in subseafloor catabolic metabolism between 1992 and 2000. These reactions are deduced from deviations in diffuse fluid compositions from conservative behavior of redox-sensitive species. We show that hydrogen is significantly reduced relative to values expected from conservative mixing. While H_2 concentrations of the hydrothermal endmember fluids were constant between 1992 and 1995, the affinities for hydrogenotrophic reactions in the diffuse fluids decreased by a factor of 15 and then remained constant between 1995 and 2000. Previously, these fluids have been shown to support subseafloor methanogenesis. Our calculation results corroborate these findings and indicate that the 1992-1995 period

was one of active growth of hydrogenotrophic communities, while the system was more or less at steady state between 1995 and 2000.

Geochimica et Cosmochimica Acta 75 (2011) 5736–5748; doi:10.1016/j.gca.2011.07.041

7. Appendix-B: Catabolic and anabolic energy for chemolithoautotrophs in deep-sea hydrothermal systems hosted in different rock types

Jan P. Amend [a,§], Thomas M. McCollom [b], Michael Hentscher [c], Wolfgang Bach [c]

[a]*Department of Earth Sciences and Department of Biological Sciences, University of Southern California, Los Angeles, CA 90089-0740, USA*

[b] *Laboratory of Atmospheric and Space Physics, University of Colorado, Boulder, CO 80309, USA*

[c] *Department of Geosciences, University of Bremen, 28334 Bremen, Germany*

[§]*Corresponding author: jan.amend@usc.edu*

7.1 Abstract

Active deep-sea hydrothermal vents are hosted by a range of different rock types, including basalt, peridotite, and felsic rocks. The associated hydrothermal fluids exhibit substantial chemical variability, which is largely attributable to compositional differences among the underlying host rocks. Numerical models were used to evaluate the energetics of seven inorganic redox reactions (potential catabolisms of chemolithoautotrophs) and numerous biomolecule synthesis reactions (anabolism) in a representative sampling of these systems, where chemical gradients are established by mixing hydrothermal fluid with seawater. The wide ranging fluid compositions dictate demonstrable differences in Gibbs energies (ΔG_r) of these catabolic and anabolic reactions in three peridotite-hosted, six basalt-hosted, one troctolite-basalt hybrid, and two felsic rock-hosted systems. In peridotite-hosted systems at low to moderate temperatures (<~45 °C) and high seawater:hydrothermal fluid (SW:HF) mixing ratios (>10), hydrogen oxidation yields the most catabolic energy, but the oxidation of methane, ferrous iron, and sulfide can also be moderately exergonic. At higher temperatures, and consequent SW:HF mixing ratios <10, anaerobic processes dominate the energy landscape; sulfate reduction and methanogenesis are more exergonic than any of the aerobic respiration reactions. By comparison, in the basalt-hosted and felsic rock-hosted systems, sulfide oxidation was the predominant catabolic energy source at all temperatures (and SW:HF ratios) considered. The energetics of catabolism at the troctolite-basalt hybrid system were intermediate to these extremes. Reaction energetics for anabolism in chemolithoautotrophs — represented here by the synthesis of amino acids, nucleotides, fatty acids, saccharides, and amines—were generally most favorable at moderate

temperatures (22–32°C) and corresponding SW:HF mixing ratios (~15). In peridotite-hosted and the troctolite-basalt hybrid systems, ΔG_r for primary biomass synthesis yielded up to ~900 J per g dry cell mass. The energetics of anabolism in basalt- and felsic rock-hosted systems were far less favorable. The results suggest that in peridotitehosted (and troctolite-basalt hybrid) systems, compared with their basalt (and felsic rock) counterparts, microbial catabolic strategies — and consequently variations in microbial phylotypes — may be far more diverse and some biomass synthesis may yield energy rather than imposing a high energetic cost.

The ISME Journal (2011) 5, 692–703; doi:10.1038/ismej.2010.157;

8. Appendix-C: Colonization of subsurface microbial observatories deployed in young ocean crust

Beth N Orcutt[1], Wolfgang Bach[2], Keir Becker[3], Andrew T Fisher[4], Michael Hentscher[2], Brandy M Toner[5], C Geoffrey Wheat[6] and Katrina J Edwards[1 §]

[1]University of Southern California, Los Angeles, CA, USA;
[2]University of Bremen, Bremen, Germany; [3]University of Miami, Miami, FL, USA; [4]Earth and Planetary Science Department, University of California Santa Cruz, Santa Cruz, CA, USA;
[5]University of Minnesota, Twin Cities, St Paul, MN, USA and [6]Global Undersea Research Unit, University of Alaska, Fairbanks, Moss Landing, CA, USA

[§]Corresponding author: kje@usc.edu

8.1 Abstract

Oceanic crust comprises the largest hydrogeologic reservoir on Earth, containing fluids in thermodynamic disequilibrium with the basaltic crust. Little is known about microbial ecosystems that inhabit this vast realm and exploit chemically favorable conditions for metabolic activities. Crustal samples recovered from ocean drilling operations are often compromised for microbiological assays, hampering efforts to resolve the extent and functioning of a subsurface biosphere. We report results from the first *in situ* experimental observatory systems that have been used to study subseafloor life. Experiments deployed for 4 years in young (3.5 Ma) basaltic crust on the eastern flank of the Juan de Fuca Ridge record a dynamic, post-drilling response of crustal microbial ecosystems to changing physical and chemical conditions. Twisted stalks exhibiting a biogenic iron oxyhydroxide signature coated the surface of mineral substrates in the observatories; these are biosignatures indicating colonization by iron oxidizing bacteria during an initial phase of cool, oxic, iron-rich conditions following observatory installation. Following thermal and chemical recovery to warmer, reducing conditions, the *in situ* microbial structure in the observatory shifted, becoming representative of natural conditions in regional crustal fluids. Firmicutes, metabolic potential of which is unknown but may involve N or S cycling, dominated the post-rebound bacterial community. The archaeal community exhibited an extremely low diversity. Our experiment documented *in situ* conditions within a natural hydrological system that can pervade over millennia, exemplifying the power of observatory experiments for exploring the subsurface basaltic biosphere, the largest but most poorly understood biotope on Earth.

Environmental Microbiology Reports (2011) 3(6), 727–737; doi:10.1111/j.1758-2229.2011.00291.x

9. Appendix-D: Driving forces behind the biotope structures in two low-temperature hydrothermal venting sites on the southern Mid-Atlantic Ridge

Mirjam Perner[1§], Michael Hentscher[2], Nicolas Rychlik[1], Richard Seifert[3], Harald Strauss[4] and Wolfgang Bach[2]

[1]*Molecular Biology of Microbial Consortia, University of Hamburg, Biocenter Klein Flottbek, Ohnhorststr. 18, 22609 Hamburg, Germany.*
[2]*Department of Geosciences, University of Bremen, Klagenfurter Street 2, 28359 Bremen, Germany.*
[3]*Institute of Biogeochemistry and Marine Chemistry, University of Hamburg, Bundesstr. 55, 20146 Hamburg, Germany.*
[4]*Institut für Geologie und Paläontologie, Westfälische Wilhelms-Universität Münster, Corrensstr. 24, 48149 Münster, Germany.*

[§]*Corresponding author: mirjam.perner@uni-hamburg.de;*

9.1 Summary

Although it has been more than 30 years since the discovery of deep-sea hydrothermal vents, comprehending the interconnections between hydrothermal venting and microbial life remains a challenge. Here we investigate abiotic–biotic linkages in lowtemperature hydrothermal biotopes at Desperate and Lilliput on the southern Mid-Atlantic Ridge. Both sites are basalt-hosted and fluids exhibit the expected chemical signatures. However, contrasting crustal permeabilities have been proposed, supporting pervasive mixing at Desperate but restricting circulation at Lilliput. In Desperate fluids, sulfide and O_2 were readily available but H_2 hardly detectable. Under incubation conditions (oxic unamended, sulfide-spiked, oxic and anoxic H_2-spiked at 18°C), only sulfide oxidation by *Thiomicrospira* fuelled biomass synthesis. Microbial phylogenies from Desperate incubation experiments resembled those of the natural samples suggesting that the incubation conditions mimicked the environment. In Lilliput fluids, O_2 was limited, whereas sulfide and H_2 were enriched. Autotrophy appeared to be stimulated by residual sulfide and by amended H_2. Yet, based on bacterial phylogenies only conditions in anoxic H_2-spiked Lilliput incubations appeared similar to parts of the Lilliput habitat. In anoxic H_2-spiked Lilliput enrichments *Campylobacteraceae* likely supported biomass production through H_2 oxidation. We argue that the diverging circulation

patterns arising from different subseafloor permeabilities act as major driving forces shaping these biotope structures.

Environmental Microbiology (2009) 11(10), 2526–2541 doi:10.1111/j.1462-2920.2009.01978.x

10. Appendix-E: Short-term microbial and physico-chemical variability in low-temperature hydrothermal fluids near 5°S on the Mid-Atlantic Ridge

Mirjam Perner[1§], Wolfgang Bach[2], Michael Hentscher[2], Andrea Koschinsky[3], Dieter Garbe-Schönberg[4], Wolfgang R. Streit[1] and Harald Strauss[5]

[1]Microbiology and Biotechnology, University of Hamburg, Biozentrum Klein Flottbek, Ohnhorststr. 18, 22609 Hamburg, Germany.

[2]Department of Geosciences, University of Bremen, Klagenfurter Str. 2, 28359 Bremen, Germany.

[3]School of Engineering and Science, Jacobs University Bremen gGmbH, Campus Ring 8, 28759 Bremen, Germany.

[4]Institute of Geosciences, Christian-Albrechts-Universität zu Kiel, Ludewig-Meyn-Str. 10, 24118 Kiel, Germany.

[5]Geologisch-Paläontologisches Institut der Westfälischen Wilhelms-Universität Münster, Corrensstr. 24, 48149 Münster, Germany.

[§]Corresponding author: mirjam.perner@uni-hamburg.de;

10.1 Summary

This study examines the representativeness of low temperature hydrothermal fluid samples with respect to their chemical and microbiological characteristics. Within this scope, we investigated short-term temporal chemical and microbial variability of the hydrothermal fluids. For this purpose we collected three fluid samples consecutively from the same spot at the Clueless field near 5°S on the southern Mid-Atlantic Ridge over a period of 50 min. During sampling, the temperature was monitored online. We measured fluid chemical parameters, characterized microbial community compositions and used statistical analyses to determine significant differences between the samples. Overall, the three fluid samples are more closely related to each other than to any other tested habitat. Therefore, on a broad scale, the three collected fluid samples can be regarded as habitat representatives. However, small differences are apparent between all samples. One of the Clueless samples even displayed significant differences (P-value < 0.01) to the other two Clueless samples. Our data suggest that the observed variations in fluid chemical and microbial compositions are not reflecting sampling artefacts but are related to short-term fluid variability due to dynamic subseafloor fluid mixing. Recorded temporal changes in fact reflect spatial heterogeneity found in the

subsurface as the fluid flows through distinctive pathways. While conservative elements (Cl, Si, Na and K) indicate variable degrees of fluid-seawater mixing, reactive components, including Fe(II), O_2 and H_2S, show that chemical and microbial reactions within the mixing zone further modify the emanating fluids on short-time scales. Fluids entrain microorganisms, which modify the chemical microenvironment within the subsurface biotopes. This is the first study focusing on short-term microbial variability linked to chemical changes in hydrothermal fluids.

Geochem. Geophys. Geosyst., 12, Q0AE05; doi:10.1029/2011GC003704

11. Appendix-F: Geochemistry of vent fluid particles formed during initial hydrothermal fluid–seawater mixing along the Mid-Atlantic Ridge

Verena Klevenz[1§], Wolfgang Bach[2], Katja Schmidt[1], Michael Hentscher[2], Andrea Koschinsky[1] and Sven Petersen[3]

[1]*Earth and Space Sciences Program, School of Engineering and Science, Jacobs University Bremen, Campus Ring 1, D-28759 Bremen, Germany*
[2]*Fachbereich Geowissenschaften, Universität Bremen, D-28334 Bremen, Germany*
[3]*Leibniz-Institut für Meereswissenschaften an der Universität Kiel (IFM-GEOMAR), D-24148 Kiel, Germany*

[§]*Corresponding author: vklevenz@jacobs-alumni.de;*

11.1 Abstract

We present geochemical data of black smoker particulates filtered from hydrothermal fluids with seawaterdilutions ranging from 0–99%. Results indicate the dominance of sulphide minerals (Fe, Cu, and Zn sulphides) in all samples taken at different hydrothermal sites on the Mid-Atlantic Ridge. Pronounced differences in the geochemistry of the particles between Logatchev I and 5°S hydrothermal fields could be attributed to differences in fluid chemistry. Lower metal/sulphur ratios (Me/H2S < 1) compared to Logatchev I result in a larger amount of particles precipitated per liter fluid and the occurrence of elemental sulphur at 5°S, while at Logatchev I Fe oxides occur in larger amounts. Systematic trends with dilution degree of the fluid include the precipitation of large amounts of Cu sulphides at a low dilution and a pronounced drop with increasing dilution. Moreover, Fe (sulphides or oxides) precipitation increases with dilution of the vent fluid by seawater. Geochemical reaction path modeling of hydrothermal fluid–seawater mixing and conductive cooling indicates that Cu sulphide formation at Logatchev I and 5°S mainly occurs at high temperatures and low dilution of the hydrothermal fluid by seawater. Iron precipitation is enhanced at higher fluid dilution, and the different amounts of minerals forming at 5°S and Logatchev I are thermodynamically controlled. Larger total amounts of minerals and larger amounts of sulphide precipitate during the mixing path when compared to the cooling path. Differences between model and field observations do occur and are attributable to closed system

modeling, to kinetic influences and possibly to organic constituents of the hydrothermal fluids not accounted for by the model.

Danksagung

Zu allererst möchte ich meinem Doktorvater Prof. Dr. Wolfgang Bach danken, der meine Leidenschaft für die thermodynamische Modellierung geweckt hat. Er half mir bei der Einarbeitung in die verschiedenen Techniken der Reaktionspfadmodellierungen aber auch in die Zusammenhänge der Gesteinsalteration und stand mir immer mit Rat und Tat zur Seite, wenn Probleme auftraten. Ich danke ihm auch für die Zeit und Geduld, die er in mich und meine Arbeit investierte; daher ist es zu großem Teil ihm zu verdanken, dass diese zustande gekommen ist.

Ich danke Herrn Prof. Dr. Kai Uwe Hinrichs für die bereitwillige Übernahme des Zweitgutachtens.

Meinen ehemaligen Büroinsassen Frieder Klein und Dominik Niedermeier: Frieder sowohl für die fachlichen Gespräche über Modellierungen und deren Ergebnisse als auch für den Spaß bei der Arbeit sowie Dominik, der maßgeblich zu der angenehmen Arbeitsatmosphäre beigetragen hat, indem er immer gelassen blieb.

Niels Jöns danke ich für die fachliche Unterstützung und seine Hilfsbereitschaft beim Überarbeiten von Manuskripten und Vorträgen, dem Ausmerzen des einen oder anderen Fehlers, aber auch für die Hilfe bei Softwareproblemen.

Svenja Rausch danke ich für die moralische Unterstützung und die vielen lustigen und interessanten Gesprächen bei einer Tasse Kaffee.

Den Mitarbeitern der Arbeitsgruppe Petrologie der Ozeankruste danke ich für das tolle Arbeitsklima und die netten Gespräche am Kaffeetisch und bei dem einen oder anderen Feierabendbier (Heike Anders, Liping Shu, Jutta Ait-Majdari, Wolf-Achim Kahl, Andreas Klügel, Elliot Hildner, Eoghan Reeves und Janis Thal).

Natürlich danke ich auch Beth Orcutt, Mirjam Perner, Verena Klevenz, Jan P. Amend und Tom McCollom für die Zusammenarbeit, die zu den Veröffentlichungen führte.

Ich danke meinen Freunden, auf die ich mich immer verlassen konnte und die immer mal wieder für eine wohltuende Ablenkung während der Zusammenschreibphase dieser Arbeit sorgten.

Mein besonderer Dank gilt meiner Mutter, Ursela Hentscher, und meinem Bruder Martin, die mich immer unterstützt haben und ohne die diese Arbeit nie zustande gekommen wäre.

Diese Arbeit wurde durch ein Projekt der Deutschen Forschungsgemeinschaft (DFG BA1605/6-1) und die Universität Bremen ermöglicht.

Lebenslauf

Persöhnliche Daten

Name	Michael Hentscher
Anschrift	Elmeloher Weg 6d 27753 Delmenhorst
E-mail	hentscher@uni-bremen.de
Geburtsdatum	12. Oktober 1975
Geburtsort	Delmenhorst
Staatsangehörigkeit	deutsch

Ausbildung

Fachgymnasium Wirtschaft Berufsbildende Schulen I Delmenhorst	1997 Abitur
Wehrersatzdienst	1997-1998
Carl von Ossietzky Universität Oldenburg	1998-2004 Studium der marinen Umweltwissenschaften Abschluß im April 2004 als Diplom Umweltwissenschaften 1998-2006 Studium der Chemie 2005-2006 Studium Lehramt Chemie und Biologie
Universität Bremen	Seit Oktober 2006 wissenschaftlicher Mitarbeiter Seit Juni 2007 Promotionsstudium (Petrologie der Ozeankruste)

Publikationsliste

Publikationen

Hentscher, M., Bach, W., 2012. Geochemically induced shifts in catabolic energy yields explain past ecological changes of diffuse vents in the East Pacific Rise 9 degrees 50‘N area. Geochemical Transactions 13, 2.

Amend, J.P., McCollom, T.M., Hentscher, M., Bach, W., 2011. Catabolic and anabolic energy for chemolithoautotrophs in deep-sea hydrothermal systems hosted in different rock types. Geochimica et Cosmochimica Acta 75, 5736-5748.

Klevenz, V., Bach, W., Schmidt, K., Hentscher, M., Koschinsky, A., Petersen, S., 2011. Geochemistry of vent fluid particles formed during initial hydrothermal fluid-seawater mixing along the Mid-Atlantic Ridge. Geochemistry, Geophysics, Geosystems 12, Q0AE05.

Orcutt, B.N., Bach, W., Becker, K., Fisher, A.T., Hentscher, M., Toner, B.M., Wheat, C.G., Edwards, K.J., 2011. Colonization of subsurface microbial observatories deployed in young ocean crust. ISME Journal 5, 692-703.

Perner, M., Hentscher, M., Rychlik, N., Seifert, R., Strauss, H., Bach, W., 2011. Driving forces behind the biotope structures in two low-temperature hydrothermal venting sites on the southern Mid-Atlantic Ridge. Environmental Microbiology Reports 3, 727-737.

Perner, M., Bach, W., Hentscher, M., Koschinsky, A., Garbe-Schönberg, D., Streit, W.R., Strauss, H., 2009. Short-term microbial and physico-chemical variability in low-temperature hydrothermal fluids near 5°S on the Mid-Atlantic Ridge. Environmental Microbiology 11, 2526-2541.

Dellwig, O., Bosselmann, K., Kölsch, S., Hentscher, M., Hinrichs, J., Böttcher, M.E., Reuter, R., Brumsack, H.J., 2007. Sources and fate of manganese in a tidal basin of the German Wadden Sea. Journal of Sea Research 57, 1-18.

Erklärung

Erklärung gemäß § 6 Abs. 5 der Promotionsordnung der Universität Bremen für die mathematischen,natur- und ingenieurswissenschaftlichen Fachbereiche.

Name: Michael Hentscher
Anschrift: Elmeloher Weg 6d, 27753 Delmenhorst

Hiermit versichere ich, dass ich

1. die Arbeit ohne unerlaubte fremde Hilfe angefertigt habe,
2. keine anderen als die von mir angegebenen Quellen und Hilfsmittel benutzt habe und
3. die den benutzten Werken wörtlich oder inhaltlich entnommenen Stellen als solche kenntlich gemacht habe.

Bremen, den 09. May 2012

Michael Hentscher